

Rutgers, The State University of New Jersey

RUTGERS
New Jersey Medical School

**SUMMER STUDENT
RESEARCH PROGRAM**

ROBERT L. JOHNSON, MD, FAAP
THE SHARON AND JOSEPH L. MUSCARELLE ENDOWED DEAN

WILLIAM C. GAUSE, PH.D.
SENIOR ASSOCIATE DEAN FOR RESEARCH

DEBORAH A. LAZZARINO, PH.D.
ASSISTANT DEAN FOR RESEARCH ADMINISTRATION

MS. GIOVANNA COMER
PROGRAM COORDINATOR



**RESEARCH OFFICE
2013
ANNUAL REPORT
OF
ACCOMPLISHMENTS**



REPORT OF ACCOMPLISHMENTS

**NO PART OF THIS BOOK MY BE USED OR REPODUCED IN ANY FORM WITHOUT PRIOR WRITTEN PERMIS-
SION OF THE SHARON AND JOSEPH L. MUSCARELLE ENDOWED DEAN, SENIOR ASSOCIATE DEAN FOR RE-
SEARCH ADMINISTRATION, ASSISTANT DEAN FOR RESEARCH ADMINISTRATION, NJMS FACULTY MEN-
TORS, STUDENT AUTHORS AND EDITOR.**



ACKNOWLEDGEMENTS

**EXPRESSIONS OF APPRECIATION TO THE
RUTGERS, NEW JERSEY MEDICAL SCHOOL ALUMNI
AND
THE NEW JERSEY HEALTHCARE FOUNDATION, INC.
THANK YOU SO MUCH FOR YOUR CONTINUOUS FINANCIAL SUPPORT.
YOUR FINANCIAL SUPPORT ENABLES STUDENTS THE OPPORTUNITY
TO BROADEN THEIR RESEARCH SKILLS.**

2013

STUDENT ABSTRACTS

REPORT OF ACCOMPLISHMENTS



Table of Contents

Preface	4
Faculty Advisory Committee	5
Faculty Mentors	5-6
Judges for Poster Competition	7
Introduction	8
Ami Shah	9-11
Ayush Parikh	12-16
Brian D. Kim	17-21
Chislaine Cruz	22-26
David Kam	27-31
Hardik Parikh	32-35
Dina Mohamed-Aly	36-39
John Prendergass	40-44
Karen Grover	45-48
Yoon Ho Park, & Peter Sharoupim	49-52
Laura Rotundo & Patrick Lundy	53-56
Michael Duan	57-62
C. Ayala	63-64
Anthony Kordahi	65-66
Phoebe Y. Ling	67-70
Ritam Ghosh	71-74
Rohit K. Reddy	75-79
Ryan Meyer	80-82
Smirnov Exilus	83-85
Poster Symposium Highlights	86-104

PREFACE

Since 1968 the New Jersey Medical School First-Second Year Students and Volunteers have participated in this organized research program. This program gives an opportunity for students and volunteers to work alongside an NJMS Faculty Mentor on a specific research project for a period of eight weeks. Over the eight week period the participants are exposed to the dynamic nature of biomedical science. During this time they learn about the methodology and results of laboratory-clinical research; sharpen diagnostic skills, and learn the value and limits of experimental results. This program has been fortunate to have had an array of enthusiastic students seeking to broaden their research knowledge in the treatment of diseases.

This the forty-fifth edition of the Summer Student Research Program Abstracts summarizing research results generated by students, volunteers, and interns working thru this year's program. The Summer Student Research Program continues to provide a significant contribution to the training of our future clinicians and research scientists. It is the continued goal of this program to inspire the next generation of physicians and scientists.

We would like to thank the NJMS Faculty and Researchers who take time from their teaching and administrative responsibilities to mentor over the eight week period. We truly appreciate your continued support and exceptional commitment. It is also with pleasure that we thank the members of the faculty advisory committee.....for their assistance and commitment in developing the program guidelines, evaluating student abstracts, selection of student participants and participation during the poster symposium. This program could not be successful without your volunteerism! Many thanks to you for your kind consideration.

MANY THANKS TO THE FOLLOWING FACULTY FOR TAKING TIME TO MENTOR THE MEDICAL STUDENTS, INTERNS AND VOLUTEERS DURING THE 2013 SUMMER STUDENT RESEARCH PROGRAM.

FACULTY ADVISORY COMMITTEE

Eric Altschuler, MD, Ph.D. Assistant Professor Physical Medicine & Rehabilitation	Carol Lutz, Ph.D. Associate Professor Biochemistry & Molecular Biology
Deborah A. Lazzarino, Ph.D. Assistant Dean for Research Administration Office of Research & Sponsored Programs	Pranela Rameshwar, Ph.D. Professor Department of Medicine
Sheldon Lin, MD Associate Professor Department of Medicine	Charles R. Spillert, Ph.D. Associate Professor Department of Surgery
Purnima Bhanot, Ph.D. Assistant Professor Microbiology & Molecular Genetics	Nila Dharan, MD Assistant Professor Department of Medicine
Diego Fraidenaich, PhD, Assistant Professor Cell Biology & Molecular Medicine	
2013 KICK-OFF TO THE SSRP SEMINAR PRESENTER Laura T. Goldsmith, Ph.D., Professor Obstetrics, Gynecology & Women's Health	2013 SSRP Poster Symposium SEMINAR PRESENTER Steven Levison, Ph.D., Professor, Neuroscience Director, Laboratory for Regenerative Neurobiology

NJMS FACULTY MENTORS

Eric Altschuler, MD, Ph.D. Assistant Professor Physical Medicine & Rehabilitation	Purnima Bhanot, PhD. Assistant Professor Microbiology and Molecular Genetics
Soly Baredes, MD Professor Neurological Surgery	Ping-Hsin Chen, Ph.D. Assistant Professor Family Medicine
Susan Feldman, Ph.D. Associate Professor Department of Radiology	Melissa Rogers, Ph.D. Associate Professor Biochemistry & Molecular Biology
Chirag Gandhi, MD Assistant Professor Neurological Surgery	Sandra Scott, MD Assistant Professor Emergency Medicine
Betsy Barnes, Ph.D. Associate Professor Biochemistry & Molecular Biology	Ziad Sifri, MD Associate Professor Emergency Medicine



NJMS FACULTY MENTORS

<p>Robert Heary, MD Professor Neurological Surgery</p>	<p>Lizhao Wu, Ph.D. Assistant Professor Microbiology & Molecular Genetics</p>
<p>Sheldon Lin, MD Associate Professor Department of Medicine</p>	<p>Charles Spillert, MD Associate Professor Department of Surgery</p>
<p>James Liu, MD Assistant Professor Neurological Surgery</p>	<p>Ellen Townes-Anderson, Ph.D. Professor Neurology & Neurosciences</p>
<p>Patrick O'Connor Associate Professor Biochemistry & Molecular Biology</p>	<p>Yongkyu Park, Ph.D. Adjunct Assistant Professor Cell Biology & Molecular Medicine</p>
<p>Alicia Mohr, MD Associate Professor Department of Surgery</p>	<p>Chaoyang Xue, Ph.D. Assistant Professor Public Health Research Institute</p>
<p>Charles Prestigiacomo, MD Professor & Chair Neurological Surgery</p>	<p>Anna Barrett, MD Professor Physical Medicine & Rehabilitation</p>
<p>Charles Spillert, Ph.D. Associate Professor Department of Surgery</p>	<p>Robert Ledeen, Ph.D. Professor Neurosciences</p>
<p>Stella Elkabes, Ph.D. Associate Professor Neurological Surgery</p>	<p>Stanley Weiss, MD Professor Preventive Medicine & Community Health</p>
<p>Misun Park, Ph.D. Assistant Professor Cell Biology & Molecular Medicine</p>	<p>Padmini Salgame, Ph.D. Professor Department of Medicine</p>
<p>Francis Patterson, MD Associate Professor Department of Orthopaedics</p>	<p>John Capo, MD Professor Department of Orthopaedics</p>



JUDGES FOR POSTER COMPETITION

<p>Rashi Aggarwal, MD Assistant Professor Department of Psychiatry</p>	<p>Petros Levounis, MD Professor & Chair Department of Psychiatry</p>
<p>Alex Bekker, MD, Ph.D. Professor & Chair Department of Anesthesiology</p>	<p>Elizabeth Moran, Ph.D. Professor Department of Orthopaedics</p>
<p>Vivian Bellofatto, Ph.D. Professor Microbiology & Molecular Genetics</p>	<p>Sabina Mushtaq, MD Professor & Chair Department of Psychiatry</p>
<p>Raymond Birge, Ph.D. Professor Biochemistry & Molecular Biology</p>	<p>Yongkyu Park, Ph.D. Adjunct Assistant Professor Cell Biology & Molecular Medicine</p>
<p>Deborah A. Lazzarino, Ph.D. Assistant Dean for Research Administration Research Office</p>	<p>Ziad Sifri, Ph.D. Adjunct Assistant Professor Department of Psychiatry</p>

INTRODUCTION

The Summer Student Research Program provides an eight-week research experience for the New Jersey first-second year medical students, as well as undergraduate students enrolled in our combined BS/MD seven-year program. Students are required to participate in research activities in a basic science or clinical laboratory. On many occasions this has been the students first research experience. Participation allows students, interns and volunteers to develop a close working relationship with their mentor.

After completing eight weeks of research in the respective laboratories, students present their research projects at the Summer Student Research Poster Symposium held the last week of July. At the symposium students are interviewed and required to explain the results displayed in their poster presentation. The abstracts preceding is a reflection of the commitment, dedication and enthusiasm of every student who participated in the Summer Student Research Program who presented at the 2013 Poster Symposium.

Congratulations to all the students, interns and volunteers enrolled in the 2013 Summer Student Research Program! Wishing you all the best and my you have continued success in your future endeavors!

Congratulations to Ms. Alisha Valdez the winner of the 2013 Summer Student Research Poster Competition!

AMI SHAH (TCNJ-NJMS 2019)

**PROJECT TITLE: ROLE OF METABOLISM IN FRUCTOSE TRANSPORTER GLUT5
REGULATION**

MENTOR: RONALDO P. FERRARIS, PH.D, PROFESSOR

DEPARTMENT: PHARMACOLOGY AND PHYSIOLOGY

Participation Description:

For this project, I was responsible for the functional assay where I incubated portions of the proximal jejunum to measure sugar uptake. I was also involved with RNA extraction, RNA clean-up, conversion to c-DNA, and PCR. I also made graphs from the data to better understand it and was involved with the statistical analysis. I was also a part of other research projects in the lab during the summer through which I learned and performed immunohistochemistry and blood collection.

Objective:

The recent surge in metabolic diseases like obesity, type II diabetes and hyperinsulinemia has been attributed to the marked increases in fructose consumption rates. It is therefore important to increase our understanding of the processes that regulate metabolism of this sugar. The Ferraris lab has already established that consumption of fructose increases the absorption of this sugar in the small intestine by inducing the expression and thus activity of the fructose-specific transporter GLUT5. While the exact mechanism of this regulation is unknown, recent results from the lab have shown, using KHK (ketoheokinase, the fructose metabolizing enzyme) $-/-$ mice, that fructose needs to be metabolized in order to upregulate GLUT5. The purpose of this study was to determine whether a downstream, fructose-specific metabolite such as glyceraldehyde can increase GLUT5 expression and activity. Based on prior results, it was hypothesized that glyceraldehyde would upregulate GLUT5 and thus would increase fructose absorption and GLUT5 mRNA levels.

Methods:

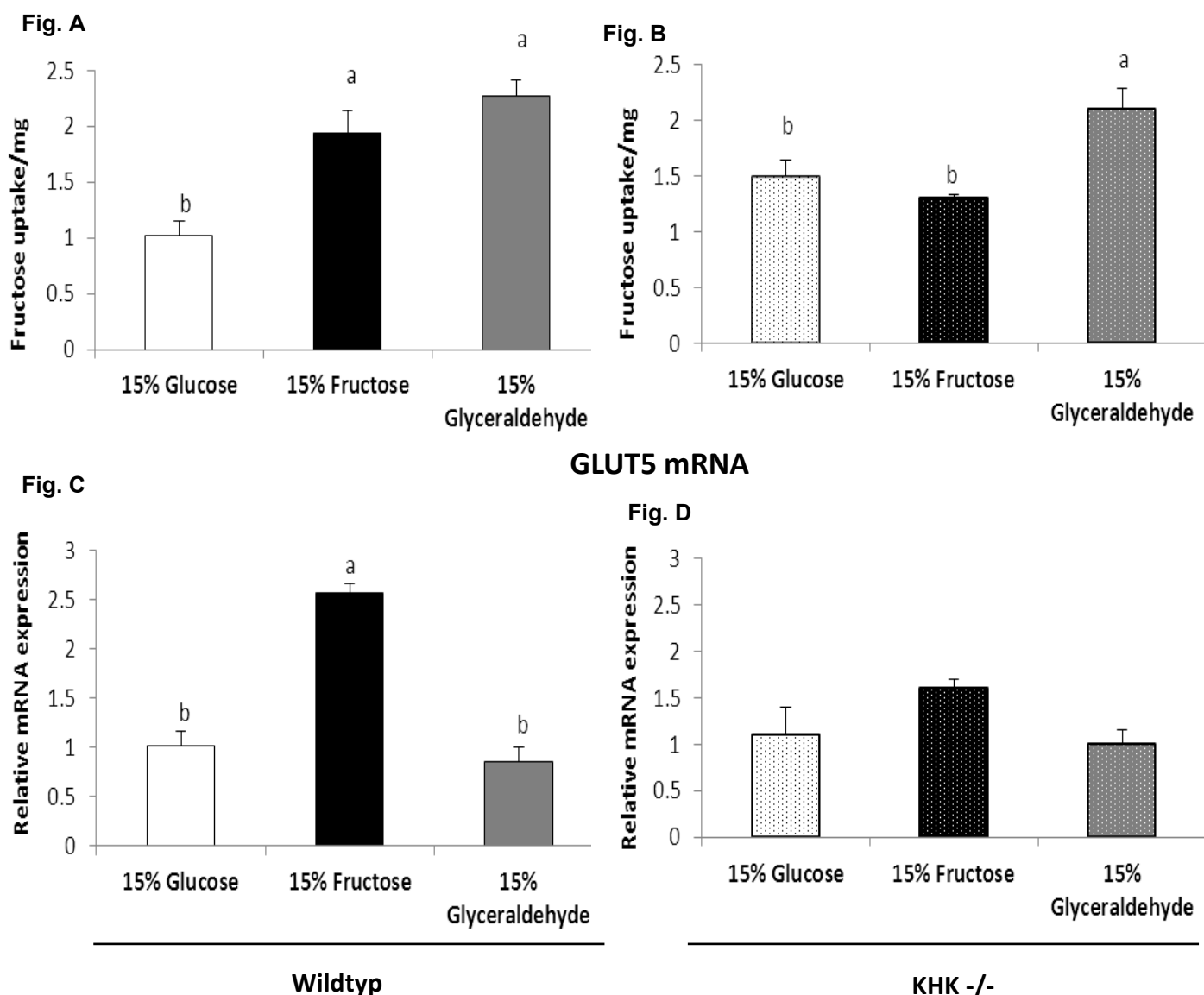
Five-week-old wildtype and KHK $-/-$ mice were gavaged twice a day for three days with a 15% glucose, fructose, or glyceraldehyde solution (n=4) at 2 ml/100 kg body weight. The mice were sacrificed and the intestine was flushed and removed. Pieces of the proximal jejunum of each mouse were inverted and incubated in radioactive glucose or fructose solutions to measure sugar uptake. Mucosal scrapes of the remaining proximal jejunum were used to determine mRNA concentrations of various proteins through RNA extraction, RNA clean-up, conversion to c-DNA, and RT-PCR.

Summary:

In wildtype mice, fructose uptake (or GLUT5 activity) was significantly higher in fructose- and glyceraldehyde-gavaged mice (Fig. A). In KHK $-/-$ mice, however, fructose uptake was only significantly higher in mice gavaged with glyceraldehyde (Fig. B). GLUT5 mRNA expression was significantly higher only in wildtype mice gavaged with fructose (Fig. C). In KHK $-/-$ mice, there was no significant difference in GLUT5 expression levels amongst all treatments (Fig. D). In order to make sure that these effects were specific to GLUT5, expression of the glucose transporter SGLT1 and glucose uptake (or SGLT1 activity) were measured as a control. Neither expression nor activity of SGLT1 was affected by sugar and glyceraldehyde treatment (not shown).

Expression levels of fructose metabolizing enzymes triokinase and aldolase were also measured. Expression of triokinase was significantly higher in wildtype mice gavaged with fructose and while the expression of aldolase was not significantly higher in any experimental group, expression did tend to increase in wildtype mice gavaged with fructose (not shown). Glyceraldehyde had no effect on the expression of either of these enzymes (not shown).

D-Fructose Uptake



Conclusion:

These results confirm past results that fructose needs to be metabolized in order to upregulate GLUT5 as expression and activity of GLUT5 did not increase with fructose in KHK $-/-$ mice (in which fructose metabolism is inhibited). Moreover, these results also suggest that glyceraldehyde does play a role in upregulating GLUT5 since GLUT5 activity did increase in both wildtype and KHK $-/-$ mice gavaged with glyceraldehyde. However, since GLUT5 expression was not affected by glyceraldehyde in either wildtype or KHK $-/-$ mice, it can be concluded that glyceraldehyde is not involved with the transcriptional regulation of GLUT5. In conclusion, while glyceraldehyde appears to mediate GLUT5 upregulation, this regulation is not transcriptional.

AYUSH PARIKH
(DR. RONALD E. MCNAIR ACADEMIC HIGH SCHOOL, 2015)

PROJECT TITLE: THE EFFECTS OF TISSUE-SPECIFIC LOCO-RPD3 DOWNREGULATION IN STRESS RESISTANCE OF *D. MELANOGASTER*
MENTOR: YONGKYU PARK, Ph.D, ASSISTANT PROFESSOR
DEPARTMENT: CELL BIOLOGY AND MOLECULAR MEDICINE

Participation in Research Project:

The procedures, experiment setups, and results collection and analysis that are included within this project were all performed by Zachary Kopp (graduate student), Dr. Park, and myself. First, we planned out the stress resistance for the various mutated strains of *Drosophila melanogaster*. We planned out three different stress experiments (oxidation, heat, and starvation), and performed the oxidation and starvation twice. First, I was responsible for male fly collection, virgin female (for mating different crosses) collection, transferring the flies into appropriate testing vials during experiments, and then counting them at 2-hour intervals during the stress experiments. Next, I planned and performed the gene expression studies, utilizing the procedures of RNA isolation, cDNA production, and real-time PCR with the help of Mr. Kopp and Dr. Park. I also aided in the subcloning process, through pipetting, preparing solutions, and calibrating machinery. Each of these was performed greater than 3 times for the various genes tested. I helped organize all of the data into Microsoft Excel files, performed data analysis, and created the graphs and charts to easily visualize the data. I also calculated median points of the data. I would like to greatly thank Dr. Park and Zachary Kopp in their strong guidance, teaching, patience, and support during my research experience with them.

Objective:

The objective of the study was to examine the effects of Loco-Rpd3 down-regulation in specific target tissue of *D. melanogaster*. Previous experiments conducted by Dr. Yongkyu Park have concluded that Loco (RGS protein – Regulator of G-protein signaling) and Rpd3 protein (HDAC-1) down-regulation in whole-body tissue have directly correlated to increased oxidative and starvation stress resistance in *D. melanogaster* (Table 1). The reasoning behind this lies in the fact that previous studies have shown that down-regulation of Loco and Rpd3 enhanced fat content in those mutated flies, resulting in healthier and more effective immune systems (Table 1). These previous experiments (Table 1) also concluded that fat-body specific loco down-regulation contributed to recognizable increases in stress resistance (Table 1). Rpd3/HDAC-1, a downstream protein of Loco, is predicted to exhibit a similar effect if it is down-regulated.

This experiment wanted to examine this effect in a tissue-specific region, specifically the heart tissue (Tinman genotype) in *D. melanogaster*, and to see if similar results would be obtained. Based on previous data, the hypothesis of this experiment is that there will be an increased stress-resistant response in *D. melanogaster* through decreases in Loco and Rpd3 (HDAC-1).

	Expression	Lifespan	Stress Resistance (hr)			Weight	Nutrients (ug/mg)	
	<i>loco</i> gene	(day)	Starvation	Oxidation	Heat	(mg/fly)	Protein	Fat
+/+	wild type	47.1	32.6	11.6	18.6	0.88	46.2	13.0
Δ <i>loco</i> /+	<i>loco</i> mutant	+20%	+27%	+63%	+26%	+16%	-8%	+36%
act/ <i>loco</i>	<i>loco</i> O/E	-20%	-22%	-25%	-28%	+3%	+17%	-34%
<i>loco</i> -dsRNAi								
+/ <i>loco</i> Ri	no	47.3	38.8	25.5	21.7	0.64	48.9	17.7
arm/ <i>loco</i> Ri	whole body	+32%	+30%	+26%	+30%	+0%	+1%	+16%
r4/ <i>loco</i> Ri	fat body	+26%	+27%	+30%	+31%	-12%	-29%	+22%
repo/ <i>loco</i> Ri	glial cells	-6%	-3%	-20%	-6%	+2%	+4%	+0%
GMR/ <i>loco</i> Ri	eye	+0%	-7%	+4%	-1%	-2%	+8%	+5%

Table 1. +/+ : the original values of 2-day-old female flies; Δ *loco*/+ and act/*loco*: the percentages changed from the wild-type (+/+) and none-overexpressed control (act/+, (2)), respectively; +/*loco*Ri: the original values of 5-day-old male flies; arm/, r4/, repo/, and GMR/*loco*Ri: the percentages changed from the control (+/*loco*Ri). Data of each Gal4/+ flies (arm, r4, repo, and GMR/+) were similar to those of +/*loco*Ri flies (data not shown, (2)). **Lifespan** (mean life time), **stress resistance** (median survival time), **weight** (fresh weight per fly), and **nutrients** (amount per fresh fly weight) represent average values from the several independent experiments (**Bolded**: increased and decreased percentages, P-value < 0.05,). Glycogen amount of nutrients was not changed between the flies (data not shown, (2)).

Methods:

The experiment tested five unique genotypes for oxidative and starvation stress resistance. For the starvation test, groups of 100-adult male flies (per genotype and 20 flies per vial) were maintained in vials containing two filters wetted with 300 ml of water at 25°C. These flies were then starved and fly counts were performed at calculated intervals. For the oxidation test, 100 adult-male flies per genotype (20 flies per vial) were starved for an initial six hours, and then were maintained in vials containing two filters wetted with 300 ml of 20 mM paraquat in 5% sucrose solution at 25°C. Fly counts were also performed at specific intervals. The oxidation test functions as an indicator of whether the flies that have been hypothesized to show increased stress-resistance do actually contain higher levels of MnSOD (Manganese super-oxide dismutase), thereby providing them increased resistance to oxidative stress (an organism's ability to detoxify free radicals, which can damage and kill cells). The starvation test examines standard nutrient-deficiency. For the heat stress test, 100 adult flies (20 per vial) per genotype were maintained in standard cornmeal vials (lab-medium) at 37°C with 30% humidity. Standard interval counts were performed.

The flies themselves were obtained through the molecular process of sub-cloning. Sub-cloning is performed when a gene of interest (insert) is moved from a parent vector to a destination vector. In this experiment, particular inserts for specific genotypes were inserted into bacteria plasmids, which were then mini-prepped and confirmed by DNA sequencing to contain the desired insert. Finally, this insert was applied into the UAS Vector (Fly Expression Vector), which was then injected into *D. melanogaster* embryos. The F0 generation that resulted from these injections implemented our transgene (insert) into the reproductive aspect of their genome, but the F0 generation flies themselves did not actually implement our transgene into their own respective genomes. Therefore, these F0 flies were crossed with wild-type males or females depending on original gender, and a marker gene was applied to see which of the progeny generations contained our transgene, signified by the marker of changed eye color – from white eye to red eye. At the same time, this process also isogenized the mutant flies with the lab stock.

Through these methods, five genotypes were tested. These genotypes utilized a transgene in which the Tinman (Tin) promoter (heart-tissue specific) binds and activates the GAL4-UAS System, which then allows for RNAi (RNA interference) to create down-regulation of either Loco or Rpd3 in cardiovascular tissue. For example, the control group, *+TinG4*, was a fly mutant that contained the TinG4 transgene. However, this transgene was not activated because the GAL4 could not bond to the UAS (which activates gene transcription), and ultimately, there was no change in these *Drosophila*. However, by experimenting with this genotype, we can ensure that the presence of our transgene alone plays no role in increased stress resistance, although it may if it is activated. Similarly, the genotypes *LocoRi2/+* and *Rpd3Ri/+* also lack the Gal4-UAS system, and so those mutated flies contain the LocoRi2 or Rpd3Ri transgene, but do not have the innate ability to activate them. Conversely, the genotypes *LocoRi2/TinGal4* and *Rpd3Ri/TinGal4* contain the Tinman promoter, Gal4-UAS system, and the RNAi mechanism. Therefore, these flies will have either effective Loco down-regulation or Rpd3 down-regulation, respectively.

Summary:

A) Oxidation Test Results

In the oxidation stress test, the experiment showed that the *Rpd3Ri/TinGal4* (Rpd3 down-regulation) mutant clearly had increased stress resistance, demonstrating a median survival time of 59.9 hours (Figure 1). Calculations showed that this genotype of flies had a 29% increase of median oxidative stress resistance compared to the standard control group, *+TinG4* (median value 46.4 hours). Furthermore, the data showed that the *locoRi2/TinG4* genotype (Loco down-regulation) had no effect in oxidative stress resistance, based upon the fact that it had a median stress-resistance value of 36 hours, lesser than the control group *+TinG4* but greater than the *LocoRi2/+* mutant (Figure 1).

B) Starvation Test Results

The starvation stress test also showed similar results. The *Rpd3Ri/TinG4* mutant displayed the highest starvation stress resistance, with a median starvation resistance value of 67.2 days, greater than both the *Rpd3Ri/+* control group and the *+TinG4* control group (Figure 2). However, in this stress study, it must be noted that the difference, or percent increase, of the stress resistance of the *Rpd3Ri* mutant compared to the *+TinG4* control group is much smaller than the oxidative value stated previously. In this trial, the *Rpd3Ri* mutants only showed a 4% increase in starvation stress resistance. Additionally, the *LocoRi2/TinGal4* mutant also had no effect on stress resistance, similar to the results of oxidative stress test.

C) Heat Test Results

The heat test also showed similar results (Figure 3). The Rpd3Ri/TinG4 mutant displayed the greatest heat stress resistance, with a median survival time of 38.6 hours, greater than both the Rpd3Ri/+ and +/TinG4 control groups, and 39% increased heat stress resistance (compared to +/TinG4) (Figure 3). Additionally, the locoRi2/TinG4 mutant also displayed the second highest heat stress resistance, with a median survival point of 31.4 hours, and 13% increased heat-stress resistance (compared to +/TinG4) (Figure 3). This is interesting because the locoRi2/TinG4 mutant only showed an increase in heat stress resistance and not in oxidative or starvation stress resistance, as compared to the Rpd3Ri/TinG4 mutant, which had greater stress resistance in all three types of stress. These results could possibly show that down-regulation of Loco in the LocoRi2/TinG4 mutant could enhance only heat stress resistance and not oxidative or starvation stress resistance. However, further trials would have to be conducted.

D) Genetic-Based Increased Stress Resistance

From the results of this experiment, it seemed as if all of the mutants tested in the experiment had a high “background,” or were genetically predisposed to have high stress resistance. The flies utilized in all three stress experiments seemed to naturally be more inclined to have higher stress resistance compared to genotypes tested in previous studies (data not shown). Future Studies will have to confirm this result.

Figure 1:

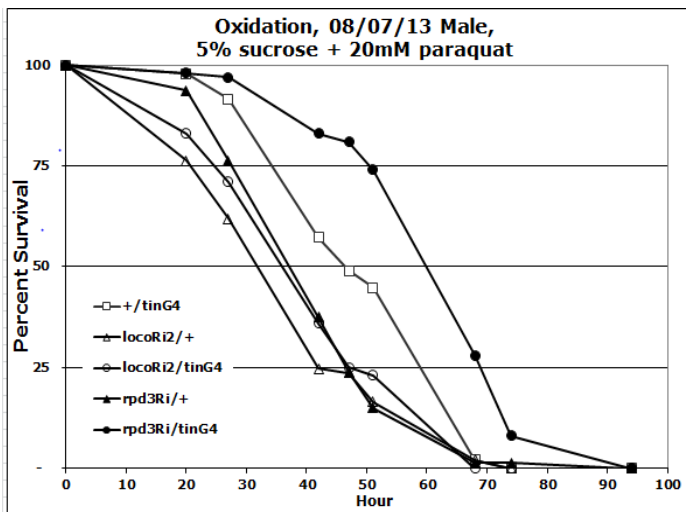


Figure 2:

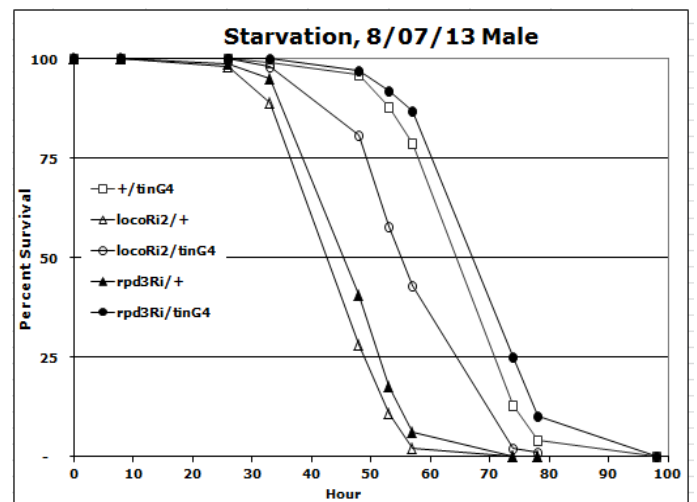
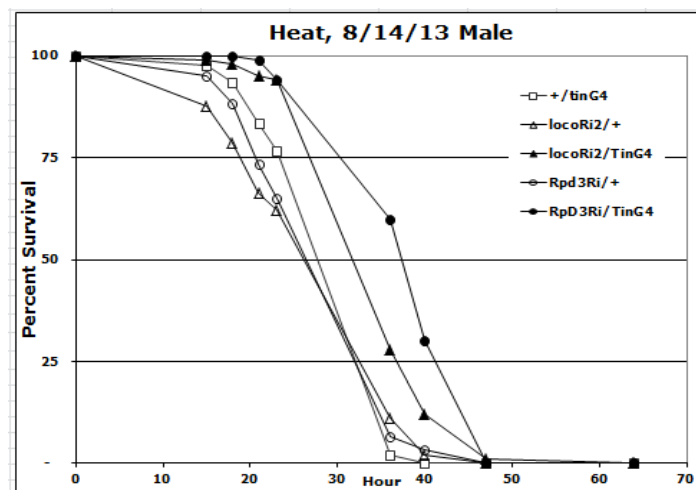


Figure 3:



Conclusion:

Heart tissue down-regulation of the Rpd3 protein in *D. melanogaster* correlates to increased oxidative, starvation, and heat stress resistance. Previous studies have interpreted that this increased stress resistance possibly may arise from extra fat (triglyceride) content that stems from the down-regulation of Loco-Rpd3 signaling. The results also showed that the down-regulation of Loco in heart tissue through the LocoRi2/TinG4 mutant may have no effect in oxidative or starvation stress resistance, but may have enhanced heat stress-resistance. Future studies could include performing further isogenization of our mutant flies (to normalize high “background” or natural stress resistance in +/TinManG4 mutant) and to use older flies (which would naturally have standard levels of stress resistance due to aging). The results of this trial could also be replicated in duplicate experiments, as to verify these results.

References:

Lin Y, Parikh H, Park Y. Loco signaling pathway in longevity. *Small GTPases* 2011; 2:158 - 161; <http://dx.doi.org/10.4161/sgtp.2.3.16390>.

Lin YR , Kim K, Yang Y, Ivessa A, Sadoshima J, Park Y. Regulation of longevity by regulator of G-protein signaling protein, Loco. *Aging Cell* 2011; 10: 438-447.

BRIAN D. KIM (NJMS 2016)

PROJECT TITLE: NOVEL POLYMER CONSTRUCTS
MENTOR: J. PATRICK O'CONNOR, PH.D, ASSOCIATE PROFESSOR
DEPARTMENT: BIOCHEMISTRY AND MOLECULAR BIOLOGY

Participation Description:

My involvement in the experiment was focused on the histomorphometry portion. After the animals were sacrificed, I took charge of preparing the samples for slide preparation. This involved numerous changes of ethanol, xylene, and methyl methacrylate to ensure that the bone samples were efficiently dehydrated for polymerization. After successful polymerization, I bisected the samples and created sections to be mounted onto slides for staining and analysis. After pictures were taken, image analysis software was used to obtain the bone areas of all the samples and subsequent statistical analyses were performed to check for significant differences in bone formation.

Introduction:

Bone segmental defects are caused by severe traumatic injuries such as crush, missile, and concussive injuries as well as resection of diseased tissue. Healing of large segmental defects is difficult and often requires use of bone grafting methods. The most widely and commonly accepted method of surgical intervention for segmental defects is the use of autologous bone grafts. This form of treatment is not without its complications though; complication rates are reported to be of up to 30%. The health risks and economic pressures associated with autologous or allogenic bone grafts mandate a more cost effective synthetic alternative that provides all the benefits of bone grafts.

A limiting factor when using biocompatible and osteoconductive scaffolds for bone regeneration is soft tissue infiltration that impedes the extent of bone regeneration. PolyAspirin[®], a poly(anhydride-ester) polymer (PA) that hydrolyzes to release salicylic acid, a non-steroidal anti-inflammatory drug, has been developed to allow for controlled, local delivery of salicylic acid. The polymer has been shown to be biocompatible and to reduce levels of inflammation with minimal bone resorption. It has also been shown that when PA is used in the form of a barrier to separate a bone defect from the overlying muscle and tissue, the PA barrier reduced cellular infiltration into the defect site, reduced apparent inflammation at the site but without reducing bone regeneration into the defect site.

Bone morphogenetic protein-2 (BMP-2) is a protein of the transforming growth factor - beta family that has been shown to have osteoinductive effects in rodent models via osteoblast differentiation. BMP-2 has undergone extensive clinical testing and is currently being used to treat severe tibia fractures and to promote spinal fusion. We believe that by combining the barrier functions of the PA polymer with BMP-2 to promote bone regeneration, we can promote bone regeneration within a defined defect space, so called guided bone regeneration, in order to heal large bone defects.

Objective:

In our experiment, we tested the effects of using BMP-2 and a PA barrier in a guided bone regeneration device for efficacy in healing of rabbit cranial defects. We hypothesized that the use of a PA barrier would decrease inflammation and cellular infiltration into the defect site while the BMP-2 would promote robust bone formation in the defect.

Methods:

46 New Zealand white rabbits were used for this experiment. 3 week and 8 week time points and 6 experimental subgroups were created for each time point (Table 1). A 4 cm incision was made through the skin and periosteum and retracted along the midline of the calvarium to expose the parietal bone. A hand-powered trephine drill was used to create a 1 cm defect in the right parietal bone posterior to the coronal suture and lateral of the sagittal suture. Rabbits received antibiotic treatment for 5 days post-surgery and pain was managed by application of a fentanyl patch for an additional 3 days post-surgery.

After the designated time point, scaffolds were harvested by using a hand saw to remove the top portion of the cranium and fixed in phosphate buffered formalin for one to two weeks. Samples were dehydrated in grades of ethanol (70%, 80%, 95%, 100%, 100%, 100%) and three changes of xylene. Grades of methylmethacrylate with differing amounts of benzoyl peroxide catalyst (0%, 1%, and 2% w/v) were used to prepare the samples for polymerization in poly(methylmethacrylate) with 2.0% benzoyl peroxide. Polymerized samples were sectioned along the midline of the scaffold and mounted onto plastic slides. Slides were ground to ~25 μm and stained with Stevenel's Blue and counter-stained with van Gieson's picrofuchsin. Image analysis was performed with Image Pro Premier (Media Cybernetics) 9.0.4.

Summary:

The data showed that BMP-2 does indeed enhance the amount of bone formed within the defect site at 8 weeks compared to controls (Figure 1). The addition of the PA barrier (fast/slow PA), however, did not affect the activity of BMP-2. It is interesting to note that at 3 weeks, the PCL scaffold with a PA barrier and BMP-2 had less bone formation than the PCL scaffold with only BMP-2, but by 8 weeks, bone growth for both groups had reached the same levels. This suggests that BMP-2 may be restoring any bone growth that the PA cap is inhibiting.

New bone growth patterns also appeared to be consistent throughout all the groups. Bone appeared to originate from the cortical bone and mainly grow inwards at the bottom (brain-side) of the scaffold close to the periosteum of the trephine defect by the end of 8 weeks (Figure 2). It was hypothesized that with use of a PA barrier would reduce tissue invasion into the defect site and so bone growth would be uniform in the defect site as the scaffold degraded.

Conclusion:

The addition of BMP-2 to a PCL scaffold shows promising results for a novel polymer in guided bone regeneration to allow for accelerated healing of bone when tested in a 1cm trephine rabbit calvarial defect.

Table 1. Experimental Design and Sample Sizes

Time Points	Guided Bone Regeneration Device Configurations					
	PCL Scaffold Only	PCL + CaSO ₄	PCL + CaSO ₄ + BMP-2	PCL + PA Barrier	PCL+ PA Barrier + CaSO ₄	PCL + PA Barrier + CaSO ₄ + BMP-2
3 weeks	3	6	4	3	3	4
8 weeks	3	6	4	3	3	4

Figures

3 Weeks vs. 8 Weeks Total Bone Area

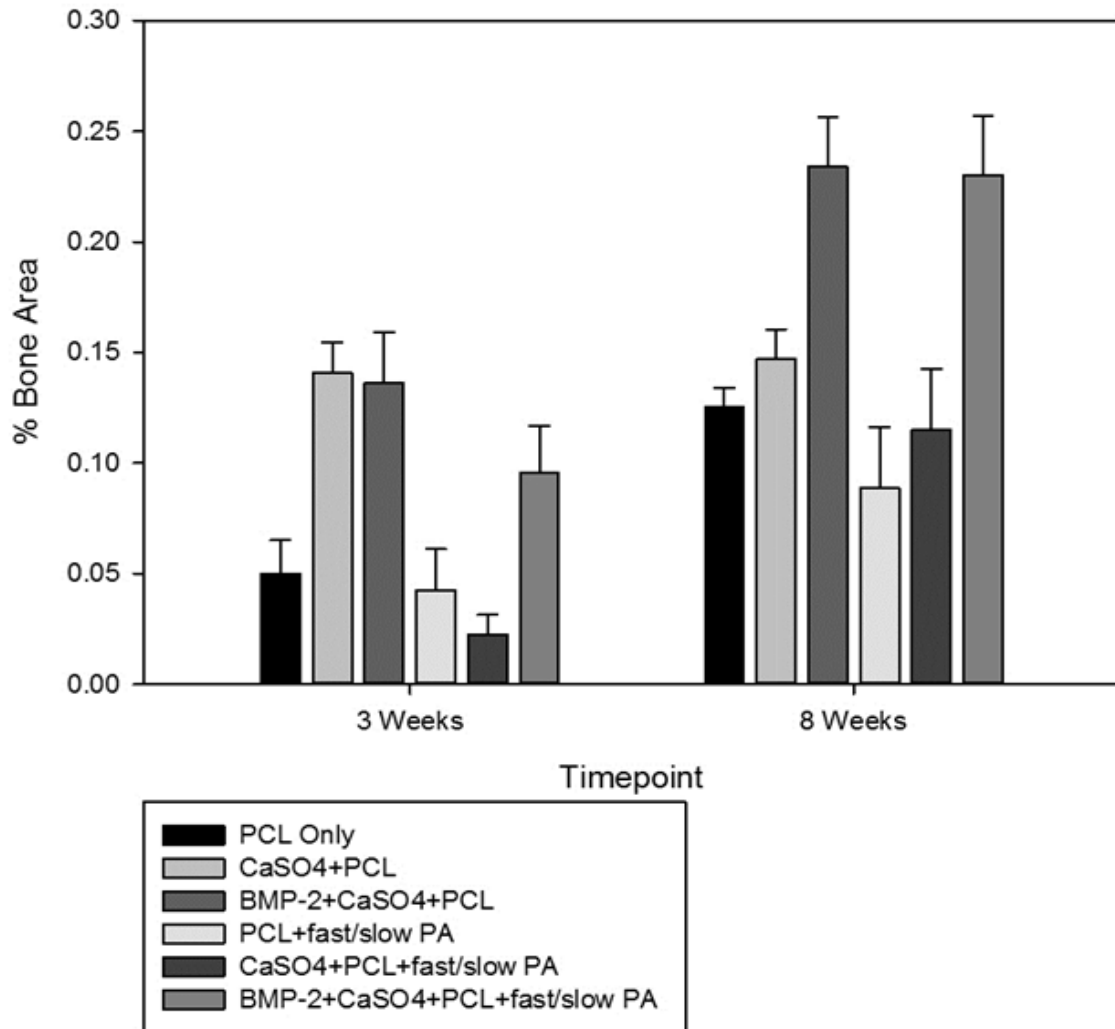


Figure 1: 3 Weeks vs. 8 Weeks Total Percent Bone Area

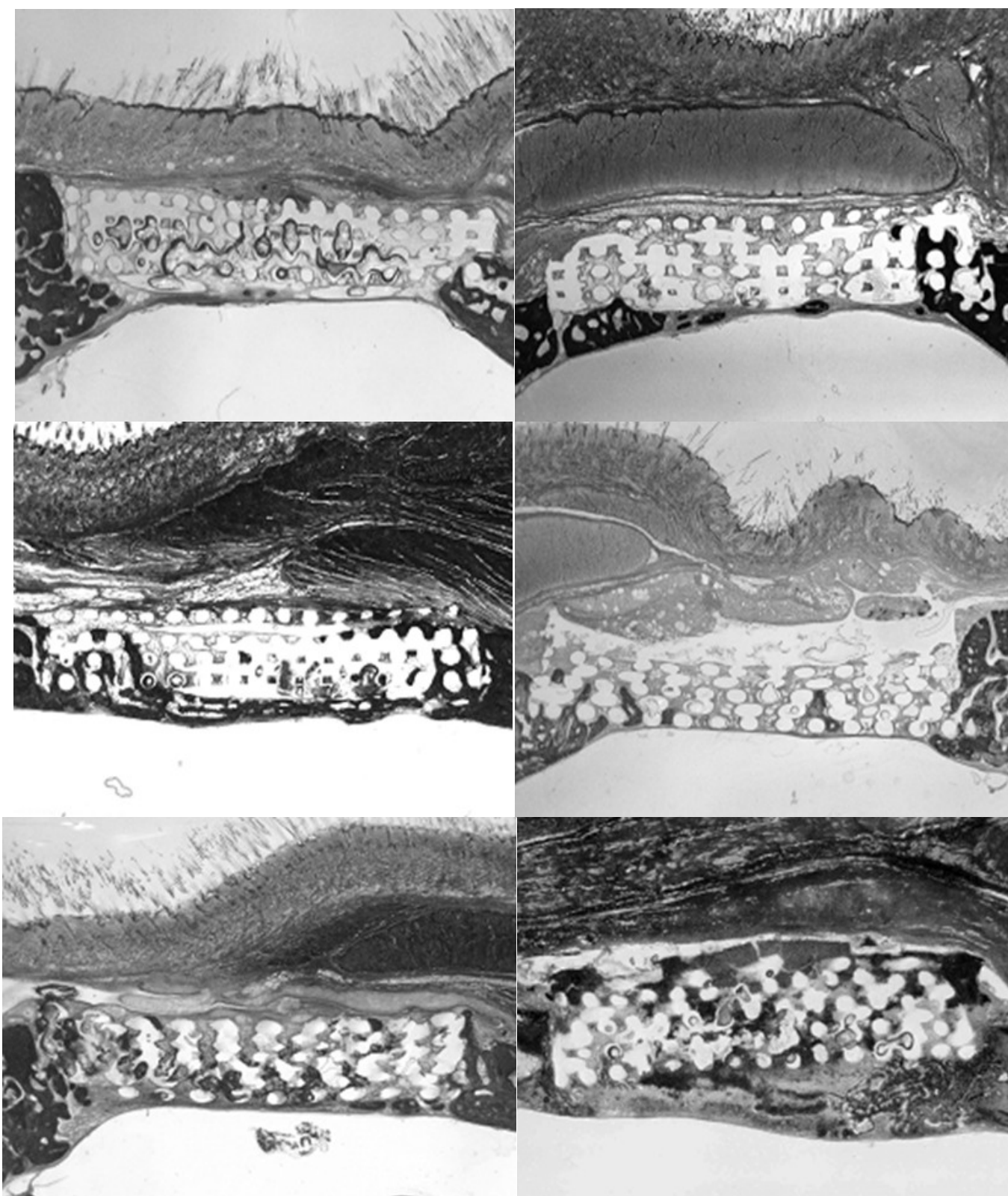


Figure 2: Representative Histological Images at 8 Weeks

From left to right: PCL Only; CaSO₄+PCL; BMP-2+CaSO₄+PCL; PCL+PA barrier; CaSO₄+PCL+PA barrier; BMP-2+CaSO₄+PCL+PA barrier

GHISLAINE CRUZ (ROWAN, 2014)

PROJECT TITLE: ENDOVASCULAR TECHNIQUES FOR TRAUMA PATIENTS WITH CEREBROVASCULAR INJURIES
MENTORS: CHIRAG D. GANDHI MD, ASSISTANT PROFESSOR
E. JESUS DUFFIS MD, ASSISTANT PROFESSOR
DEPARTMENT: NEUROLOGICAL SURGERY

Participation Description:

My participation in this research project mainly consisted of a review of the published literature. The purpose of the review was to summarize existing data on patients with traumatic injuries to the head and neck that were treated with endovascular techniques. There is currently no consensus on the optimal treatment of patients presenting with cerebrovascular injuries, the published literature consists of mainly just case series and case reports. Through the literature review, the use of endovascular techniques for trauma patients deemed to be successful with high rates of positive outcomes and a low rate of complications post-procedure. However, further review still needs to be done to establish endovascular techniques as the optimal management in such cases.

Objective:

Introduction:

The use of endovascular techniques in head and neck applications in the last two decades has continuously expanded . expanded. Endovascular techniques offer several advantages over traditional surgical procedures including their less invasive nature, lower mortality and morbidity rates, while surgical intervention has an associated high mortality rate of 20-40 % . The purpose of this study was to review diagnosis and treatment options for patients presenting with traumatic cerebrovascular injuries. .

Methods:

A systematic review of the medical literature was performed using Pubmed and Google Scholar to identify published literature documenting endovascular techniques performed on trauma patients with a variety of cerebrovascular injuries. A research index was created based on the published findings of the diagnosis and treatment of traumatic cerebrovascular injuries using endovascular techniques.

Summary:**Results:**

Cerebrovascular injuries in trauma patients were commonly confirmed using computerized tomographic angiography (CTA). Diagnostic and treatment options were determined based on the extent of the injuries of each individual patient. Endovascular techniques were applied to various types of injuries both after blunt and penetrating trauma including dissection, pseudoaneurysm formation, fistulas, and transections. Based on clinical presentations and diagnosis, patients were treated with stents, balloons, detachable coils, or liquid agents. Endovascular treatment is associated with a decrease in anesthetic requirement, blood loss and preservation of the parent artery. Patient outcomes were successful with complete occlusion or obliteration, with minimal or no complications.

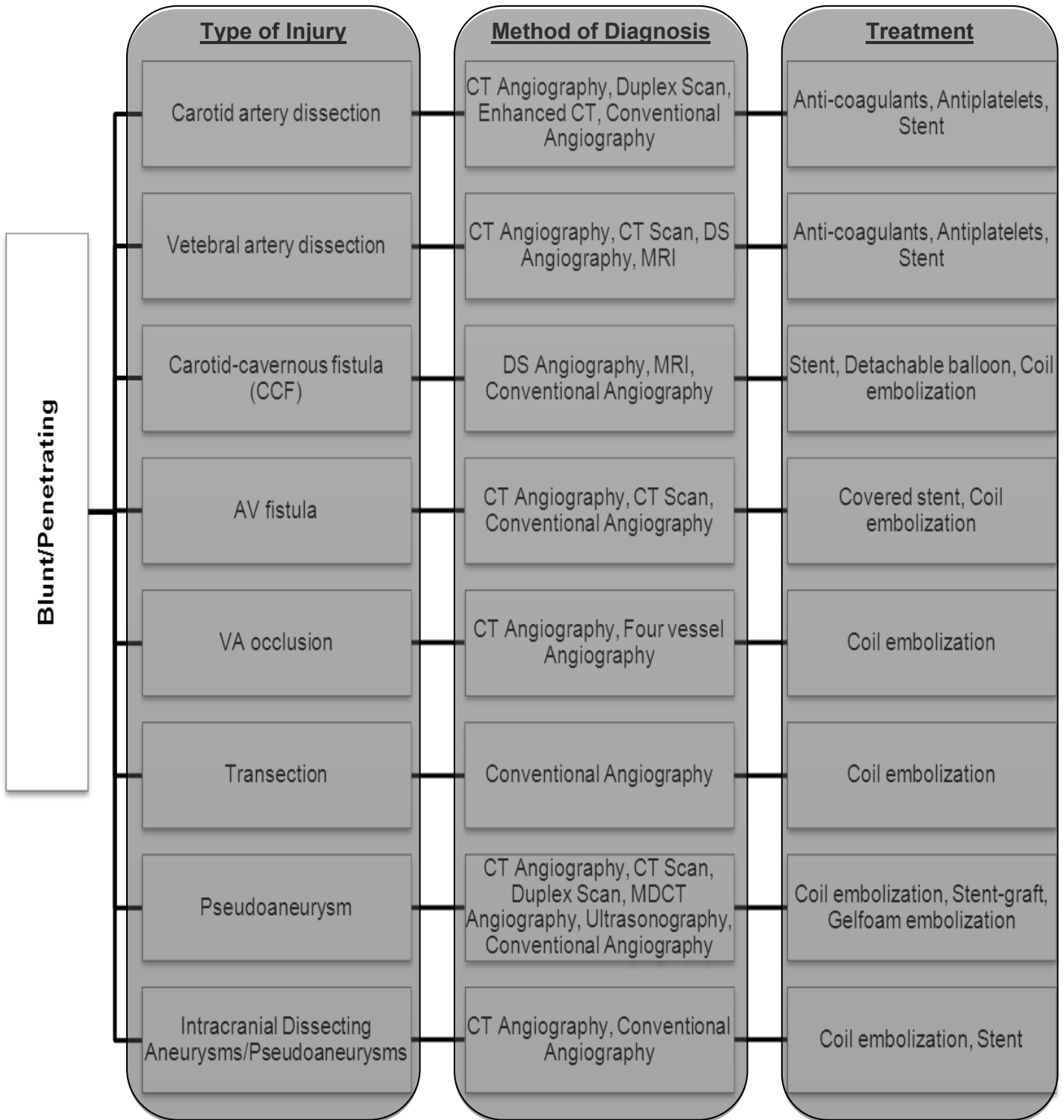


Figure 1. Research Index of patients that sustained blunt or penetrating injuries to the head and neck that were diagnosed and treated using endovascular techniques.

Conclusion:

Endovascular treatment of cerebrovascular trauma patients, with both blunt and penetrating injuries, has been shown to be effective. It has proven to be advantageous over surgical treatment and associated with positive outcomes. Consensus on the optimal management of patients with cerebrovascular injury due to trauma still needs to be established.

Reference:

- Witz M, Gepstein R, Paran H, Shnaker A, Lehmann J, Gryton I, et al. Endovascular treatment of an open cervical fracture with carotid artery tear. *European Spine Journal*. 2006;15(5):650-2.
- Seth R, Obuchowski A, Zoarski G. Endovascular repair of traumatic cervical internal carotid artery injuries: a safe and effective treatment option. *American Journal of Neuroradiology*. 2013;34(6):1219-26.
- Rao PM, Ivatury R, Sharma P, Vinzons AT, Nassoura Z, Stahl WM. Cervical vascular injuries: a trauma center experience. *SURGERY-SAINT LOUIS*. 1993;114:527-.
- Faure E, Canaud L, Marty-Ané C, Alric P. Endovascular Repair of a Left Common Carotid Pseudoaneurysm Associated With a Jugular–Carotid Fistula After Gunshot Wound to the Neck. *Annals of Vascular Surgery*. 2012.
- Mclaughlin DJ, Modic M, Masaryk T, Pratt D, Huang D. A New Approach to the Treatment of Penetrating Injuries to the Vertebral Artery A Case Report. *Vascular and Endovascular Surgery*. 1998;32(6):639-46.

Dr. Rogers' lab previously generated a mouse bearing a novel BMP2 allele (floxed) with loxP sites flanking the UCS. Once bred to a Cre recombinase expressing mouse, the floxed UCS will be deleted in the offspring. Our hypothesis is that UCS deletion, mediated by Cre expression, will increase BMP2 levels and alter ESC differentiation and transgenic pup viability. My aim was to test the differentiation of ESCs transfected with a flippase- or Cre recombinase-expressing vector, relative to non-transfected cells and cells transfected with only a luciferase-expressing vector (controls).

Methods:

ESCs containing the floxed allele and the selectable Neomycin resistance gene (Fig. 1) were cultured on Mitomycin C-treated mouse embryonic fibroblasts (MEFs), in Knockout DMEM (KO-DMEM) containing leukemia inhibitory factor (LIF). Growth on MEFs and LIF prevented ESC differentiation.

Transfection of the ESCs was achieved via electroporation (250 V, 250 μ F, 0.04 ms) with linearized pcDNA3.1Hygro (hygromycin resistance) and either pDIRE (Cre recombinase), pGKFLP (flippase), or pC β SLuc (luciferase). Hygromycin provided the selectable marker for those cells which took up DNA. The Cre recombinase-expressing plasmid allows for the removal of the sequence between the loxP sites. The flippase-expressing plasmid allows for the removal of the sequence between the FRT sites. The luciferase-expressing plasmid allows for a positive control quantification via a luciferase assay.

After electroporation, each of the three cell lines were rested for 2 days, with KO-DMEM media changed daily. They were then passaged into KO-DMEM containing LIF and hygromycin. The selection with hygromycin occurred for 7 days, with media changed daily. At the end of this week, the cells were rested again on KO-DMEM + LIF for 2 days, then were plated for differentiation. The cells were split either onto p150 Petri dishes for embryoid body culture with DMEM, or onto gelatinized 12 well plates for culture with α MEM or DMEM. The cells grown in the plates also received added osteogenic factors: β -glycerophosphate; ascorbic acid; calcitriol; and DMSO.

DNA was extracted from the cells using Dneasy (Qiagen) and run in a PCR with set 2 primers. PCR products electrophoresed on 3.5% Seakem 3:1 agarose gel, 70 V, 1 hour. After fixing the cells, the following stains were performed: benzidine HCl, Alcian blue, Alizarin red, methylene blue, and alkaline phosphatase. Embryoid bodies (EB) were visualized and counted via light microscopy, and methylene blue-stained plates were eluted and the amount of dye quantified via spectroscopy.

DAVID KAM (NJMS 2016)

**PROJECT TITLE: CONDITIONAL KNOCKOUT OF THE BMP2 ULTRA-CONSERVED
 REGULATORY ELEMENT**

MENTOR: MELISSA B. ROGERS, PH.D., ASSOCIATE PROFESSOR

DEPARTMENT: BIOCHEMISTRY AND MOLECULAR BIOLOGY

Participation Description:

Most of the theoretical planning was done by Dr. Rogers, while my participation involved running the experiments. I isolated and digested plasmids, electroporated the cells using those plasmids, collected the cells via centrifugation, isolated their DNA, performed genotyping PCRs, electrophoresed their products, and analyzed the gels using spectroscopy. At the same time, I gelatinized plates, on which I cultured two sets of cells, changed media daily, electroporated with the plasmids of interest, and fixed and stained embryoid bodies and plates with methylene blue, alkaline phosphatase, alizarin red, benzidine HCl, and Alcian blue. I assayed stain concentration using spectrophotometry and visualized the embryoid bodies using light microscopy. I also performed the data collection, tallying cells positive for staining or beating, as well as the statistical analysis (SD and SEM). I'd like to thank Dr. Rogers for all her support and hard work, as well as the other members of her lab for their assistance in teaching me techniques throughout this summer.

Objective:

To test the differentiation potential of the embryonic stem cells (ESCs) used to generate a mouse bearing a novel BMP2 allele, and to provide preliminary genotyping data.

Background:

Bone morphogenetic protein 2 (BMP2) is a potent morphogen that controls the normal differentiation of mesenchymal precursors into myocytes, adipocytes, chondrocytes, and osteoblasts. Additionally, BMP2 dysregulation in adults has been directly implicated in aberrant calcification: atherosclerotic lesions; calcified cardiac valves; and calcified medial arteries. A sequence in the 3'-untranslated region (3'-UTR) of the BMP2 mRNA is 73% identical between mammals and fishes. The evolutionary conservation of this ultra-conserved sequence (UCS), over the 450 million years since divergence, suggests a fundamental role in modulating development. 3'-UTR-mediated mechanisms that naturally restrain BMP2 synthesis are relevant to congenital heart and vasculature malformations as well as to adult vascular calcific diseases involving aberrant BMP2 levels and activity.

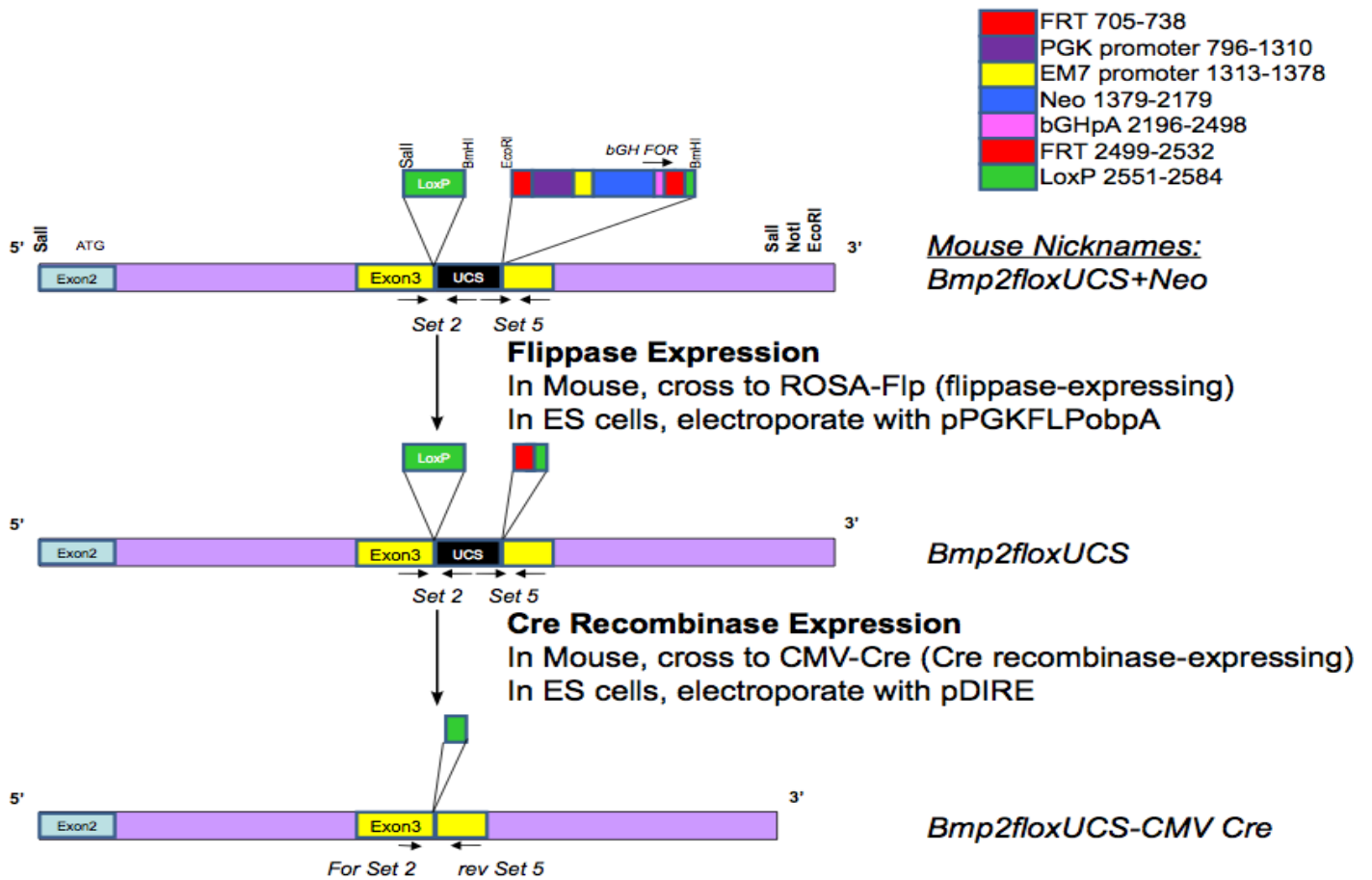


Figure 1: BMP2floXUCS genotypes and PCR primer locations.

Summary:

The three transfections produced three different alleles with three different 3'-UTRs. The cells transfected with FLP have a structure closest to the wildtype 3'-UTR. With the Neomycin resistance gene flipped out, all that remains in exon 3 of the flippase-expressing cells is a frt scar and the two loxP sites (Fig. 1, construct 2). In contrast, the non-transfected and Luc-transfected cells had 3'-UTRs with an inserted Neomycin coding sequence (Fig. 1, construct 1). The Cre-transfected cells lacked the Neo gene and the UCS (Fig. 1, construct 3). Quantification of methylene blue staining revealed an approximately 30% increase in cell density of the FLP cells, relative to Cre and Luc.

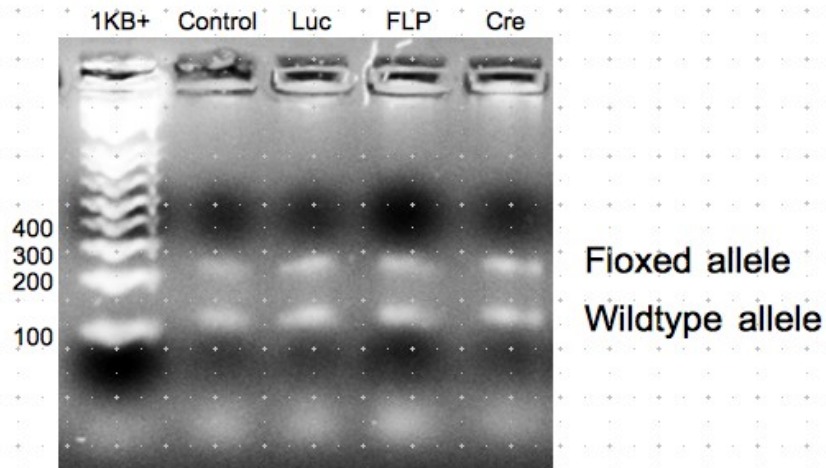


Figure 2: Genotyping of ESC DNA reveals the amplicons expected from the floxed allele and the wildtype allele .

This is the first attempt at transfecting these ESCs, and the transfection efficiency was relatively low (Fig. 2). As such, a small difference in activity was expected. However, the change in growth of the FLP-transfected cells appears to be significant, and warrants further study. The effect of the inserted Neo on the activity of the control and the Luc cells is similarly unpredictable.

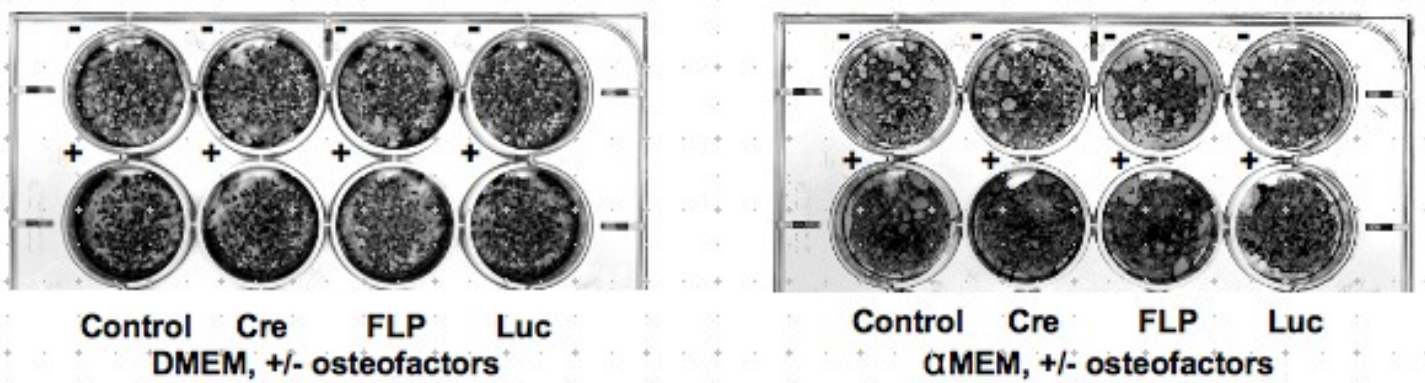


Figure. 3: Alizarin red staining for calcium deposition.

Cells cultured on gelatinized plates using DMEM or α MEM. Osteofactors or negative control solvents (H₂O + DMSO) added on day 5 after differentiation plating. Plates fixed with 70% ethanol and stained with 40 mM Alizarin red, pH 4.2, on day 10.

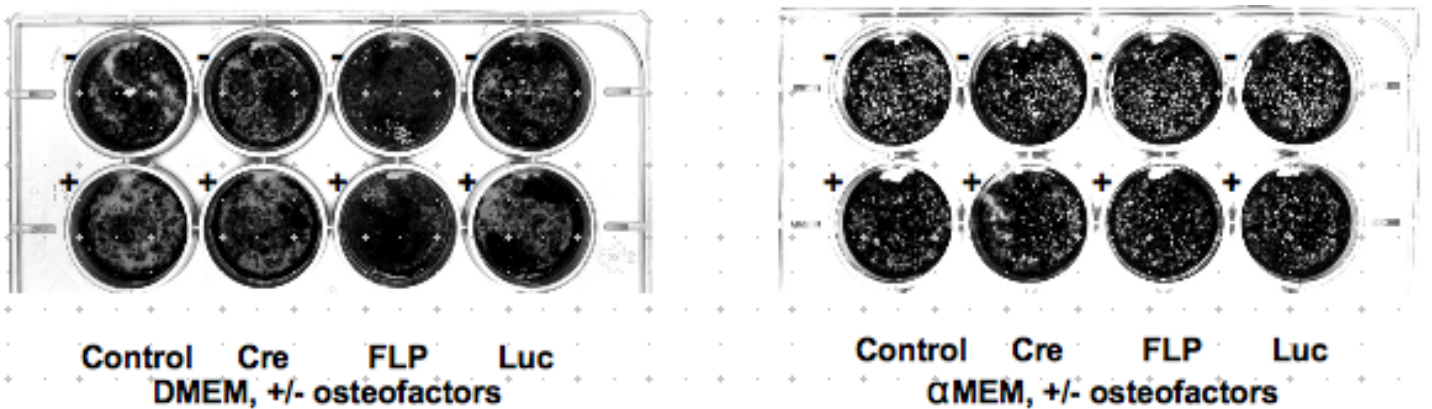


Figure. 4: Methylene blue staining for cell density.

Cells cultured on gelatinized plates using DMEM or α MEM. Osteofactors or negative control solvents added on day 5 after differentiation plating. Plates fixed with 100% methanol and stained with 1% methylene blue in 0.01 M borate buffer on day 15.

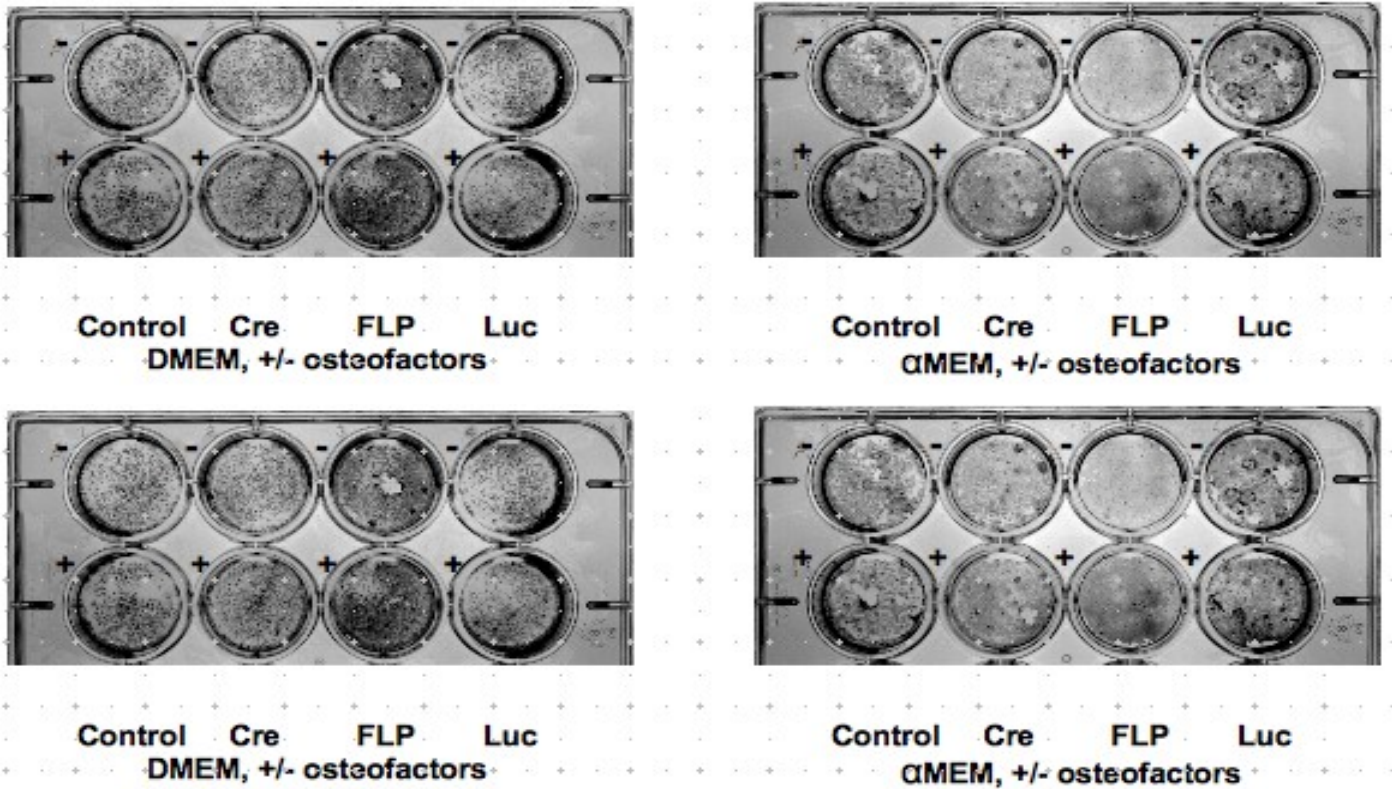


Figure. 5: Alkaline phosphatase staining (an early osteogenesis marker).

Cells cultured on gelatinized plates using DMEM or α MEM. Osteofactors or negative control solvents added on day 5 after differentiation plating. Plates fixed with 100% methanol and stained with BCIP / NBT (Promega) on day 10.

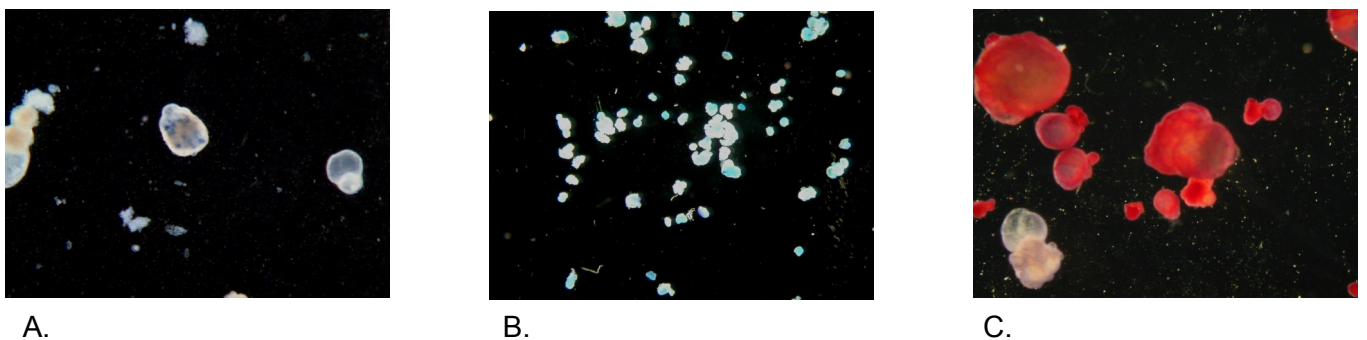


Figure. 6: Representative EB stains visualized via light microscopy.

A. Benzidine HCl stained erythroblast (blue). Sample fixed and stained with 0.2% benzidine HCl and 0.3% hydrogen peroxide in 3% acetic acid. Visualized via light microscopy.

B. Alcian blue stained chondrocytes (turquoise). Sample fixed in 10% neutral buffered formalin and stained with Alcian blue in 3:1 ethanol : glacial acetic acid.

Cell type %	Control	Luc	FLP	Cre
Beaters	1.97±0.53	1.38±0.63	1.88±0.52	1.82±0.71
Erythroblasts	0.56±0.56	0.56±0.56	0±0	0±0
Chondrocytes	19.9±4.86	7.61±2.21	11.27±2.07	16.76±4.95
Osteoblasts	64.09±19.66	75.64±15.98	71.29±10.4	67.22±10.11

Figure 7: Percent relative differentiation of the four cell types.

The live mice derived from these cell lines may be unaffected due to their heterozygosity. Concurrent in vivo studies are underway, with several generations of transgenic mice that require identification of the developmental effects of the UCS knockout. To date, 18 pups have been born from the chimeric founders mated to CMV-Cre. The gender of the pups had a ratio of 10 male : 8 female. This suggests that any potential phenotype did not affect development in a gender-specific manner. Genotyping of these pups is in process.

Conclusion:

The BMP2floxUCS transgene, in the presence of recombinase which knocks out the UCS, alters the differentiation and growth rate of embryonic stem cells.

Future Work:

Optimization of the electroporation and hygromycin selection is needed to increase transfection efficiency. Additional quantification of differentiation is required. For example, additional stains will be solubilized and measured by spectroscopy.

Inheritance of the floxed allele with a ubiquitously expressed Cre allele (e.g., CMV Cre) may be lethal or cause significant congenital malformations. If so, then mice bearing the floxed allele will be bred to mice expressing a Cre allele that can be induced by tamoxifen. Tamoxifen-dependent conditional deletion of the UCS will permit the identification of specific stages where UCS deletion is problematic.

HARDIK PARIKH (NJMS 2016)

PROJECT TITLE: DOWNREGULATION OF THE IMD PATHWAY ENHANCES STRESS RESISTANCE AND LONGEVITY IN DROSOPHILA MELANOGASTER
MENTOR: YONGKU PARK, PHD, ADJUNCT ASSISTANT PROFESSOR
DEPARTMENT: CELL BIOLOGY AND MOLECULAR MEDICINE

Objective:

Although non-genetic and genetic approaches have been used to understand the complex biological features of aging, the mechanisms of the eukaryotic aging process have not been clearly understood because of its global and epigenetic aspects. Various signaling pathways are involved in the regulatory mechanisms of aging, and these pathways are evolutionarily conserved in different species such as yeast, nematodes, fruit flies, and mammals. Preliminary studies have revealed that the Loco/RGS14 protein in a G-protein signaling pathway modulates stress resistance and lifespan in the several species.^{1,2} It has also been shown that Loco signaling modulates phosphorylation levels of Rpd3 protein (HDAC1, histone deacetylase 1). It is reported that reduced expression of Rpd3 protein extends fly lifespan³. However, it is not characterized how Rpd3/HDAC1 activity is regulated for the longevity mechanism.

The purpose of this experiment is to create expression vectors with genetically modified Rpd3 inserts that can induce varying levels of Rpd3/HDAC1 phosphorylation at the S419/S421 sites (wild type: SDS). The S419A/S421A Rpd3 protein mutation (ADA) will have no phosphorylation while the S419D/S421D (DDD) protein mutation will have hyper-phosphorylation. After these mutant flies have been created, future goals will be to test stress resistance and lifespan. Based on previous experiments regarding the loco gene, the hypothesis is that decreases in Rpd3/HDAC1 phosphorylation at S419/S421 will lead to extension of lifespan and stress resistance.

Methods:

Each type of Rpd3 insert (SDS, ADA, DDD) in a pAC vector was provided to our lab from a collaborator.

Polymerase chain reaction (PCR) was performed to amplify each of the inserts using Taq polymerase and the primers XhoI-Rpd3 and Rpd3-XbaI for 20 cycles.

A ligation reaction was performed to insert each Rpd3 insert into the pTOPO vector.

The pTOPO vector was then inserted into an electro-competent bacterial cell via electroporation at 1640 Volts.

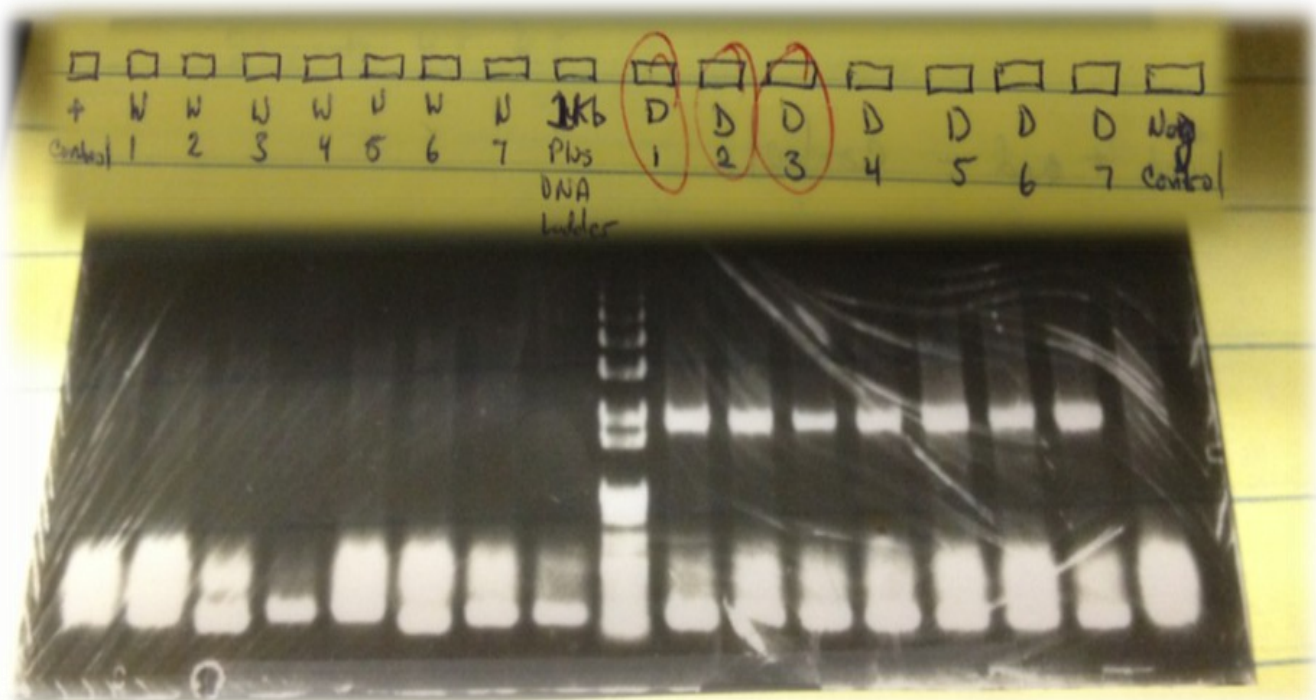
The bacteria were then spread on an agar plate that has been prepared with ampicillin and X-gal. It was grown at 37°C overnight.

Colony PCR was performed (using M13F and M13R primers) to determine if the insert could be found within the plasmid in the colonies.

Specific colonies were inoculated to grow the desired plasmid.
 The Qiagen QIA Spin Miniprep protocol was used to purify the plasmid.
 The plasmid was then sent out for gene sequencing (using primers sp6 and T7)
 Enzyme digestion was performed, using XbaI and XhoI of the pTOPO recombinant vector and the pUAST-attB expression vector.
 The Rpd3 insert was cut and eluted. A ligation reaction was performed at 25°C for 1 hour with the Rpd3 insert and the pUAST-attB expression vector.
 The recombinant pUAST-attB vector was then inserted into bacteria via electroporation.
 The bacteria were then spread onto plates as described previously, and incubated at 37° overnight.

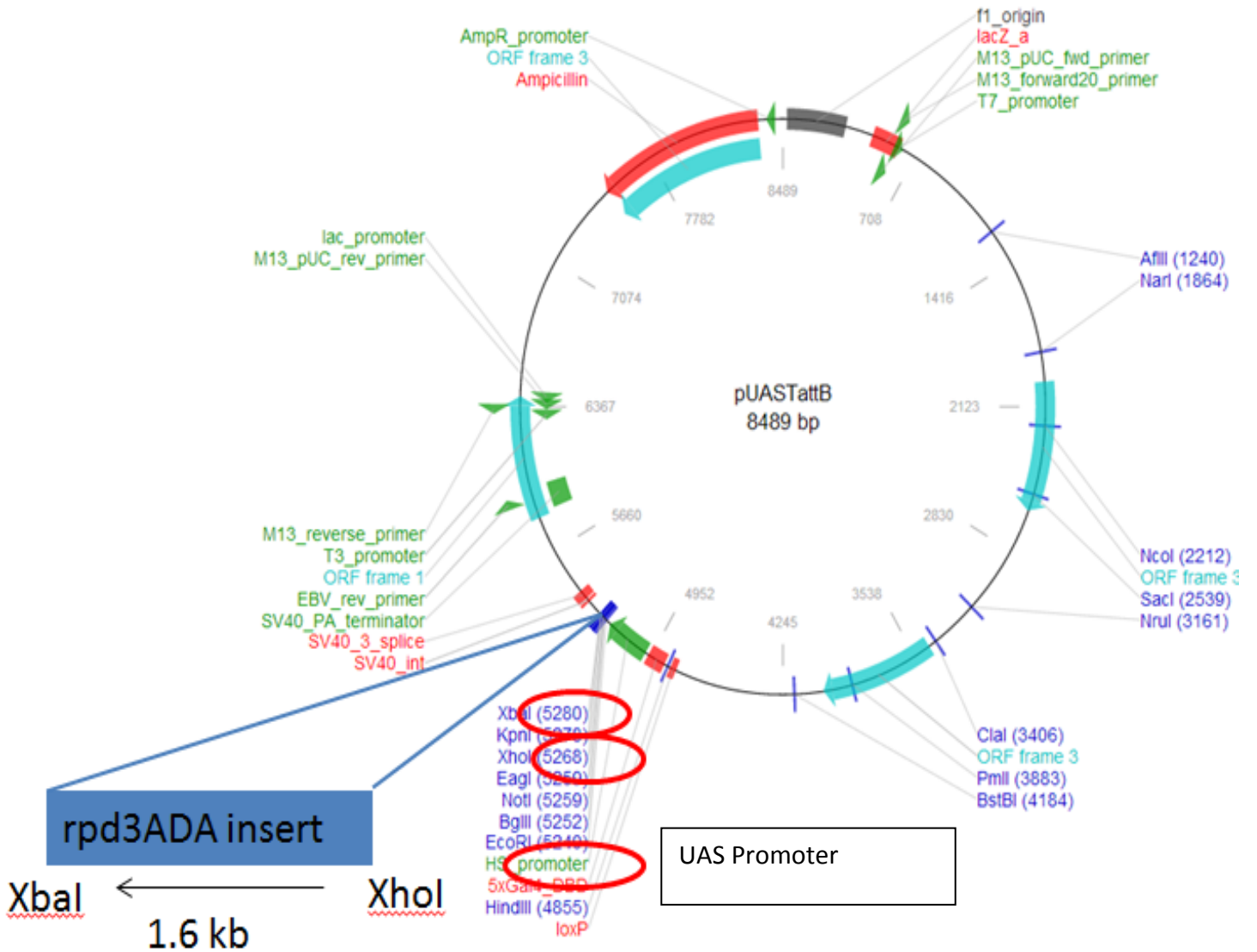
Results:

Figure 1: Colony PCR results of Rpd3-DDD showing the 1.8 kb expected product



The Rpd-DDD insert was actually 1.6 kb. We expected a 1.8 kb product, however, because the primers we used (M13F and M13R) amplified both the insert and the a small portion (~250 bp) of the vector. Using these primers allowed the colony PCR to be more specific and amplify only the fragment of interest.

Figure 2: Final Map of PUASt-attB expression vector with the 1.6 kb rpd3ADA insert shown



The UAS promoter region upstream of the Rpd3 gene allows it to be expressed in the PUASt-attB expression vector. This promoter is acted upon by the yeast transcription activator protein Gal4, which serves as a driver of gene transcription.

Conclusion:

All three of the Rpd3 inserts (SDS, ADA, DDD) were successfully transferred from the pAC vector into the pTOPO vector, and then from the pTOPO vector into the PUASt-attB expression vector. The reason why the insert had to be transferred is because pUASt-attB is an expression vector for *Drosophila melanogaster*. When the UAST recombination vector is injected into the fly and incorporated into the fly genome, the fly will express a red eye color instead of the white eye color. This phenotypic expression will allow us to sort and collect flies for longevity and stress resistance tests. This is the next stage of the experiment, which will be continued by Dr. Yongku Park and Zachary Hopp (graduate student). The results that they will generate will then prove whether no-phosphorylation/hyper-phosphorylation at the S419/S421 sites lead to changes in aging and lifespan.

References:

1. Lin YR, Parikh H and Park Y: Loco signaling pathway in longevity. *Small GTPases* 2: 158-161, 2011.
2. Lin YR, Kim K, Yang Y, Ivessa A, Sadoshima J and Park Y: Regulation of longevity by regulator of G-protein signaling protein, Loco. *Aging Cell* 10: 438-447, 2011.
3. Rogina B, Helfand SL and Frankel S: Longevity regulation by *Drosophila* Rpd3 deacetylase and caloric restriction. *Science* 298: 1745, 2002.

**DINA MOHAMED-ALY
(GETTYSBURG COLLEGE, 2011)**

PROJECT TITLE: FUNCTIONAL ANALYSIS OF CLEAVAGE AND POLYADENYLATION FACTORS IN CELL PROLIFERATION AND DIFFERENTIATION
MENTOR: BIN TIAN, PH.D., ASSOCIATE PROFESSOR
DEPARTMENT: BIOCHEMISTRY AND MOLECULAR BIOLOGY

Objective:

In this study, we aim to examine the functions of three cleavage and polyadenylation (C/P) factors which are involved in site choice in alternative polyadenylation (APA). Using mouse 3T3-L1 pre-adipocytes and C2C12 myoblasts, we have performed experiments to measure changes in cell migration, proliferation, and differentiation.

Methods:

All reagents and solutions purchased from Sigma Chemical Company unless otherwise noted.

Cell culture and differentiation

Late passage C2C12 cells were maintained in Dulbecco's Modified Eagles Medium (DMEM) supplemented with 10% Fetal Bovine Serum (FBS). C2C12 cells were induced to differentiate with 2% Horse Serum in DMEM. 3T3-L1 cells were maintained in DMEM supplemented with 10% Calf Serum. 3T3-L1 cells were differentiated to mature adipocytes for a maximum of 8 days with an IBMX/ dexamethazone/insulin medium containing 10% FBS. Insulin and 10% FBS/DMEM was replenished every two days. Small interfering RNAs (siRNAs) were used to knock down expression of three known C/P factors: *Cpsf5*, *Cstf3* (*Cstf-77*), and *Pabpc4*. Transfection was carried out using Lipofectamine 2000 (Invitrogen) using a half-dosage of RNA and Lipofectamine. C2C12 cells were plated with siRNA transfection reagent and after reaching confluence (~24h), were induced to differentiate for 2 days. RNA was harvested using TriZol (Invitrogen) and the Qiagen RNeasy Kit. An RT-qPCR was performed to check levels of differentiation markers and of each factor. Relative curves were normalized to GAPDH reporter.

Migration

C2C12 cells were plated with a seeding density of 6×10^4 cells and grown overnight. 3T3-L1 cells were seeded with a density of 6×10^4 cells and grown overnight. Wounds were made with a 200uL pipette tip in a straight line down each well. A 10uM dosage of cytosine arabinoside was used to inhibit proliferation. Photographs were taken at T=0h and T=18h and stitched using Microsoft Image Composite Editor™. Images of the same size and wound area were analyzed with ImageJ. Quantification of migration rate was done by measuring the difference in space after 18h relative to 0h returning a % migration.

Morphology, Proliferation, and Cell cycle by flow cytometry

Proliferating cells were monitored for morphology changes after 48 hours of siRNA transfection. After 48 hours of knock down, cells were counted and stained with propidium iodide for fluorescence-activated cell sorting (FACS) analysis to check cell cycle levels.

Summary:

Differentiation

Differentiation of wildtype C2C12 cells show that myotube formation is greatly increased by 4 days of differentiation (not pictured). Myoblast differentiation is characterized by an elongated appearance of myocytes and increased myotube formation. Accumulation of lipid droplets and a rounded cell appearance are characteristics of adipocytes as modeled by the Oil Red O staining of fully differentiated 3T3-L1 cells (not pictured). Data generated for C2C12 cells show that differentiation seems to be downregulated by *Pabpc4* KD after assessing three markers for myogenesis (Figure 1). Conversely, *Cstf3* KD appears to have overexpressed myogenic markers. *Cpsf5* KD data is inconsistent but shows a general trend of downregulation of differentiation reporter genes.

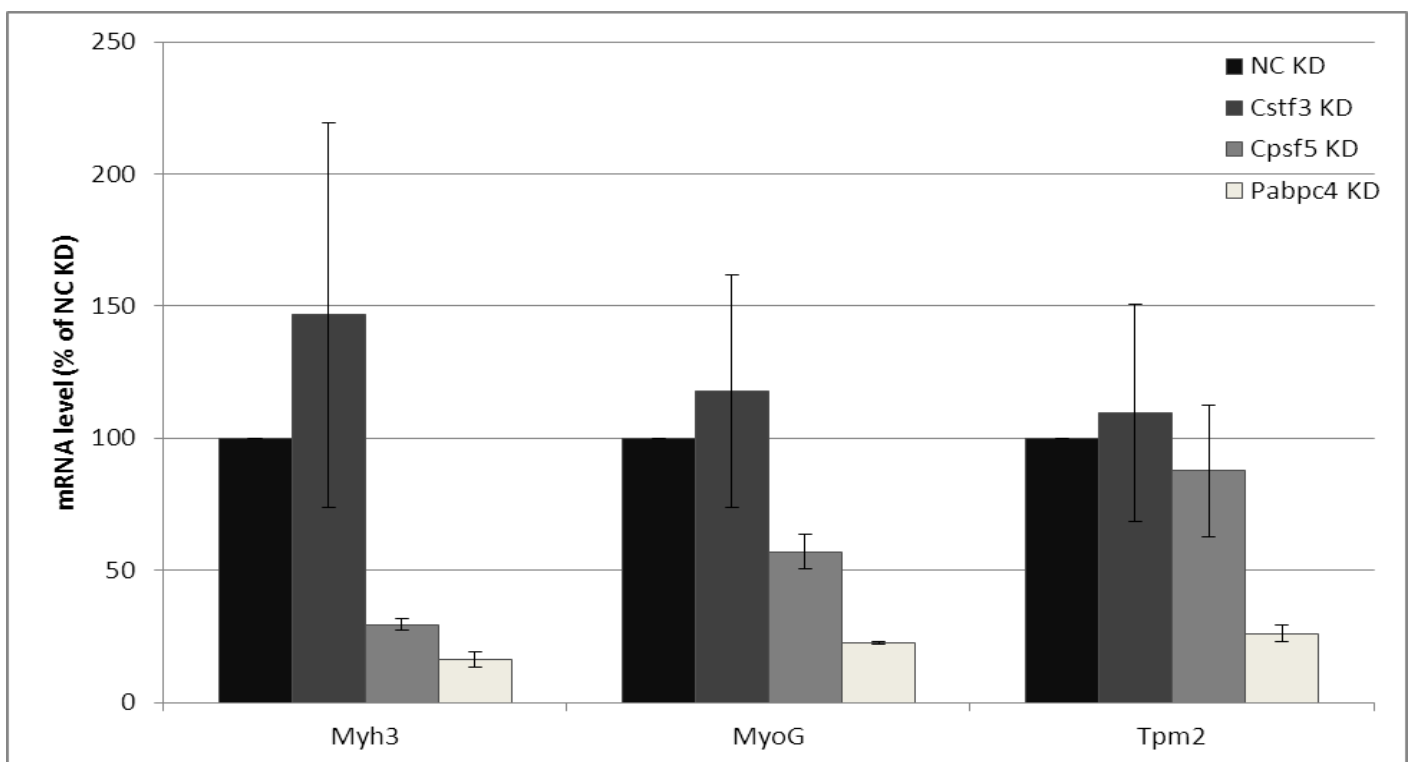


Figure 1. Expression of mRNA for markers associated with C2C12 differentiation: *Myh3*, *MyoG*, and *Tpm2*.

Migration

Preliminary wound healing data suggests that *Cstf3* and *Pabpc4* play a role in affecting cell motility and chemotaxis (Figure 2). From these results *Cstf3* appears to downregulate migration and *Pabpc4* appears to upregulate migration.

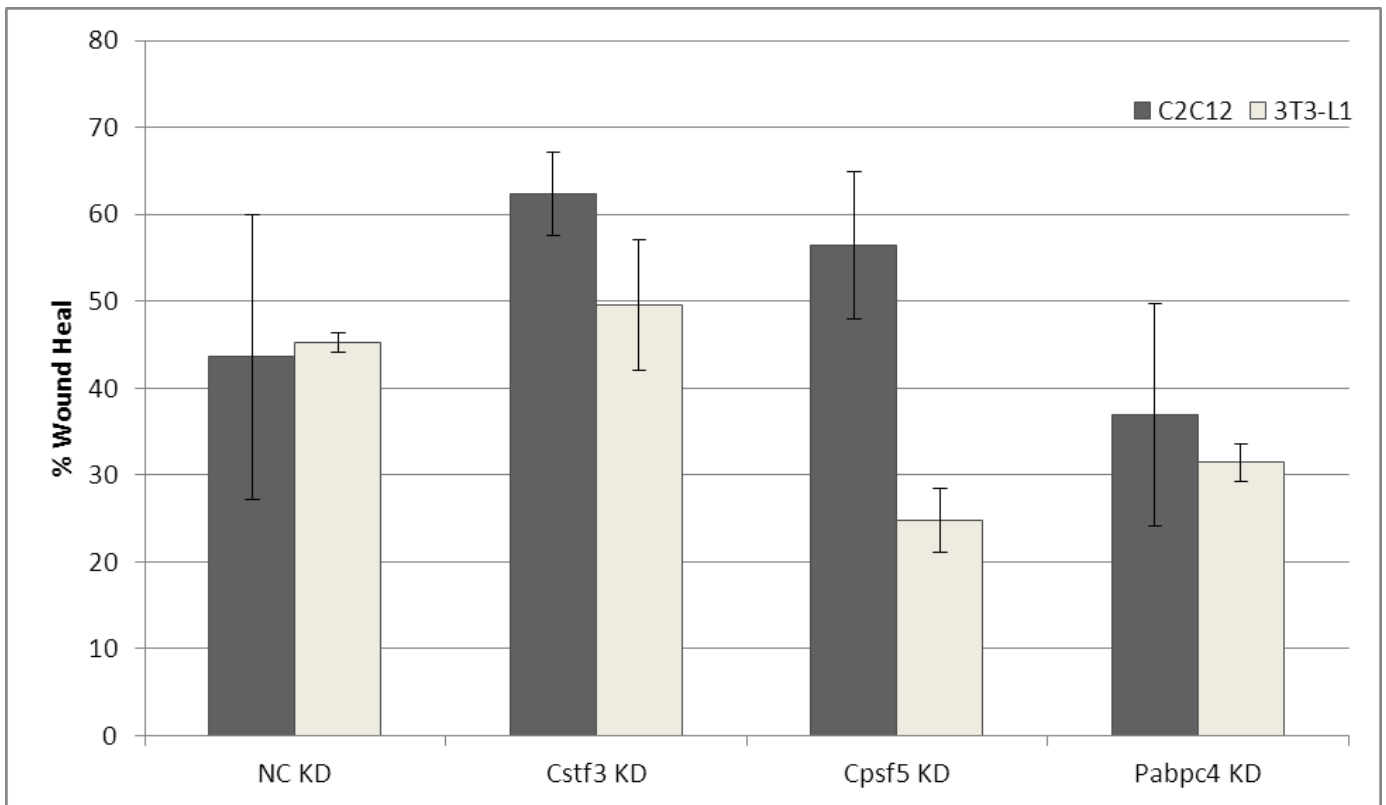


Figure 2. Analysis of % mean wound heal (\pm SD) of scratch assays in C2C12 and 3T3-L1 cells. (C2C12 n=2, 3T3-L1 n=1, p=0.440087, df=3)

Proliferation and Cell cycle by flow cytometry

Cell density was measured by counting the cells after 48 hours of transfection and results were as follows: *Pabpc4* KD displayed the lowest density overall. *Cstf3* KD also displayed a high density in C2C12 cells but it was lower than both Mock (non-transfected) and NC KD. Cell cycle analysis was performed using FACS data and relative stages of the cell cycle in C2C12 and 3T3-L1 were obtained (Figure 3). *Pabpc4* KD resulted in a lower density of cells but a higher percentage of cells in G2/M phase compared to controls. Other KDs did not display as much deviation from the cell cycle pattern of the controls.

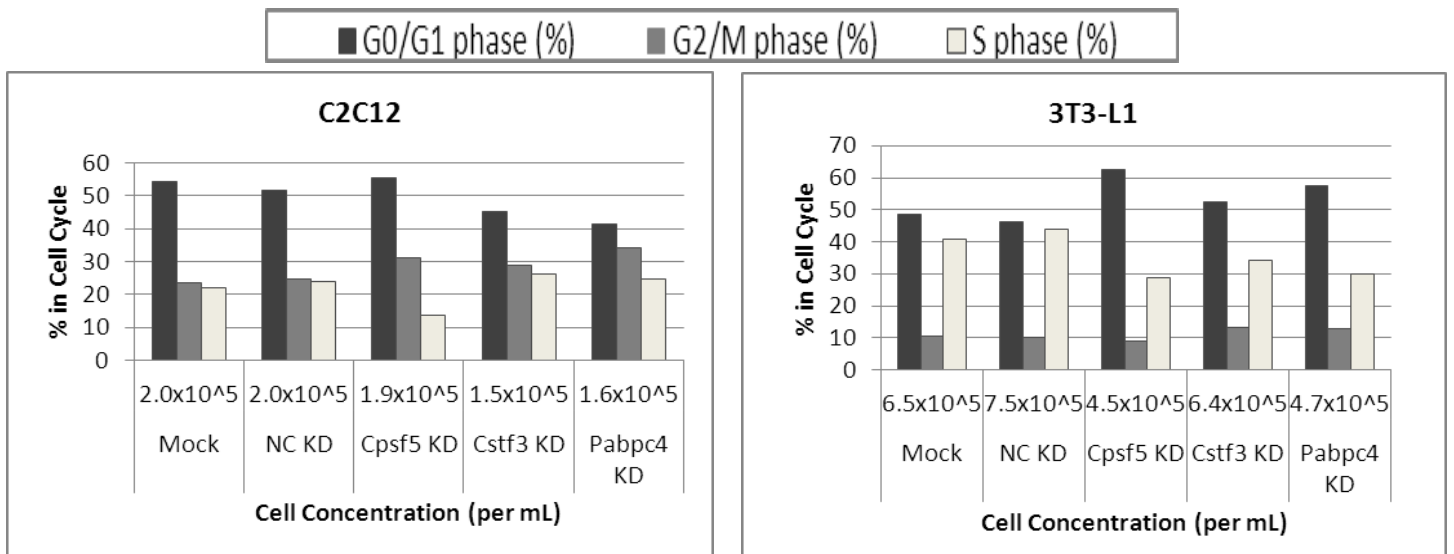


Figure 3. Proliferation and cell cycle quantification by flow cytometry. Levels of cell cycle arrest for C2C12 and 3T3-L1 cells, respectively.

Conclusion:

The findings of this study implicate *Pabpc4* as a highly involved factor in APA and its effects on the migration, proliferation, and differentiation in C2C12 and 3T3-L1 cells. As results show, migration was severely downregulated in *Pabpc4* KD cells suggesting that *Pabpc4* is an important element for chemotaxis and cellular motility. However, it appears that different C/P factors may have varied effects on differentiation factors adding to the complexity of APA.

This study has relevance for possible early detection of tumors or cancerous tissue from a specific set of genes affecting the proliferation and/or differentiation of the cells. Additionally, this study can also be used to further study the genetic mechanism by which cells, such as fat cells and muscle cells, commit to differentiation. The results of this preliminary work may indicate key players in the regulation of gene expression as they pertain to APA and provide interesting information about cells in which such mechanisms are deficit or overabundant.

Further experiments are needed to examine how different genes are affected by different knockdowns and to improve methods of siRNA transfection. Improved methods for executing and analyzing wound healing assays need to be considered for large-scale experiments if it is to be continued in the study. Further replications of the differentiation and proliferation (FACS) assays will be done with samples appearing to have interesting results and to measure significance. In addition, the testing of other potentially interesting C/P factors is under way and will eventually lead to large-scale knockdowns of several other C/P factors.

Summary of contributions:

In this experiment, I helped to maintain the cell lines, passaging them every few days, and seeding them to prepare them for assays. I mainly worked on the scratch/migration assays and developed techniques to perform and refine them. Dinghai Zheng helped to develop the quantification, which I later modified and used to analyze the images. Bei You mostly did the transfection experiments and the RNA extraction and qPCR experiments as well as FACS staining for analysis. I reviewed and interpreted all the data on my own but Bei You also helped me initially analyze the qPCR data.

JOHN PRENDERGASS (NJMS 2016)

PROJECT TITLE: GLUCONO-DELTA-LACTONE (GDL) POTENTIATES ANTICOAGULANT PROPERTIES OF LOW MOLECULAR WEIGHT HEPARIN

MENTOR: CHARLES SPILLERT, PH.D, ASSOCIATE PROFESSOR

DEPARTMENT: SURGERY

Following an introduction to the lab and the past work that has been conducted, Dr. Spillert and I set out to look into a novel area of GDL research. We decided to study the interplay between GDL, low molecular weight heparin, and whole blood. While there was certainly precedent set for the general design of the experiment, I was solely responsible for adjusting the techniques used to fit our specific project. The only machines used were the Sonoclot Coagulation Analyzer, to measure blood clotting times, and an incubator. Since this was my first time working in a lab, becoming proficient and consistent with the techniques involved several days of trial and error which culminated in a process finally producing consistent results. Dr. Spillert's outstanding advice combined with hours of my personal background reading helped us begin to understand the clinical potential for GDL, particularly its use in combination with heparin treatment.

OBJECTIVE:

Heparin is used to prevent blood clotting and reduce the tendency to form life-threatening clots. It is used primarily to treat clotting disorders, as well as to prevent clots from forming in patients undergoing kidney dialysis, blood transfusions, and vascular surgery. Heparin exists in two medically useful forms: Unfractionated heparin (UFH) and low molecular weight heparin (LMWH). LMWH was developed as a safer alternative to UFH and is capable of preventing some types of blood clots from growing and traveling to distant areas of the body. It is commonly employed postoperatively and used ubiquitously in hospitals. Low molecular weight heparin works by activating antithrombin, a protease inhibitor, which normally works late in the coagulation cascade to inhibit thrombin and mitigate the clotting process (2).

Glucono-delta-lactone (GDL) is a low molecular weight, non-toxic substance that is found naturally in the human body, in many food and cosmetic products, and is on the FDA's Generally Recognized As Safe (GRAS) list. Previous studies have shown that GDL has an anticoagulant effect in blood via antithrombin and anti-tissue factor properties (1). The goal of this experiment was to study whether GDL will have a synergistic effect with low molecular weight heparin to increase the clotting times of human citrated whole blood. Prolongation of the clotting times with GDL may prove clinically useful as an adjuvant to heparin therapy.

METHODS:

Two-day-old human citrated whole bloods (CWB) were obtained from University Hospital's clinical labs according to IRB Protocol. The bloods were pooled into aliquots containing different reagents (n=10) of approximately 500ul each. The aliquots were gently mixed and incubated for 15 minutes at 37°C to allow enough time for the reagents to react. Three hundred microliters of each aliquot was then added to cuvettes containing 32ul of 0.1M CaCl₂ (to initiate clotting). Final blood concentrations of reagents are listed below.

The heparin employed was Fragmin (dalteparin sodium) which is utilized for subcutaneous injection to reduce clotting tendency.

Experiment 1 (n=10)

0.85% saline (Control)

0.2 units LMWH final concentration

2mg/ml GDL

0.2 units LMWH + 2mg/ml GDL

Experiment 2 (n=10)

0.2 units LMWH + 0.5mg/ml GDL (Control)

0.2 units LMWH + 1mg/ml GDL

0.2 units LMWH + 2mg/ml GDL

The samples were analyzed using the Sonoclot Coagulation Analyzer (Sienco, Wheat Ridge, CO, USA), a mini-viscometer that is sensitive to fibrin clot formation (3). This instrument is currently FDA approved for evaluating human blood coagulation. The Sonoclot was used to measure activated clotting times of the samples.

Activated clotting times were compared using a statistical program to perform paired t-tests and repeated measure analysis of variance (ANOVA). Significance was defined as test values with $p < 0.05$.

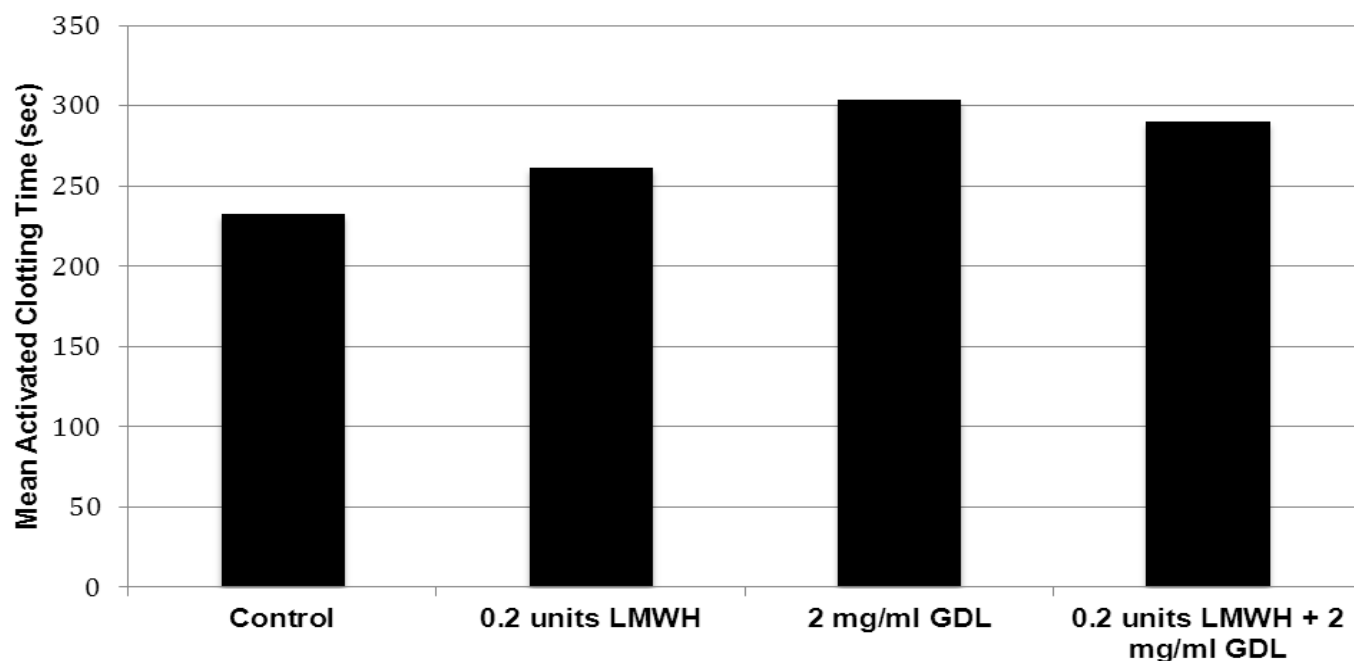
SUMMARY OF RESULTS:

Experiment 1 – What is the effect of GDL and heparin on blood coagulation?

Table 1: Effect of GDL and heparin on blood coagulation (N=10)

<u>Sample</u>	Mean activated clotting time (sec)
Control	232 ± 58
0.2 units LMWH	262 ± 65
2mg/ml GDL	304 ± 79
0.2 units LMWH + 2mg/ml GDL	290 ± 72

Effect of GDL and Heparin on Blood Clotting Time

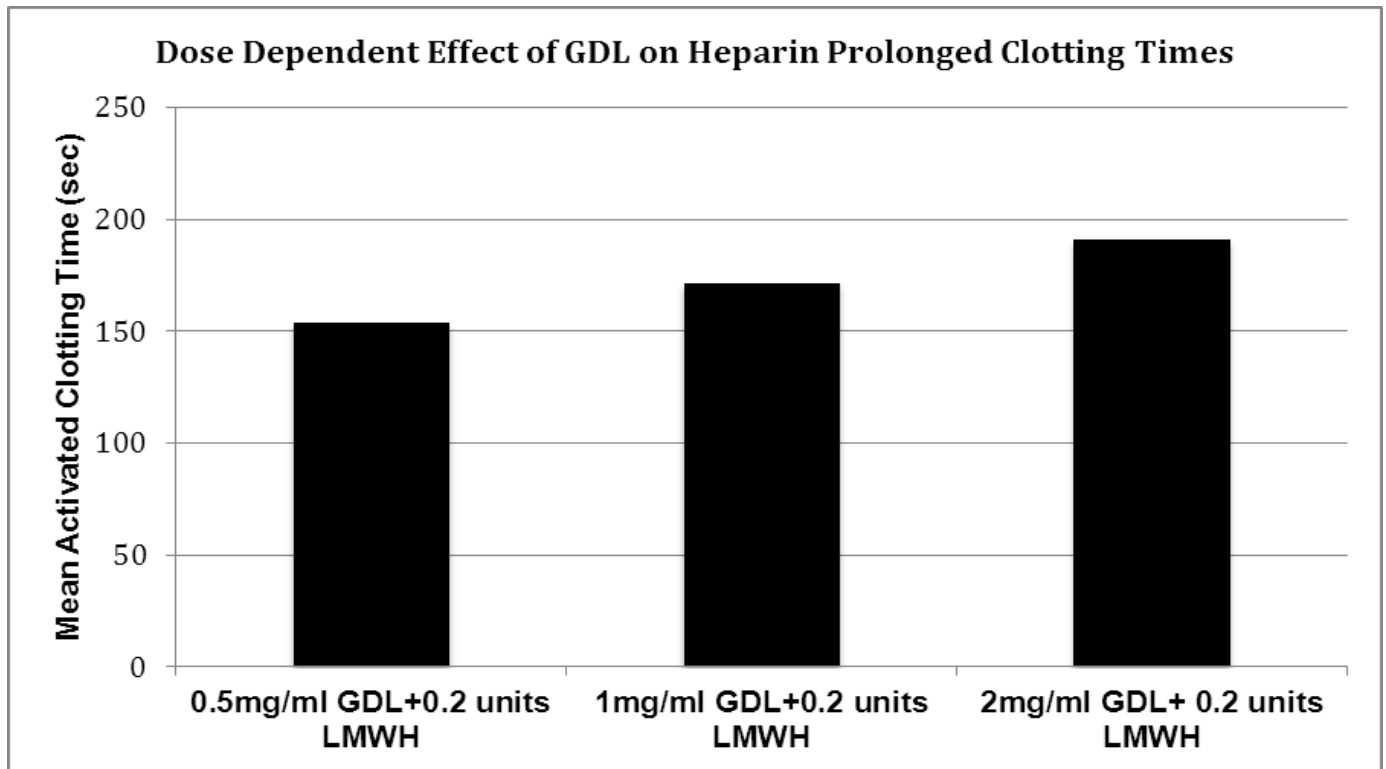


GDL administered at 2mg/ml final concentration combined with 0.2 units heparin was found to significantly lengthen the activated clotting times of citrated whole bloods compared to heparin alone. Two tailed t-tests indicated a significant increase in clotting time between samples treated with saline versus 0.2 units heparin ($p=0.008$), 2mg/ml GDL ($p=0.0002$), and 0.2 units heparin combined with 2mg/ml GDL ($p=0.004$).

Experiment 2 – Is there a dose-dependent effect of GDL on heparin during blood coagulation?

Table 2: Dose-dependent effect of GDL on heparin during blood coagulation (N=10)

<u>Sample</u>	Mean activated clotting time (sec)
0.5mg/ml GDL+0.2 units LMWH	154 ± 52
1mg/ml GDL+0.2 units LMWH	172 ± 60
2mg/ml GDL+ 0.2 units LMWH	191 ± 53



GDL was previously shown to significantly potentiate the anticoagulant properties of heparin on citrated whole blood. To determine whether this increase is dose dependent we tested three increasing concentrations of GDL on 0.2units LMWH in blood. Two tailed t-tests indicated a significant increase in activated clotting times between samples treated with 0.5mg/ml GDL combined with heparin in blood versus 1.0 mg/ml GDL ($p=0.026$), and versus 2.0 mg/ml GDL ($p=0.0005$). A significant increase was also detected between the 1.0mg/ml and 2.0mg/ml GDL aliquots ($p=0.021$)

CONCLUSION:

Low molecular weight heparin activates antithrombin, a protease inhibitor. Antithrombin normally works late in the coagulation cascade to inhibit thrombin and Factor Xa. Many anticoagulants are administered at this stage in the coagulation cascade when prothrombin is converted to thrombin. Previous experiments have suggested that GDL may function at this stage by antagonizing thrombin and tissue factor, the exact mechanism of which is still unknown. This mechanism allows GDL to attack more than one portion of the coagulation cascade, unlike LMWH. Because LMWH does not affect tissue factor, GDL has the potential to be a more versatile anticoagulant with a wider spectrum of anticoagulant effects.

This experiment showed that GDL is capable of potentiating the anticoagulant properties of low molecular weight heparin in a dose dependent manner. Further, under the conditions of this experiment we found that 2mg/ml GDL had a significantly prolonged clotting time compared to 0.2units of heparin. The mechanism is possibly based on GDL working synergistically with heparin to potentiate the inhibition of thrombin in addition to GDL inhibiting tissue factor. Patients with clotting disorders may one day be benefited from the addition of GDL to heparin therapy, resulting in a more comprehensive inhibition of the coagulant cascade. Future studies will investigate the steps of the coagulation cascade affected by GDL in combination with LMWH.

REFERENCES:

Ngo, G and Spillert CR. August 2012. Glucono-Delta-Lactone (GDL) Inhibits Tissue Factor and Thrombin During Human Blood Coagulation. Summer Reserarch Abstracts; 30-34

"Fragmin (Delteparin Sodium) Injection." *DailyMed*. Oct. 2010. Web. 17 July 2013. <<http://dailymed.nlm.nih.gov/>>.

Spiess BD, Spence RK, Shander A. 2006. Perioperative Coagulation Monitoring. *Perioperative Transfusion Medicine*. 2nd ed. Lippincott Williams & Wilkins; 349-356

KARAN GROVER, PHARMD (NJMS 2016)

PROJECT TITLE: THE EFFECT OF LATE NIGHT USAGE OF ELECTRONICS ON SCHOOL PERFORMANCE IN ADOLESCENTS
MENTOR: SUE MING, MD, PH.D, PROFESSOR,
DEPARTMENT: NEUROSCIENCES

Participation:

Karan Grover conducted the literature review, came up with the concept for the study, performed part of the statistical analysis, and authored the presentation, abstract, and the manuscript.

Background:

Instant messaging and video gaming in young people increased from 6.5 hours to 7.5 hours between 2004 and 2009. The late night usage of technology may compromise the sleep schedule and school performance of adolescents. Previous studies have shown that mobile phone usage after lights out is associated with significantly increased risk of feeling tired, however effects on school performance remain unstudied.

Objectives:

This study aimed to determine whether an association between video gaming/messaging and reported school performance existed. The association between video gaming/messaging on a constellation of daytime sluggishness symptoms (naps, perception of inadequate sleep, daytime sleepiness) was also evaluated.

Methods:

Anonymous questionnaires were completed voluntarily by 9th-12th graders at three high schools in New Jersey. The questionnaire consisted of 16 categories assessing school day and weekend sleep schedules; sleep duration; daytime sluggishness symptoms; messaging habits; video game usage; and self-reported academic performance. Logistic regression and odds ratios were applied for statistical analysis.

Results:

2,165 students completed the survey of which 2,140 were included in the analysis. Academic Performance: There were no significant differences in reported school performance between students messaging and not messaging prior to lights out. Students messaging after lights out, however, reported poorer grades compared to students not messaging after lights out ($P=0.04$). Timing of messaging was important: students messaging both before and after midnight reported poorer performance than those messaging only before midnight ($P<0.0001$). Students who denied playing video games on school days reported better performance than students playing < 30 minutes ($P=0.04$), and > 2 hours ($P<0.0001$). Daytime Sluggishness: Prior to lights out, students denying messaging were less likely to report daytime sluggishness than students messaging 30-60 minutes ($P<0.0001$), 1-2 hours ($P=0.01$), and > 2 hours ($P=0.003$). After lights out, students denying messaging were less likely to report daytime sluggishness than students messaging < 30 minutes ($P=0.01$), 30-60 minutes ($P<0.0001$), 1-2 hours ($P=0.001$), or > 2 hours ($P=0.01$). Students messaging both before and after midnight were more likely to report daytime sluggishness than students messaging before midnight ($P=0.002$). Though students denying both messaging and video gaming tended to report less daytime sluggishness than those who did message and/or play video games, the overall difference was not significant.

Conclusions:

Extended periods of messaging are associated with poorer school performance and increased risk of daytime sluggishness, especially messaging after lights out. Video gaming is associated with poorer school performance but not necessarily daytime sluggishness.

KARAN GROVER, PHARMD (NJMS 2016)

PROJECT TITLE: THE EFFECT OF LATE NIGHT USAGE OF ELECTRONICS ON SCHOOL PERFORMANCE IN ADOLESCENTS
MENTOR: SUE MING, MD, PH.D, PROFESSOR
DEPARTMENT: NEUROSCIENCES

Participation:

Karan Grover conducted the literature review, came up with the concept for the study, performed part of the statistical analysis, and authored the presentation, abstract, and the manuscript.

Background:

Adolescents have delayed circadian rhythms and tend to sleep and rise late. It is perceived that early morning sleep (equivalent to REM sleep) is important for learning and memory. However, high school start times mandate early rising, which may put adolescents at a disadvantage for daytime performance and sleepiness. This study analyzes whether rising time alone impacts school performance.

Objectives:

1) To determine whether there is an association between early rise time and self-reported school performance, a constellation of daytime sluggishness symptoms (after school naps, perception of inadequate sleep, daytime sleepiness) while sleep duration is controlled; 2) To measure the effect of changes, if any, in sleep schedule since 5th grade and 7th grade impacts on school performance.

Methods:

Anonymous questionnaires were completed voluntarily by 9th-12th graders at five high schools in New Jersey. The questionnaire consisted of 16 categories assessing school day and weekend sleep schedules; sleep duration; daytime sluggishness symptoms; sleep schedule changes since 5th and 7th grades; and current, 5th, 7th grade school performance. Logistic regression and odds ratios were applied for statistical analysis. All analyses were controlled for sleep duration.

Results:

3,894 students completed the survey. Contradictory to the authors' hypotheses, when sleep duration is similar, students with earlier rise times on school days were more likely to report a better performance ($P=0.001$). Additionally, the authors observed that in students getting less than 7.5 hours of sleep on school days, students rising before 6AM were less likely to experience daytime sluggishness symptoms than those rising 6-6:30AM ($P=0.02$), 6:30-7AM ($P=0.047$), and 7-7:30AM ($P=0.001$). Those with at least 7.5 hours of sleep, rising before 6AM were more likely to experience daytime sluggishness symptoms than those rising 6-6:30AM ($P=0.01$), 6:30-7AM ($P=0.003$), and 7-7:30AM ($P=0.01$). Changes in sleep schedule from prior grades were not associated with changes in self-reported school performance.

Conclusion:

When sleep duration is controlled, rising time is not important for daytime performance and sleepiness in this cohort of adolescents.

YOON HO PARK (NJMS 2016)
PETER SHAROUPIM (NJMS 2016)

**PROJECT TITLE: STUDY OF GANGIOSIDE DEFICIENCY IN PARKINSON’S DISEASE
REGARDING COGNITIVE IMPAIRMENTS**

MENTOR: ROBERT LEDEEN, PH.D, PROFESSOR

DEPARTMENT: NEUROLOGY & NEUROSCIENCES



Participation Description:

Peter and Yoon Ho were involved in deciding the parameters of the T-maze experiment, including retention time and resting time. We performed all T-maze experiments and were responsible for collection, interpretation, and statistical analysis of the experimental results. We performed 23 trials on each mouse. Peter, Yoon Ho, and Victoria Nguyen (undergraduate) contributed equally to the project.

Objective:

Parkinson’s disease (PD) is one of the most common late-onset neurodegenerative diseases. It is primarily characterized by motor impairments, such as tremor, bradykinesia, and rigidity. However, it also has a wide variety of non-motor symptoms, including cognitive disturbances and autonomic dysfunctions, which can sometimes precede the hallmark motor symptoms of PD. Mice lacking the GM1 family of gangliosides is being explored as a model for PD. This model, which is created by knocking out gene B4galnt1, shows many characteristic of PD including motor dysfunction that worsens with age, histological findings of Lewy body-like formations, and loss of dopamine in the striatum [1,2]. The objective of this experiment is to explore any short-term spatial memory deficits in the mice model lacking GM1 gangliosides. The hypothesis is that the mouse model will have significantly lower spatial memory compared to age-matched wild types. Furthermore, supplementation of GM1-deficient mice with LIGA-20 – a GM1 analog that is able to pass through the blood-brain barrier – is expected to increase their spatial memory.

Methods:

Mice

Age-matched littermates, aged 25-61 weeks, were used for all behavioral experiments. Genotypes used were B4galnt1 (+/+) (WT), B4galnt1 (+/-) (HT), B4galnt1 (-/-) (KO). Males (n=18) and females (n=41) of all genotypes were used for the experiments. Mice were divided into two groups based on age: “Young” group (n=27) aged 25-43 weeks and “Old” group (n=32) aged 46-61 weeks.

Genotype count of each group is as follows:

“Young”: WT (n=5), HT (n=18), KO (n=4)

“Old”: WT (n=4), HT (n=26), KO (n=2)

Memory Test (T-maze Test)

T-maze forced-trial spontaneous alternation test was conducted on mice of all genotypes to test for differences in spatial memory capacity [3] (Fig. 1). The mice were initially placed in the center start path where they were forced to enter one of the two arms (left or right) determined

by the experimenter, and then kept there for 60 seconds. The mice were then placed in an isolated, stimulus-free cage for a 60 second retention interval. After the retention interval, the mice were placed back into the starting path, where they were able to freely choose between the initially forced arm or the novel arm. A normal mouse's instinct is to choose the new arm for exploration, provided he retains the memory [3]. The exploration of the initial arm was recorded as incorrect and the exploration of the novel arm was recorded as correct.

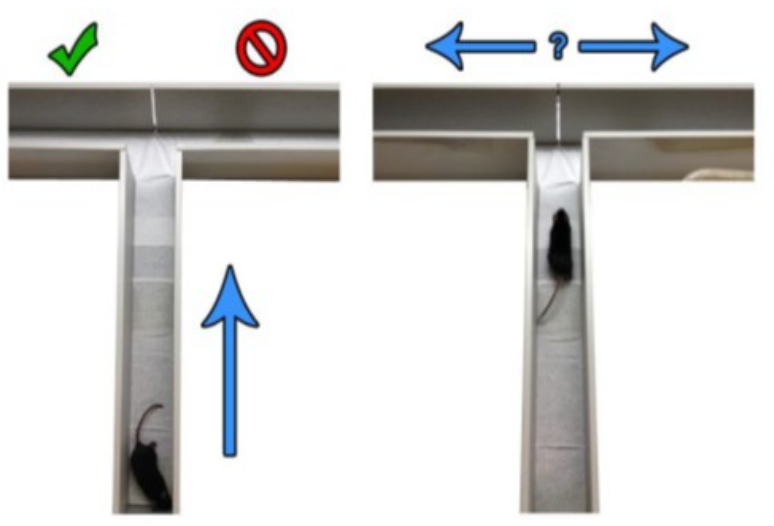


Figure 1. T-maze procedure testing spontaneous alternation.

LIGA-20 Injection

Selected mice from both “Young” and “Old” group were intraperitoneally injected with 0.10-0.15 mL of LIGA-20 to be supplemented with GM1. The T-maze tests were repeated for all genotypes after injection to determine any changed in spatial memory capacity.

Genotype count of mice injected with LIGA-20 is as follows:

“Young”: HT (n=13), KO (n=4)

“Old”: WT (n=4), HT (n=26), KO (n=2)

Summary:

The following data are the average of the rates of spontaneous alternation of all the mice without any treatments with respect to their genotype. The lowest possible rate would be 0.5, which describes a random 50-50 choice in the T-maze.

Note: p-values from Student's t-test have not yet been calculated due to the complexity of the data (multiple trials for each mouse). This will be done in due course by a statistician.

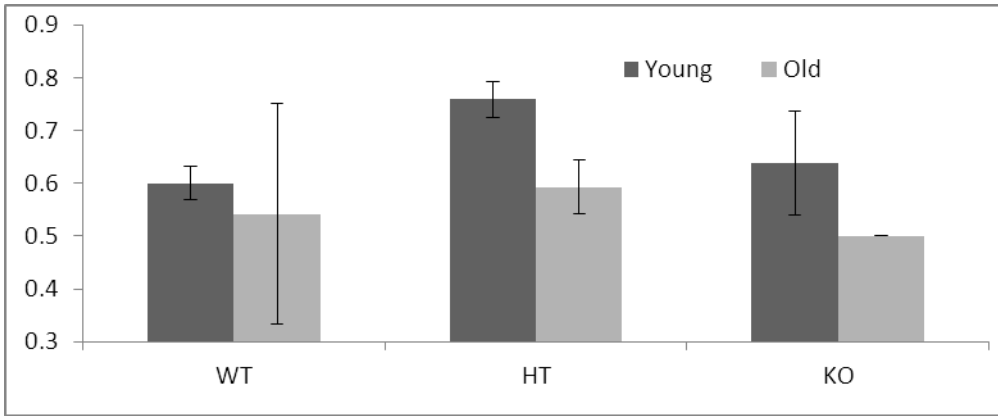


Figure 2. Rate of spontaneous alternation in both young and old mice with no injections. Young mice (25-43 weeks) consistently outperformed old mice (46-61 weeks). There was no significant difference among all genotypes. These result included 9 trials for each young mouse and 4 trials for each old mouse.

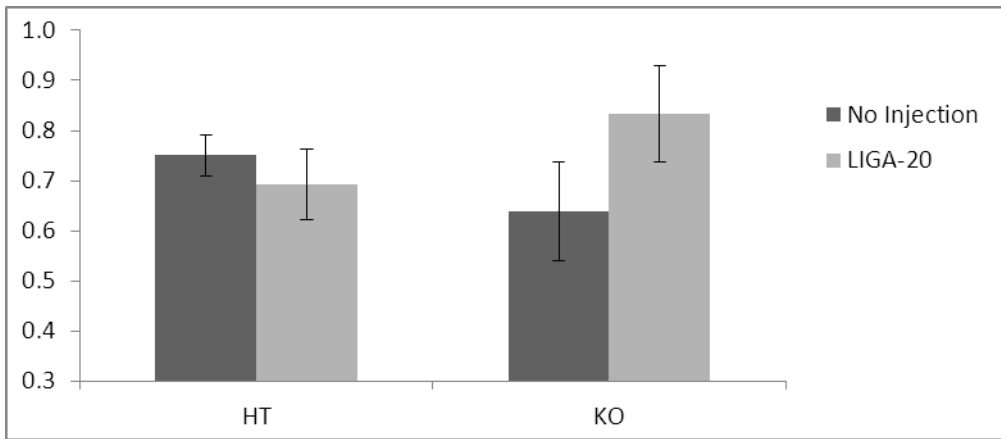


Figure 3. Rate of spontaneous alternation in young mice (25-43 weeks) comparing no injections to LIGA-20 injections. These results included 5 trials for each mouse.

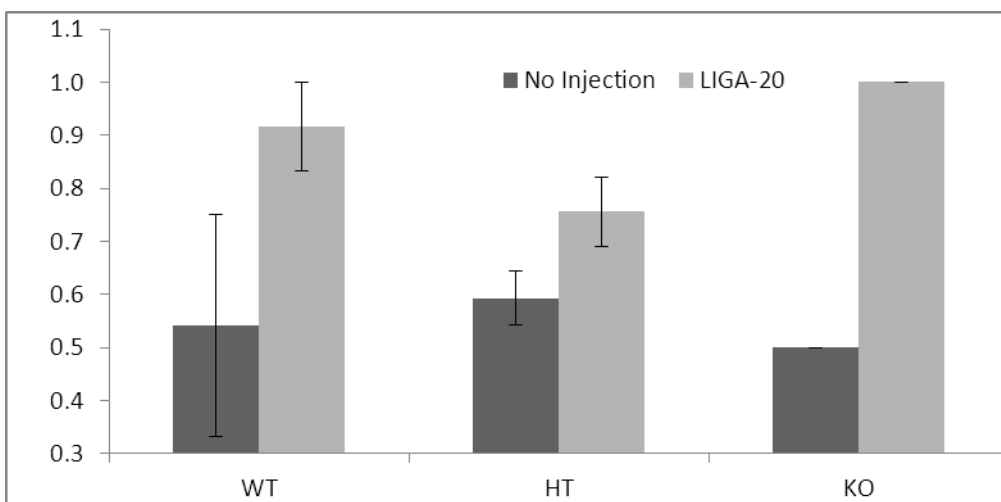


Figure 4. Rate of spontaneous alternation in old mice (46-61 weeks) comparing no injections to LIGA-20 injections. These results included 5 trials for each mouse.

Conclusions:

Previous studies have shown that GM1 deficient mice have significant decrease in cognitive abilities compared to their age-matched controls. However, our results show no significant differences between genotypes in mice with no injections (Fig. 2). Possible reasons include a small sample size for WT and KO, a change in testing parameters, and a wide age range among old mice and young mice.

Older mice tended to have low rates of spontaneous alternation, close to 50%, across all genotypes (Fig. 2). This suggests that older mice have more cognitive impairments regardless of the genotype.

Injections with LIGA-20 generally showed improvements in the rates of spontaneous alternation across all genotypes (Fig. 3 and Fig. 4). This suggests that supplementation of GM1 improves cognitive impairments such as diminished spatial memory. This was especially apparent in older mice for all genotypes, which indicates that older mice are more deficient in GM1 regardless of genotype. This is consistent with the finding [2] that GM1 decreases progressively with aging.

References:

1. Wu G, Lu ZH, Kulkarni N, Amin R, Ledeen RW. 2011. Mice lacking major brain gangliosides develop parkinsonism. *Neurochem Res* 36:1706-1714.
2. Wu G, Lu ZH, Kulkarni N, Ledeen RW. 2012. Deficiency of Ganglioside GM1 Correlates With Parkinson's Disease in Mice and Humans. *J. Neurosci. Res.* 90:1997-2008.
3. Lalonde R. 2001. The neurobiological basis of spontaneous alternation. *Neuroscience and Biobehavioral Reviews* 26:91-104.

**LAURA ROTUNDO (NJMS 2016)
PATRICK LUNDY (La Salle 2014)**

PROJECT TITLE: A CASE REPORT OF AN IATROGENIC ARTERIOVENOUS FISTULA BETWEEN THE SUBCLAVIAN ARTERY AND INTERNAL JUGULAR VEIN
**MENTORS: CHIRAG GANDHI MD, ASSISTANT PROFESSOR
VIVEK TANK MD,
CHARLES PRESTIGIACOMO MD, CHAIR**
DEPARTMENT: NEUROSURGERY

Participation Description

In order to complete this case report, we reviewed related literature concerning iatrogenic arteriovenous (AV) fistulas, dural sinus thrombosis, and other similar case reports to compare to our particular patient and her treatment outcomes. The patient's individual chart was also read to gain a clear understanding of her clinical presentation and risk factors; the angiogram imaging results were also reviewed to look at the outcome of the surgery to close off her arteriovenous fistula. We also met with Dr. Gandhi and Dr. Tank to further discuss the patient's history and the course of her AV fistula. The overall conclusion of the management of this patient as well as an overview of her presentation and of arteriovenous fistulas was compiled into a unique case report.

Objective:

The right internal jugular vein (IJV) is a common site of cannulation in hemodialysis patients and of insertion of central venous catheters for heart surgery patients.[1] Although this location is considered to be safer than other sites, there are some rare, but serious, complications that can occur. There have been a few incidences in literature that show iatrogenic arteriovenous (AV) fistulas that resulted from the placement of catheters into the IJV because of its proximity to other large arteries.[2-4] There are even fewer reports of subclavian artery-IJV fistulas, with only six reported occurrences.[1, 5-9] Common physical presentation of iatrogenic AV fistulas includes neck murmur, pulsating mass in the neck, high-output heart failure and neurological symptoms, such as seizures and syncope.[2-4, 6, 10, 11] This case outlines the detection of an AV fistula in a patient with uncommon presentation of symptoms that included rapid neurological decline and the options for management of the fistula.

Methods:

To complete this case report, the patient's history and relevant visits leading up to the treatment of her arteriovenous fistula (AVF) were reviewed in detail. This information was essential in understanding the development of the patient's AVF and the best way to treat it. Since the location of the AVF is so rare, details of the clinical presentation of the patient are important when considering management outcomes. A comparative literature review was also performed to note the differences in this AVF. The patient's clinical presentation and history is outlined below.

A 43 year old woman with a history of cardiac transplant due to non-ischemic cardiomyopathy was admitted in November 2012 was admitted after presenting with headaches and visual changes. She was found to have decreased visual acuity, constricted fields of vision, papilledema, and pseudotumor cerebri. She had placement of a ventriculoperitoneal shunt complicated by a lack of CSF outflow secondary to clot formation in the lateral ventricle. She developed seizures following her shunt placement, thus her shunt was revised. During a diagnostic cerebral angiogram, it was determined that the patient had poor venous filling after the arterial phase of contrast injection. Because the patient moved during the procedure, the right side of her neck was not catheterized at the time.

Due to decreasing mental status, the patient was admitted, placed under general anesthesia, and had another diagnostic cerebral angiogram performed, with both sides of the neck examined at this time. The angiogram showed an AVF between the right subclavian artery and right IJV. The arterial side of the fistula was located on the posterior superior wall of the subclavian artery about 1 cm proximal to the origin of the right vertebral artery. The angiogram showed significant retrograde flow from the right IJV into the jugular bulb, the sigmoid sinus, the transverse sinus and the superior sagittal sinus.

There was cortical venous reflux to the bilateral cortical venous system with markedly elevated transit times. Treatment of the AVF was first attempted with coils, but there was persistent herniation of the coils into the subclavian artery. After consultation with our vascular surgery colleagues, it was determined that a covered stent would be the appropriate treatment, and an 11mm x 5 cm covered Viabahn Endoprosthesis stent graft (W. L. Gore & Associates, Flagstaff, Arizona) was placed at the proximal end at the origin of the innominate artery with the stent ending 2 cm distally to the fistula. Evaluation at the time revealed the stent graft was patent with no significant flow entering the fistula site.

There was persistence of the patient's decreased mental status, but she was able to wiggle her toes on her left foot to commands. A repeat angiogram performed in June 2013 revealed no evidence of AVF, see Figure 2. The stent occluded both the origins of the right vertebral and right internal mammary artery. The angiography showed diffusely dilated cortical veins more on the left than the right. There was normal antegrade flow of contrast in the veins. There was evidence of stenosis or occlusion of the left transverse sinus with veins draining into the sigmoid sinus to bypass the lesion.

Summary:

The catheterization of the IJV is a procedure commonly used in hemodialysis, pacemaker lead insertion, and central venous pressure monitoring. [1] While this location is chosen because of its minimal risks as compared to other sites, there are still rare, but serious complications. These include psuedoaneurysms, hematoma, and the formation of AV fistulas, with the most common fistula occurring between the IJV and common carotid artery.[5] Because of its more obscure location, and the possibility of underreported number of cases, an AV fistula between the IJV and subclavian artery is rarely seen in literature.

In this case, the formation of the iatrogenic AV fistula is speculated to be the result of needle puncture during central line placement into the IJV when the patient underwent weekly biopsies for her heart transplant in 2004. The unidentified AV fistula was initially considered to be a dural sinus thrombosis in cerebral angiogram imaging because the abnormal connection and retrograde flow presented as poor venous filling after contrast injection. The condition of the patient prevented catheterization and imaging of her right side, delaying the identification of the AV fistula. The patient also presented with vision problems, elevated intracranial pressure, and seizures, which are the nonspecific clinical findings associated with dural sinus thrombosis as well as AV fistulas.[12] The importance of a thorough vascular physical exam is highlighted in this case. Because the patient had a history of rapid neurologic deterioration not seen in other literature, it is possible that the AV fistula could have been detected earlier through palpation and physical exam findings to help distinguish the AV fistula from a dural sinus thrombosis.

Untreated AV fistulas can lead to high-output heart failure as a result of left-to-right shunting of blood.[2, 5] Over time, AVFs can lead to dilation of collateral veins, continuous murmurs, decreased distal pulses, arrhythmias, and thromboembolic episodes.[5, 13] Immediate treatment poses the best outcome for patients with AV fistulas. Treatment options have included coil and/or Onyx embolization, covered stent placement, or surgical repair with or without a sternotomy.[10, 14, 15] Treatment of iatrogenic AV fistulas can be considered similar to treatment of AV fistulas secondary to penetrating trauma, which is itself a rare complication accounting for about 4% of arterial injuries.[11]

Conclusion:

The goal of AVF treatment is to close the abnormal connection while keeping the surrounding vessels patent. When possible, endovascular treatment is preferred over surgical intervention because there is less risk to the surrounding structures and shorter operative time.[16] Coil embolization has been successfully utilized in the past and would be preferred to allow for patency of the vertebral artery. However, due to the geometry of this specific case, a stent graft was the better option and has led to successful occlusion of the fistula and stabilization of the patient's mental status.

References:

- Acri, I.E., et al., *Ipsilateral Jugular to Distal Subclavian Vein Transposition to Relieve Central Venous Hypertension in Rescue Vascular Access Surgery: A Surgical Report of 3 Cases*. *Annals of Thoracic and Cardiovascular Surgery*, 2013. **19**(1): p. 55-59.
- Patel, H.V., et al., *Carotid-jugular arteriovenous fistula: a case report of an iatrogenic complication following internal jugular vein catheterization for hemodialysis access*. *Hemodialysis international. International Symposium on Home Hemodialysis*, 2011. **15**(3): p. 404-6.
- Bahcebasi, S., et al., *Carotid-jugular arteriovenous fistula and cerebrovascular infarct: a case report of an iatrogenic complication following internal jugular vein catheterization*. *Hemodialysis international. International Symposium on Home Hemodialysis*, 2011. **15**(2): p. 284-7.
- Droll, K.P. and A.G. Lossing, *Carotid-jugular arteriovenous fistula: case report of an iatrogenic complication following internal jugular vein catheterization*. *Journal of clinical anesthesia*, 2004. **16**(2): p. 127-9.
- Prakash, J., et al., *Subclavian Artery-Internal Jugular Vein Fistula and Heart Failure: Complication of Internal Jugular Vein Catheterization*. *Journal of the Association of Physicians of India*, 2013. **61**: p. 56-58.
- Singh, K., et al., *Traumatic arteriovenous fistula involving the subclavian artery and jugular vein*. *Journal of vascular surgery*, 2013. **57**(4): p. 1127.
- dos Santos, M.L., et al., *Radiculopathy due to iatrogenic fistula between subclavian artery and internal jugular vein*. *Clinical Neurology and Neurosurgery*, 2008. **110**: p. 80-82.
- Finlay, D., L. Sanchez, and G. Sicard, *Subclavian artery injury, vertebral artery dissection, and arteriovenous fistulae following attempt at central line placement*. *Annals of Vascular Surgery*, 2002. **16**(6): p. 774-778.
- Merino-Angulo, J., et al., *Subclavian artery to internal jugular vein fistula following percutaneous internal jugular vein catheterization*. *Catheterization and Cardiovascular Diagnosis*, 1984. **10**(6): p. 593-595.
- Chloroyiannis, Y. and G.J. Reul, *Iatrogenic left subclavian artery-to-left brachiocephalic vein fistula: Successful repair without a sternotomy*. Vol. 31. 2004, Houston, TX, ETATS-UNIS: Texas Heart Institute. 3.
- Maher, F.S.M., et al., *Traumatic Arteriovenous Fistula*. *The Annals of thoracic surgery*, 1997. **63**(6): p. 1792-1794.
- Osborn, A.G., *Diagnostic Cerebral Angiography*. 2 ed. 1999: Lippincott Williams & Williams. 462.
- Amiridze, N., Y. Trivedi, and K. Dalal, *Endovascular repair of subclavian artery complex pseudoaneurysm and arteriovenous fistula with coils and Onyx*. *Journal of vascular surgery*, 2009. **50**(2): p. 420-3.
14. Kakkar, S., et al., *Successful closure of post-traumatic carotid-jugular arteriovenous fistula complicated by congestive heart failure and cerebrovascular insufficiency*. *Cardiovascular Disease*, 1979. **6**(5): p. 457-462.
15. Cohen, J.E., et al., *Urgent endovascular stent-graft placement for traumatic penetrating subclavian artery injuries*. *Journal of the neurological sciences*, 2008. **272**(1-2): p. 151-7.
16. du Toit, D.F., et al., *Long-term results of stent graft treatment of subclavian artery injuries: Management of choice for stable patients?* *Journal of Vascular Surgery*, 2008. **47**(4): p. 739-743.

MICHAEL DUAN (TCNJ 2016/NJMS 2019)

PROJECT TITLE: DETERMINATION AND CHARACTERIZATION OF THE INOSITOL OXIDATION PATHWAY IN *CRYPTOCOCCUS NEOFORMANS*
MENTOR: CHAOYANG XUE, PH.D, ASSISTANT PROFESSOR
DEPARTMENT: MICROBIOLOGY AND MOLECULAR GENETICS

Participation:

My role in this study was to identify and characterize the remaining enzymes in the inositol catabolic pathway using homologues from phylogenetically similar species. I identified (through BLASTp searches) two enzymes that may be involved in the glucuronate to UDP-Glucuronate conversion in *C. neoformans*. I located the two genes that code for the two enzymes, and I performed gene knockout and transformation to determine whether the inositol utilization pathway is affected. Laboratory techniques that I utilized include: culturing different strains of *C. neoformans* (inoculation, measuring concentrations, serial dilutions, plating), PCR (standard, split, overlap), gel electrophoresis, fungal transformation, and fungal miniprep/PCR.

Objective:

Cryptococcus neoformans is a yeast pathogen that is the most common cause of fungal infection of the central nervous system (CNS) in HIV-infected persons. These cryptococcal CNS infections may present as encephalitis, meningitis, or cerebral-space-occupying lesions. Due to its ubiquity and virulence, it is important to understand the molecular mechanisms and pathways of *C. neoformans*. Increased knowledge of this pathogen may help current treatment efforts become more effective.

Inositol, which is abundant in the human brain, is essential for cellular structure and signaling in all eukaryotes. Recent studies show that inositol uptake and utilization is crucial in the pathogenesis of *C. neoformans*, because inositol promotes the growth, reproduction, and invasion mechanisms of the pathogen. Intracellular inositol can be utilized as a carbon source to produce energy or as a precursor for production of cell surface components. One of those components is the polysaccharide capsule, an important fungal virulence factor that is essential for blood-brain barrier crossing and cryptococcal pathogenesis. Despite the importance of inositol for cell virulence, the inositol utilization pathway for capsule formation remains undefined. The first enzyme in this inositol catabolic pathway, *myo*-inositol oxygenase (MIO), which converts *myo*-inositol to glucuronate, has been identified, but the enzymes that potentially convert glucuronate to UDP-Glucuronate, an essential substrate of the capsule, are still unknown. Isolating and characterizing the genes that code for the aforementioned enzymes can help develop a better understanding of the inositol oxidation pathway. The goal of this project is to identify additional genes encoding enzymes in the inositol catabolic pathway and to ultimately study gene deletion mutants, which will provide further insight into how *C. neoformans* utilizes inositol.

Methods:

Functional Analysis of *myo*-Inositol Oxygenase (MIO) - Using strains *C. neoformans* var. *grubii* H99 and *mio1/2/3Δ*, several growth studies were performed to illustrate the role of inositol and the enzyme MIO.

Identification of Additional Proteins in the Inositol Catabolic Pathway - In the model plant *Arabidopsis thaliana*, there is a pathway that converts glucuronate into UDP-Glucuronate in two steps. This pathway exists in certain species of bacteria and fungi as well. Homologues for the two enzymes in *C. neoformans* were identified through BLASTp searches.

Construction of Gene Knockout Cassettes - Two approaches were used to construct the gene knockout cassettes: (1) Overlap PCR, (2) Cloning vectors containing overlap PCR product.

Generation of the Null Mutants – The gene knockout cassettes were transformed into H99 cells using a biolistic particle delivery system, and gene deletion mutants were identified through PCR screening.

Summary:

***Myo*-inositol oxygenase (MIO) and inositol study** – MIO was identified as essential for cell growth on media with inositol as a sole carbon source. In order for cell cultures to effectively utilize inositol, the MIO genes must be activated. Otherwise, the inositol oxidation pathway cannot be completed and the fungal cells cannot grow on inositol medium.

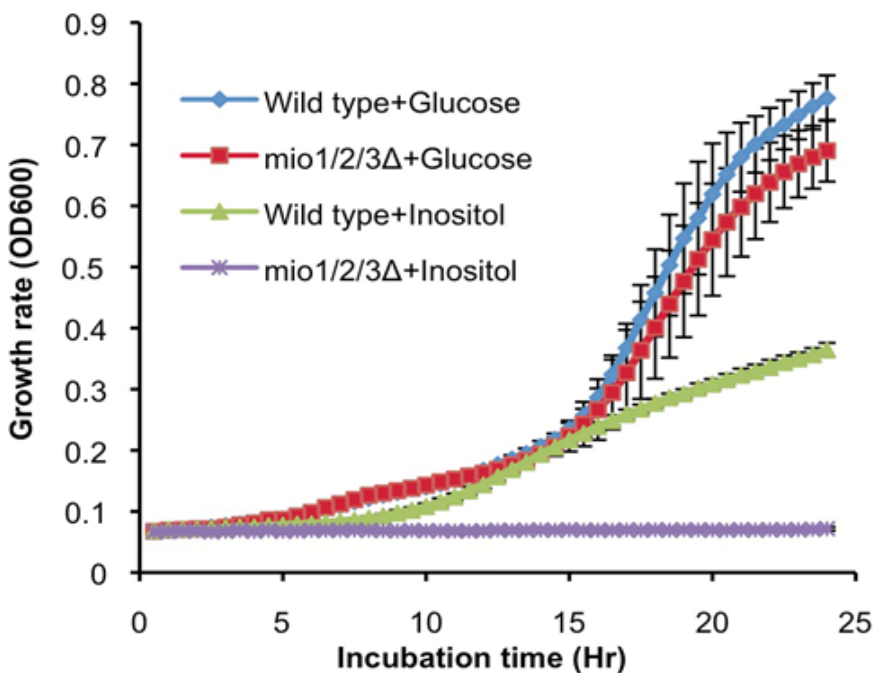


Figure 1 – Growth Assay on Glucose/Inositol Media

Using different combinations of H99 (wild type) and *mio1/2/3Δ* cells with glucose or inositol as the sole carbon source, the effects on inositol oxidation are shown.

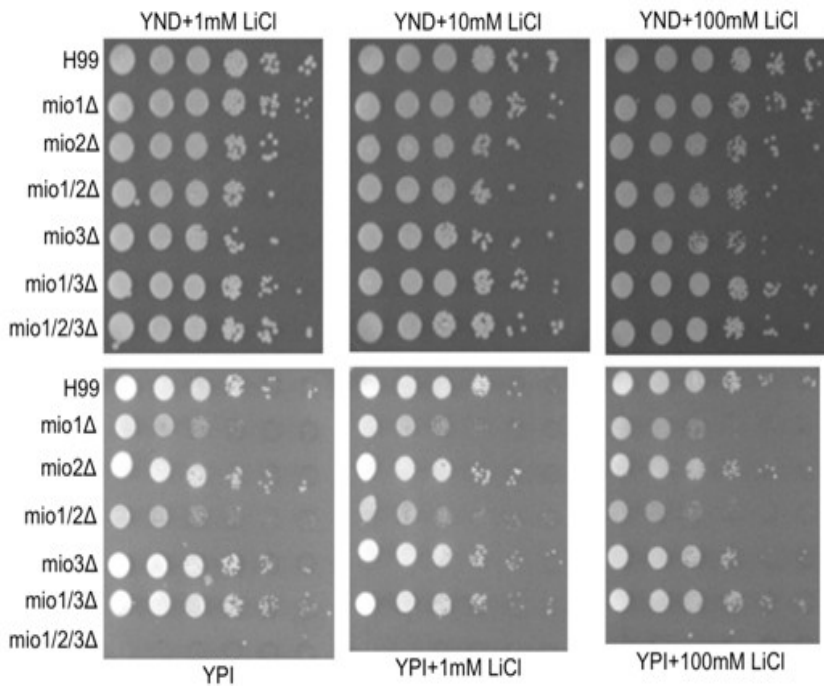


Figure 2 – MIOs are Required for Growth under Inositol Conditions

There are three MIO genes that code for three separate *myo*-inositol oxygenases. The three enzymes are of unequal importance. When all three enzymes are missing, the cells fail to grow when inositol is the sole carbon source. LiCl is an FDA-approved drug for treating manic patients by regulating brain inositol level. Adding Li⁺ does not show an obvious effect in our assay.

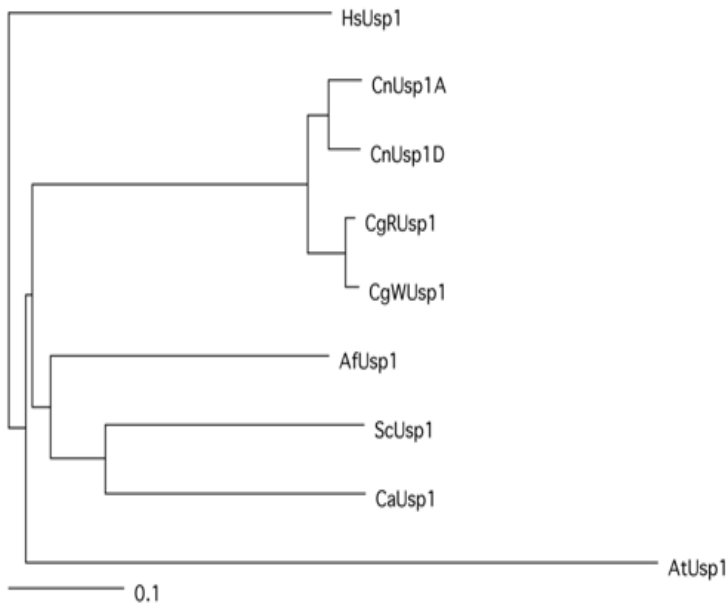


Figure 5 – USP1 Genes

After homologues were identified through BLASTp searches, sequence alignment using ClustalX was performed to generate the phylogenetic tree. (Sc: *Saccharomyces cerevisiae*, Ca: *Candida albicans*, Af: *Aspergillus fumigatus*, Cg: *Cryptococcus gattii*)

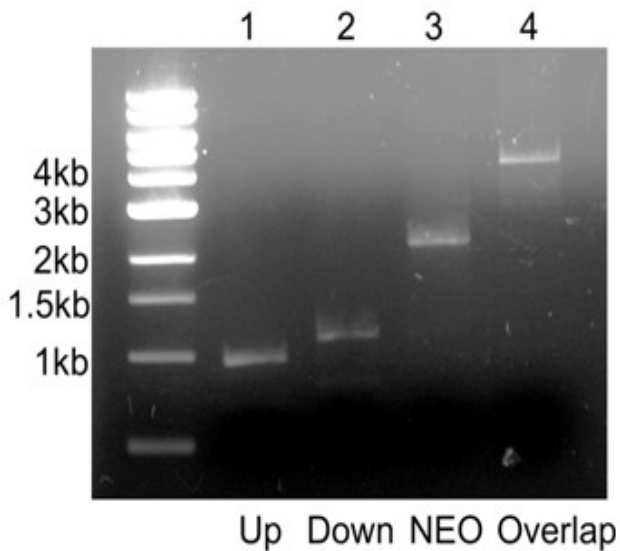


Figure 6 – PCR Fragments

The upstream (1) and downstream (2) fragments were amplified from the H99 genome, and the NEO marker (3) fragments were amplified from the pJAF1 plasmid. The overlap (4) fragments were amplified via overlap PCR of the three previous fragments.

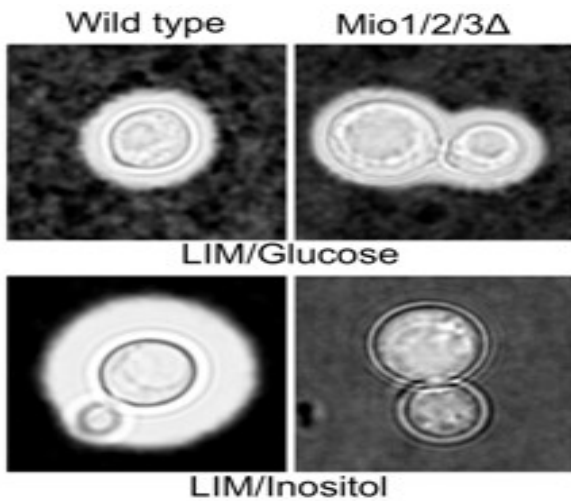


Figure 3 – Capsule Formation

Low ion medium (LIM – necessary for capsule formation) containing glucose or inositol as a carbon source shows the effects of inositol and *myo*-inositol oxygenase on capsule formation.

Identification of remaining genes in the inositol oxidation pathway – The two genes that code for the enzymes responsible for converting glucuronate to glucuronate-1P (GUK1) and glucuronate-1P to UDP-glucuronate (USP1) were located and analyzed.

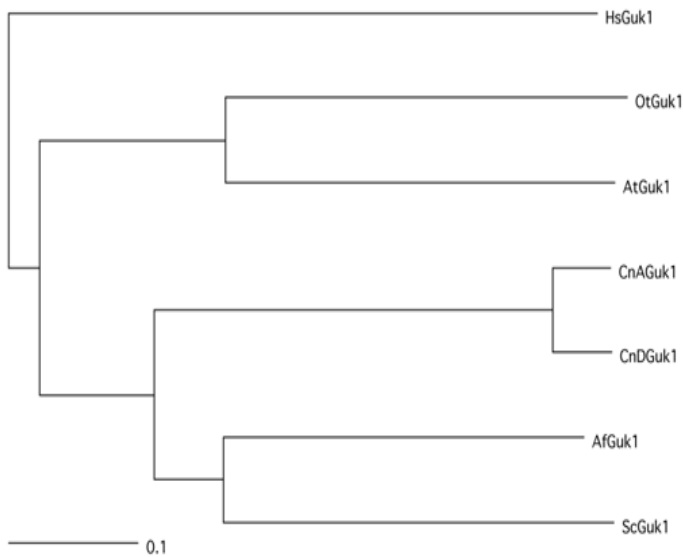


Figure 4 – GUK1 Genes

After homologues were identified through BLASTp searches, sequence alignment using ClustalX was performed to generate the phylogenetic tree. (At: *Arabidopsis thaliana*, Hs: *Homo sapiens*, Cn: *Cryptococcus neoformans*)

Conclusion:

C. neoformans can use inositol as a sole carbon source, and utilizes a unique inositol oxidation pathway to modify cell surface structure. Homologues with other species may reveal additional enzymes in the inositol oxidation pathway. The two genes that we identified using homologues identified through BLASTp searches are GUK1 (conversion of glucuronate to glucuronate-1P) and USP1 (conversion of glucuronate-1P to UDP-glucuronate). We are in the process of generating null mutants, which will provide substantial insight into the inositol oxidation pathway in *C. neoformans*. Identification and characterization of mutants in future work will advance our understanding of the enzymes that enable *C. neoformans* to utilize inositol and modulate its cell surface structure and capsule.

C. AYALA

PROJECT TITLE: THE UTILITY OF PRE-PROCEDURAL VERIFYNOW ANTI-PLATELET ASSAYS IN PREVENTING COMPLICATIONS IN NEUROVASCULAR STENT INTERVENTIONS

MENTORS: P. JIN, T. KASS-HOUT MD, J. DUFFIS MD

DEPARTMENT: NEUROLOGICAL SURGERY

Background and purpose:

Patient reactivity to platelet therapy has been shown to be variable. Our study describes a single-center experience with continuous preoperative VerifyNow Anti-platelet Assay[®] for neurovascular stenting procedures. The VerifyNow assay was used to individualize anti-platelet therapy. We compare our end point performance to recently reported outcomes in literature.

Methods:

Starting in September 2007 our institution employed preoperative VerifyNow Anti-Platelet Assay[®] for all neurovascular stenting procedures. If a patient was a clopidogrel non-responder (<38% inhibition of platelet activity by clopidogrel), their intraoperative and post-operative anti-platelet therapy would be switched from the standard aspirin and clopidogrel to aspirin with another antiplatelet (eptifibatid or ticlodipine). A retrospective study of patient medical records from 2007 to 2013 was conducted. Patients selected were elective neurovascular stent recipients that received pre-operative VerifyNow salicylic acid and clopidogrel anti-platelet assays and that had a periprocedural follow up of at least 30 days. Data was collected on the pathology presented, preoperative antiplatelet regimen, stent neurovascular location, aspirin platelet reactivity, clopidogrel platelet reactivity, type of stent used and periprocedural primary end point. If patients were found to be non-responders, the impact in change of anti-platelet regimen was recorded. A parallel Pubmed literature search was made to retrieve articles describing the periprocedural primary endpoint incidence in intracranial and extracranial stent procedures from 2007 to 2013 without a pre-procedural anti-platelet assay. The primary endpoint was defined as thromboembolic event, intracranial hemorrhage, or death within 30 days of the procedure. The incidence of periprocedural outcomes from our medical records review was then compared to those reported in recent literature.

Results:

Our literature review yielded 7323 patients without a preprocedural antiplatelet assay. Of these, 40.3% had intracranial and 59.7% extracranial stents placed. The incidence of ipsilateral stroke was 3.52% for extracranial and 6.31% for intracranial stents. The incidence of intracranial hemorrhage was 6.48%. Our retrospective study included 30 patients of which 57%(17/30) had extracranial and 43% (13/30) intracranial stents placed. Eight patients were found to be clopidogrel resistant (<40% inhibition) and their antiplatelet therapy was periprocedurally changed to integrillin in 6 patients and ticagrelor in 2 patients. Two patients were resistant to salicylic acid (>550ARU) and did not have any change in management. The incidence of stroke was 5.88%(1/17) for extracranial and 23.1%(2/13) intracranial procedures. Subarachnoid hemorrhage occurred in one intracranial procedure (3.33%). The collective rate of complications amongst all patients was 13.3% (4/30) The incidence of complications in patients that were clopidogrel resistant with antiplatelet therapy modifications was overall 25%(2/8). Both of these patients were non-diabetics. The incidence of complications of patients that were clopidogrel resistant and had antiplatelet therapy modification was 0% (0/4). The 2 patients in the therapy modification population that had complications were both also diabetics. The remaining 6 out of 8 patients that had therapy modification without complications were diabetics.

Conclusions: Our continuous single center experience in preoperative application of the VerifyNow assay showed similar overall incidence of complications in neurovascular stenting procedures as those reported in current literature. This is consistent with the current literature that suggests the use of VerifyNow assay for neurovascular stenting does not improve short term outcomes. Our study shows that a change in management of platelet therapy is beneficial for patients with higher risk factors for thrombus formation. We suggest the Verify now assay as a management tool to those with higher risk factors.

ANTHONY KORDAHI

PROJECT TITLE: HEAD AND NECK RECONSTRUCTION UTILIZING FREE TISSUE TRANSFER, DOES TRAINING IN OTOLARYNGOLOGY OR PLASTIC SURGERY HAVE AN EFFECT ON OUTCOMES

MENTOR: EDWARD LEE, MD, CLINICAL ASSISTANT PROFESSOR

DEPARTMENT: SURGERY

Introduction:

The reconstruction of defects resulting from the extirpation of head and neck neoplasms is performed by both otolaryngology and plastic surgery services, mostly dependent on the institution. Very little, if any, literature exists comparing differences between these two services and their reconstructions, specifically outcomes. The American College of Surgeons' National Surgical Quality Improvement Project (NSQIP) provides a unique opportunity to examine a predefined set of variables with regards to free vascularized tissue transfers performed by each service.

Methods:

Following institutional review board approval the NSQIP Participant Use Files for 2005 – 2011 were examined for all Current Procedural Terminology codes regarding free tissue transfer. The results were further refined to include only primary ICD-9 codes involving a neoplasm of the head or neck. Each record was examined to determine which service performed the free tissue reconstruction. Outcome variables examined included total operative time, total hospital stay, wound complications, flap failures, and other selected outcomes.

Results:

During this time period a total of 534 flaps were performed, 213 by plastic surgery and 321 by otolaryngology. The average age was 61.8, with 367 males and 166 females (sex of 1 patient not provided). The average operative time was 578 and 567 minutes for plastic surgery and otolaryngology, respectively ($p = 0.52$). When further refining the analysis to resections performed by otolaryngology, there was no difference in operative time when the same surgical team performed the flap, or when another team performed the reconstruction. Total hospital length of stay was 12.9 and 11.2 days for plastic surgery and otolaryngology, respectively ($p < 0.05$). There were no significant differences noted between surgical site infections, wound dehiscence, and flap failure between flaps performed by plastic surgery and otolaryngology. In addition there were no significant differences noted between blood transfusion, return to operating room, postoperative pneumonia, and myocardial infarctions between the two services. Patients undergoing flaps performed by plastic surgery were significantly more likely to be on a ventilator 48 hours postoperatively ($p < 0.005$).

Conclusions:

This study shows similar results with regards to free vascularized tissue transfers when performed by plastic surgery and otolaryngology. Plastic surgeons may be less familiar with airway management than otolaryngologists, possibly explaining the increased likelihood of the patient being ventilated for more than 48 hours postoperatively. The similar outcomes between the two services indicate that each specialty receives adequate training in microsurgery.

PHOEBE Y. LING (NJMS 2016)

PROJECT TITLE: RECONSTRUCTION AFTER RETROSIGMOID APPROACHES USING AUTOLOGOUS FAT GRAFT-ASSISTED MEDPOR TITAN CRANIOPLASTY: ASSESSMENT OF POSTOPERATIVE CEREBROSPINAL FLUID LEAKS AND HEADACHES IN 46 CASES

MENTOR: JAMES K. LIU, MD, FAANS
DEPARTMENT: NEUROLOGICAL SURGERY

Participation description:

I, Phoebe Ling, participated in the data collection and analysis for the retrospective chart review of all 46 patients who had received our reconstruction technique in this study, and literature reviews for incidences of CSF leaks and headaches after using prophylactic surgical techniques in retrosigmoid approaches.

Objective:

The retrosigmoid approach used in skull base surgery offers an excellent corridor to access various tumors and vascular lesions in the posterior fossa and cerebellopontine angle. Postoperative CSF leaks and headaches, however, still remain frequent complications. The authors therefore describe a simple repair technique with an autologous fat graft-assisted Medpor Titan cranioplasty, and investigate the incidence of postoperative CSF leaks and headaches using this technique.

Methods:

A retrospective chart review was conducted on all patients who underwent our multilayer reconstruction technique after retrosigmoid approach performed by the senior author (JKL) between September 2009 and May 2013. Variables examined included postoperative CSF leak (incisional, rhinorrhea, otorrhea), pseudomeningocele formation, postoperative headache, length of hospital stay, and length of follow-up. Findings from this study were compared to those in the literature using other prophylactic techniques for postoperative CSF leaks and headaches after retrosigmoid approaches (Tables 1 and 2).

The study consisted of 44 patients who underwent a total of 46 operations; one patient had bilateral surgery for bilateral trigeminal neuralgia (TGN), and one patient had repeat surgery at the same site for recurrent TGN. The study population included 27 females and 17 males. Their mean age was 53.5 years (range 27-80 years). There were 49 indications for surgery; three cases had dual pathology of TGN and a CPA epidermoid cyst. Indications for surgery were TGN 18/49 (36.7%), acoustic neuromas 12/49 (24.5%), posterior fossa meningiomas 9/49 (18.4%), epidermoid cysts 4/49 (8.2%), and other pathology 6/49 (12.2%).

The reconstruction technique involved obtaining a watertight dural closure and sealing off any visible mastoid air cells with bone wax (Fig. 1 A and B). An autologous fat graft was then placed over the dural suture line and up against the waxed-off air cells, filling the retrosigmoid cranial defect (Fig. 1 C). The fat graft was then bolstered with a cranioplasty using a Medpor Titan implant (Stryker Craniomaxillofacial, Kalamazoo, MI), a titanium mesh plate embedded in a sheet of porous polyethylene (Fig. 1 D). A postoperative mastoid pressure dressing was applied for 48 hours and prophylactic lumbar drainage was not used.

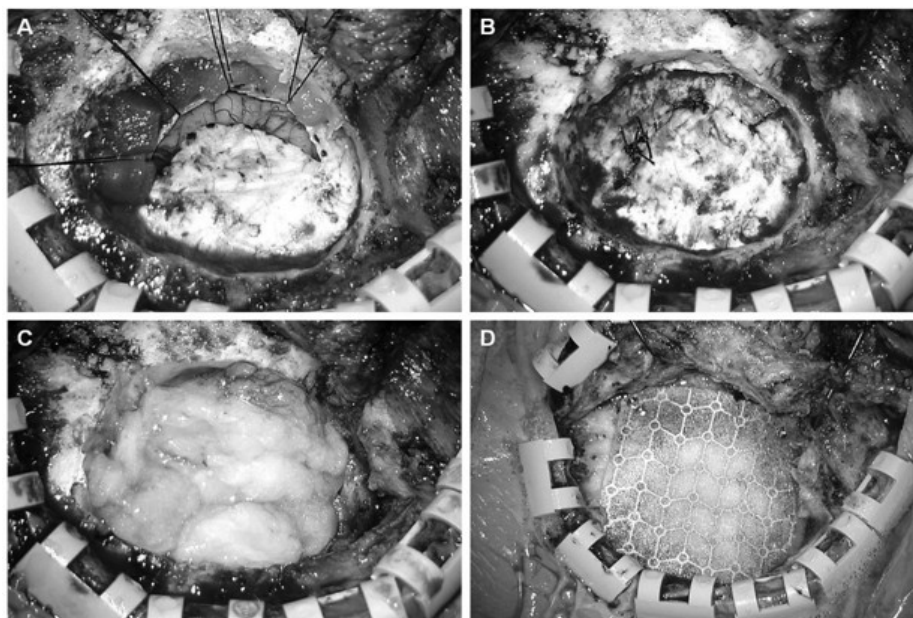


Fig. 1

Summary:

No patients developed postoperative CSF leaks (0%), pseudomeningoceles (0%), or new-onset postoperative headaches (0%) with our repair technique. There were no cases of graft site morbidity such as hematoma or wound infection. Mean duration of postoperative hospital stay was 3.8 days (range 2-10 days). Mean postoperative follow-up was 11.4 months (range 1.2-41.1 months).

Meticulous multi-layer reconstruction at every step of the closure, including dural closure, occlusion of air sinuses, and cranioplasty, is critical for successful outcomes. In our the repair technique, the fat graft serves as an excellent natural tissue sealant and accomplishes the following goals: 1) bolster the dural suture line to prevent any CSF leakage through the suture line or any other residual dural openings; 2) obliterate the retrosigmoid craniectomy dead space; and 3) provide a secondary sealant for the waxed-off air cells. The Medpor Titan cranioplasty applies external pressure to the fat graft, provides cosmetic and structural reconstruction of the bony defect, and creates a physical barrier to prevent muscle and soft tissue adhesions to the dura which may contribute to postoperative headaches.

Conclusion:

The authors' preliminary study suggests that our reconstruction technique for retrosigmoid approaches using an autologous fat graft-assisted Medpor Titan implant cranioplasty prevents postoperative CSF leaks and postoperative headaches.

TABLE 1: Postoperative CSF leak incidences and prophylactic techniques in retrosigmoid approach*

Study	CSF Leak	Prophylactic Technique
Millen and Meyer, 1993	9.7% (16/165)	fat, post-op mastoid pressure dressing
Hoffman, 1994	15.7% (37/235)	bw, mus, Gelfoam, fg
Nutik & Korol, 1995	14.1% (22/156)	bw, fat
Fishman et al., 1996	22.0% (20/91)	fat, fas, post-op mastoid pressure dressing, fg
Gormley et al., 1997	14.0% (22/157)	bw, mus, fas, Surgicel, fg
Samii & Matthies, 1997	9.2% (92/1000)	bw, mus, fg
Valtonen et al., 1997	14.5% (9/62)	bw, fat [†]
Gal & Bartels, 1999	2.9% (1/35)	bw
Tonn et al., 2000	3.2% (16/508)	mus, unspecified bone cement, fg
Brennan et al., 2001	7.9% (12/151)	bw, fas, lumbar drain
Leonetti et al., 2001	7.9% (15/191)	bw, fat, mus, fas, bp, lumbar drain, post-op mastoid pressure dressing
Bani and Gilsbach, 2002	6.3% (14/224)	mus, bp, collagen sponge
Becker et al., 2003	10.0% (10/100)	bw, fat, mus
Fishman et al., 2004	8.5% (6/71)	bw, fat, fas, fg
Yamakami et al., 2004	4.0% (2/50)	lumbar drain
Cueva and Mastrodimos, 2005	0.0% (0/160)	bw, blood-impregnated microfibrillar collagen hemostat
Galer et al., 2006	3.2% (1/31)	hydroxyapatite cement, titanium mesh, lumbar drain, closed suction wound drain
Baird et al., 2007	10.0% (13/130)	bw, hydroxyapatite cement
	18.7% (28/150)	bw, fat, mus, fg
Ludemann et al., 2008	5.7% (16/283)	mus, fg
	2.2% (3/137)	fat, fg
Stieglitz et al., 2010	4.2% (22/519)	fat, mus, polymethylmethacrylate, fg
Arlt et al., 2011	7.3% (3/41)	multilayer dural closure [‡] , mus, polymethylmethacrylate [§] , fg
	10.0% (4/40)	monolayer dural closure , mus, fg
Current study	0.0% (0/46)	bw, fat [†] , Medpor Titan implant, post-op head wrap pressure dressing

*Some studies compared multiple prophylactic techniques which are listed here in separate rows under the study.

bw = bone wax, fat = free fat graft, fat[†] = fat graft to fill retrosigmoid craniectomy defect, fas = temporalis fascia or fascia lata graft, mus = temporalis or nuchal muscle graft, bp = bone pate, fg = fibrin glue

[‡]Multilayer dural closure consisted of a subdural closure with TissuFleece and Spongostan, dural sutures, and an epidural closure with Tachosil

[§]polymethylmethacrylate used in five cases only

Monolayer dural closure consisted of dural sutures and an epidural closure with Tachosil

Study	Pre-Operative Headache	Post-Operative Headache	New Onset Post-Operative Headache	Length of Follow-up (months)	Prophylactic Technique
Schesse l et al., 1993		67.3% (37/55)		Mean 60	craniectomy with no cranioplasty
		5.3% (1/19)		Mean 60	craniotomy with bone flap replacement
Harner et al., 1993		9.1% (19/209)		24	none
Pedrosa et al., 1994		72.6% (98/135)		Range 8 – 120	IAC bone dust suctioning
Harner et al., 1995		16.7% (4/24)		3	none
		4.2% (1/24)		3	PMMA cranioplasty
Soumek h et al., 1996		12.5% (7/56)		Range 15 – 38	none
		0% (0/50)		Range 15 – 38	unspecified cranioplasty
Catalano et al. 1996			64.3% (18/28)	Range 5 – 48	none
			81.5% (22/27)	Range 5 – 48	only cranioplasty
			10.3% (3/29)	Range 5 – 48	cranioplasty, IAC bone dust suctioning
Feghali and Elowitz, 1998		5.6 % (1/18)		12	split calvarial graft cranioplasty
Wazen et al., 2000	20% (6/30)	43.3% (13/30)	30% (9/30)	Range 6 – 60	none
	26.7% (8/30)	43.3% (13/30)	23.3% (7/30)	Range 6 – 60	titanium mesh-PMMA cranioplasty
Schaller and Bau-mann, 2003			40% (52/130)	3	direct dural closure
			0% (0/25)	3	duraplastic closure
			94%	3	no bone flap replacement
			27%	3	bone flap replacement
Porter et al., 2009	45.5% (15/33)	48.5% (16/33)		24	IAC bone dust removal
	40.4% (21/52)	36.5% (19/52)		24	IAC bone dust removal, fat graft to fill craniotomy defect
Current study	30.4% (14/46)	13.0% (6/46)	0% (0/46)	Mean 10.9	IAC bone dust suctioning, fat graft-assisted Medpor Titan cranioplasty

*All values reported when possible and applicable. Some studies assessed and compared multiple prophylactic techniques which are listed here in separate rows under the study. Length of follow-up was reported differently among the studies; therefore, it is presented here as a specific time whenever possible, then mean, then range if a specific time of follow-up or mean is not reported. PMMA = polymethylmethacrylic, IAC = internal auditory canal

RITAM GHOSH (NJMS, 2016)

PROJECT TITLE: A META-ANALYSIS OF DRUG ELUTING STENTS VS. BARE METAL STENTS FOR TREATMENT OF EXTRACRANIAL VERTEBRAL ARTERY DISEASE
MENTOR: CHIRAG D. GANDHI, MD, ASSISTANT PROFESSOR
DEPARTMENT: NEUROSURGERY

Participation Description:

This summer, I worked with Chirag D. Gandhi, M.D. in the department of Neurosurgery. My work was on a meta-analysis on drug eluting stents vs. bare metal stents in the treatment of extra-cranial vertebral artery disease. This project was actually started last year by another medical student who actually found the papers in question and compiled the data for the initial statistical analysis. This summer, I finished the statistical analysis and compiled all of the information together as well as did thorough background research on the topic. Furthermore, after compiling the data together, I was the one who wrote the full manuscript, including a discussion and conclusion of the topic at hand. Finally, I presented a poster of the work at the NJMS summer symposium.

Objective:

For many years, vertebral artery stenosis was thought to be an entity of limited clinical significance, with some authors going so far as to say it was essentially benign. However, it has been shown that out of the almost 700,000 strokes occurring annually, 20% of these affect the posterior circulation. Furthermore, somewhere between 9-20% of these cerebrovascular ischemic events occur as a result of vertebral artery stenosis (VAS). The mortality associated with vertebrobasilar circulation stroke is as high as 30%, and patients experiencing vertebrobasilar transient ischemic attacks (TIAs) have a 25%-35% risk of stroke within 5 years.

The vertebral artery is the 2nd most common area of stenosis after to the carotid bifurcation, with the stenosis most frequently occurring near the origin (V_0) and proximal area of the vessel (V_1). The etiology of the stenosis is a result of hemodynamics or occlusion and hypoperfusion of the posterior circulation. However, more frequently, it is the result of artery-artery embolism, from usually the heart, aorta, or a proximal vessel such as the subclavian artery.

When vertebral artery stenosis occurs, symptoms include dizziness, syncope, diplopia, hemiparesis, leg weakness, and possible cerebellar dysfunction. Due to good collateral circulation from the contralateral artery, treatment is usually only necessary for bilateral stenosis, severe stenosis of the dominant vertebral artery, or severe ipsilateral stenosis with vertebrobasilar insufficiency. Treatment starts with a regimen of antiplatelet agents such as aspirin or clopidogrel, or anticoagulant agents such as warfarin. However, when symptoms are persistent, surgical options need to be explored. To date, the most common open surgical vascular procedures are endarterectomy, surgical bypass, and carotid-vertebral transposition. While these procedures have been shown to have good technical success, it is evident that a great deal of experience is needed to perform these procedures. They have also been associated with considerable postoperative complications, such as Horner's syndrome and lymphocele. Furthermore, the mortality associated with some surgeries has been reported as high as 20%.

Since the 1980's, endovascular approaches to VAS have been gaining popularity due to the low rates of complications as well as high technical success. The two most common forms of endovascular surgery are angioplasty and stenting. Balloon angioplasty, while maintaining high technical success, can be associated with poor outcomes due to the angioarchitecture of the vertebral artery, primarily in the ostium. Due to a high level of elastin and smooth muscle in the tunica media, there is a considerable risk of elastic recoil, vessel dissection, and restenosis.

Endovascular stenting has proved to have excellent immediate results and low periprocedural complications. The two main forms of stents are bare metal (BMS) and drug-eluting (DES) stents. Bare metal stents (BMS), which are older and more commonly used, have been shown to have high levels of in-stent restenosis (ISR). ISR rates range from 10-67% and can be attributed stent fracture as well as neointimal hyperplasia, which is the thickening of the tunica intima of the blood vessel due to a surgical procedure or injury. This is due to the aforementioned anatomical features of the vertebral artery, as well as the tortuous nature of the ostium and V1 segments which places great mechanical strain on the stents. These complications with BMS lead to high rates of target vessel revascularization (TVR), which is defined by a repeat intervention of the target vessel driven by recurrent clinical symptoms with a >70% stenosis.

To combat these complications, drug eluting stents (DES), coated with a variety of substances such as sirolimus and paclitaxel have been used with increased efficacy in the coronary arteries. The immunosuppressant and immunomodulatory drugs released by the stents reduce the risk of ISR by limiting macrophage accumulation and smooth muscle cell proliferation around the stent. However, there has not been extensive research done comparing BMS and DES stents in the clinical treatment of VAS. Therefore, this meta-analysis was undertaken to compare BMS and DES stents in terms of clinical success, technical success, mortality, perioperative complications, recurrent symptoms, and target vessel revascularization.

Methods:

A Medline search was performed using the terms "stents," "drug-eluting stents," "atherosclerosis," "vertebral artery," and "vertebrobasilar insufficiency". The criteria included that the studies all presented a large series of cases, were published within the last 5-7 years, looked specifically at BMS & DES, and were testing for similar outcome measures of interest. Five studies met the criteria for a comparative meta-analysis. The bare metal stents were either made of cobalt chromium or stainless steel, while the drug eluting stents were either coated with sirolimus or paclitaxel.

The technical and clinical success, periprocedural complications, target vessel revascularization (TVR), rates of restenosis and recurrent symptoms and overall survival were compared between the BMS and DES groups. Technical success was defined by resolving stenosis to between 20-30%, while clinical success was defined by technical success as well as a resolution of symptoms. Finally, the recurrent symptoms we were looking for included transient ischemic attacks (TIA), stroke, or vertebrobasilar insufficiency (VBI).

Summary:

The mean pretreatment stenosis was $83.8 \pm 4.2\%$ in the DES group ($n = 156$) and $80.12 \pm 2.7\%$ in the BMS group ($n = 148$), which was not significant. The rates of technical success, clinical success and periprocedural complications were 98.78%, 95.77% and 1.94% for the DES group vs. 100%, 97.96% and 2.96% for the BMS group. However, there was significant difference in the technical success (OR = 1.528, $p = 0.622$), clinical success (OR = 1.917, $p = 0.274$) and periprocedural complications (OR = 0.741, $p = 0.614$) between the two cohorts. There was no periprocedural mortality, stroke or TIA. The mean clinical and radiological follow-up times were 19.1 ± 6.9 and 14.23 ± 1.5 months respectively, for the DES arm and 26 ± 7.6 and 20.5 ± 3.3 months, respectively, for the BMS group. When compared with the DES group, the BMS group had a significantly higher rate of recurrent symptoms (2.76% vs. 11.26%; OR = 3.319, $p = 0.011$) and TVR (4.83% vs. 19.21%; OR = 4.099, $p = 0.001$). There was no significant difference between overall survival (OR = 0.655, $p = 0.32$). A 0.388 odds ratio of no-restenosis in the BMS to DES arms ($p = 0.001$) indicated a significantly higher restenosis rate in the BMS group relative to the DES group (33.57% vs. 15.49%, respectively).

Thus, the DES group was significantly different from the BMS group in terms of restenosis rates, recurrent symptoms, and TVR rate.

Conclusion:

Vertebral artery stenosis (VAS) is a medical occurrence that is still not fully understood. Despite the fact that it accounts for up to 20% of posterior circulation ischemia, the natural history and prognosis of vertebral artery disease has not been as extensively delineated as it has with carotid artery disease. Furthermore, it has been reported as hard to diagnose, since the most common symptoms, syncope and dizziness, can be associated with a myriad of etiologies.

VAS has been found to occur to patients who have risk factors for atherosclerosis, such as diabetes, hypertension, hyperlipidemia, and smoking. To date, the usual sequence of treatment is to first start the patient on antiplatelet agents such as aspirin and clopidogrel, or anticoagulant agents such as warfarin. However, when symptoms are persistent, surgical options are then considered, such as endarterectomy and carotid artery transposition. These open surgical techniques require considerable technical skill, and a study by Ausman and colleagues reported mortality and morbidity rates up to 8.4% and 13.3% respectively.

Endovascular surgery is seen as an alluring alternative, as the rates of mortality and morbidity have been reportedly low as 1.5% and 3.3% respectively. Bare metal stents have been used with great technical and clinical success since first reported by Storey and colleagues in 199. However, they have also been associated with high rates of in-stent restenosis on follow up, ranging from 10-67%. In a study by Werner and colleagues, the 2 main reasons for restenosis were stent fracture, with a rate of 32.1%, as well as intimal hyperplasia, which occurred at a rate of 20.7%. It has been theorized that the anatomical nature of the vertebral artery ostium, which contains larger relative amounts of smooth muscle and elastin, leads to higher recoil and increases the mechanical stress on stents. The tortuous nature and continuous mobility of the subclavian-vertebral artery junction may also promote in-stent restenosis due to stent fracture caused by mechanical stress. Finally, longer lesion lengths are also associated with higher ISR rates. A study by Stayman and colleagues reported lesions of less than 5 mm, between 5-10 mm, and greater than 10 mm to have ISR rates of 21%, 29%, and 50% respectively.

In order to combat the high ISR rates associated with BMS, drug eluting stents coated with anti-proliferative agents such as paclitaxel and sirolimus have been engineered to mitigate the macrophage accumulation and smooth muscle cell proliferation which leads to ISR. No significant difference was found in aspects such as peri-procedural mortality, stroke, and TIA. Furthermore, there was no significant difference in technical success and clinical success. However, there was a significant difference between BMS and DES in terms of recurrent symptoms, restenosis, and target vessel revascularization (TVR). The BMS group had 3 times a higher rate of recurrent symptoms, twice the rate of restenosis, as well as a four times higher rate of TVR. This may be clinically significant; while DES has been used to great efficacy in coronary arteries, this implies that it may also be preferred to BMS in treatment of extra-cranial vertebral artery stenosis. However, one of the complications is that DES use in the coronary arteries has been associated with clot formation, often resulting in thrombosis at the stent site, which necessitates patients to stay on clopidogrel for up to a year. Thus, more long-term research is necessary to accurately gauge the use of DES in the vertebrobasilar system.

ROHIT K. REDDY (NJMS 2017)

PROJECT TITLE: SKULL BASE RECONSTRUCTION AFTER FAR LATERAL TRANSCONDYLAR APPROACHES USING AUTOLOGOUS FAT-ASSISTED MEDPOR TITAN CRANIOPLASTY: SURGICAL TECHNIQUE AND NUANCES

MENTOR: JAMES K. LIU, MD, FAANS

DEPARTMENT: NEUROLOGICAL SURGERY

Participation Description:

I, Rohit K. Reddy, participated in the collection of data and subsequent analysis through retrospective chart review of all 12 patients who had received the reconstruction technique described in this study, as well as literature reviews for the incidence of CSF leaks after using prophylactic surgical techniques in far lateral transcondylar approaches.

Objective:

We describe a novel multilayer repair technique using an autologous fat graft-assisted Medpor Titan implant cranioplasty following the far lateral transcondylar approach as a way to prevent post-operative CSF leaks. We describe our surgical nuances and report our incidence of postoperative CSF leak and postoperative headaches.

Methods:

Between September 2009 and June 2013, 12 patients underwent far lateral craniotomy and multilayer cranioplasty with the Medpor Titan implant at the University Hospital in Newark, New Jersey. With IRB approval, a retrospective chart review was conducted, revealing a total of 13 procedures performed during this time period; one patient was diagnosed with bilateral neurenteric cysts. Factors examined included postoperative CSF leak (incisional, rhinorrhea, otorrhea), postoperative headache, and length to follow-up (Table 1). Study findings were compared to prophylactic techniques for postoperative CSF leaks found in the literature after far lateral approaches (Table 2).

The study population included 3 males and 9 females with a mean age of 34.6 years and a range of 10-71 years. Patients presented with cerebellopontine angle (CPA) epidermoid cyst 2/13 (15.4 %), CPA schwannoma 1/13 (7.7 %), CPA hemangioblastoma 1/13 (7.7 %), cerebellar cyst 1/13 (7.7 %), foramen magnum meningioma 5/13 (38.5 %), neurenteric cyst 2/13 (15.4 %), and left PICA aneurysm 1/13 (7.7 %).

At the time of closure, any exposed mastoid air cells were sealed with bone wax. (Figure 1) Primary watertight closure of the dura was performed using 4-0 Nurolon (Ethicon) sutures, with a dural allograft as needed. An autologous fat graft was then harvested from the abdomen and placed over the dead space of the far lateral craniectomy defect. The fat graft was strategically positioned over the dural suture line and up against the waxed off mastoid air cells and the suture line, with the fat graft placed into the mastoid defect to firmly seal off the dural incision and mastoid air cells. Additional fat graft was paced over the craniocervical dura and in the dead space of the cervical musculature. A Medpor Titan cranioplasty (76 mm x 50 mm x 0.85 mm; MTM, Stryker CMF) was performed to bolster the underlying fat graft and to reconstruct the suboccipital bony defect. Care was taken not to overpack the fat graft in order to avoid excessive mass effect on the cerebellum. The implant is secured to the bony edges with titanium screws and meticulous multi-layer soft tissue wound closure was performed. (Figure 2). Postoperatively, a mastoid pressure dressing was applied for 48 hours and no lumbar drainage was used.

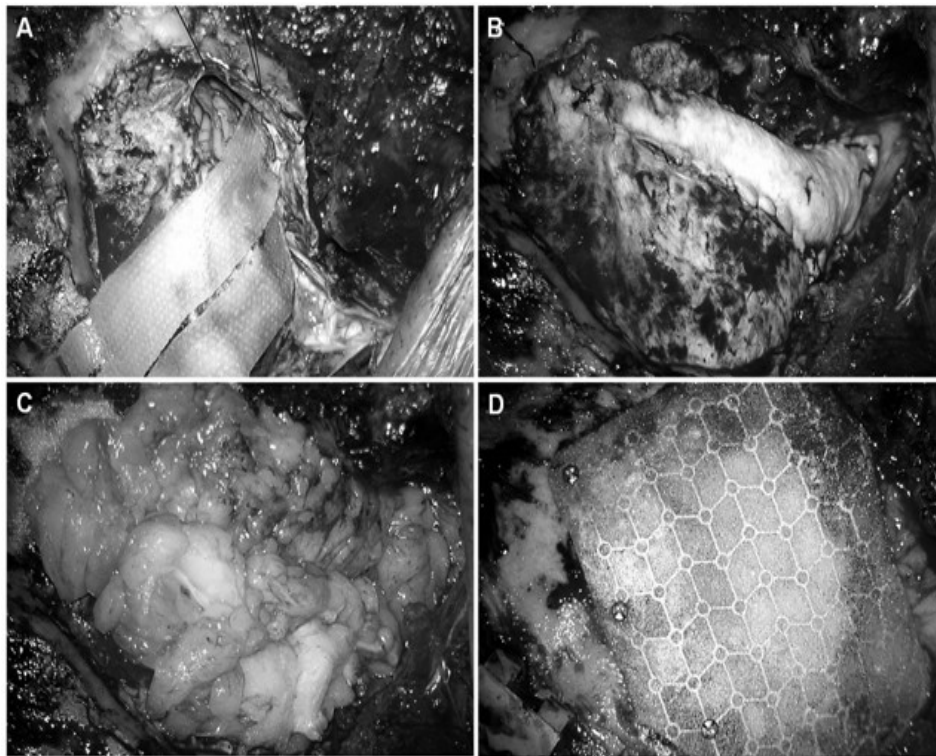


Figure 1. A: Dural incision of a right-sided far lateral approach. B: Primary watertight dural closure is performed with an allograft dural patch. The mastoid air cells are waxed off. C: An autologous fat graft is placed into the craniectomy defect over the suture line and cervical dead space. D: Medpor Titan cranioplasty is used to bolster the fat graft repair.

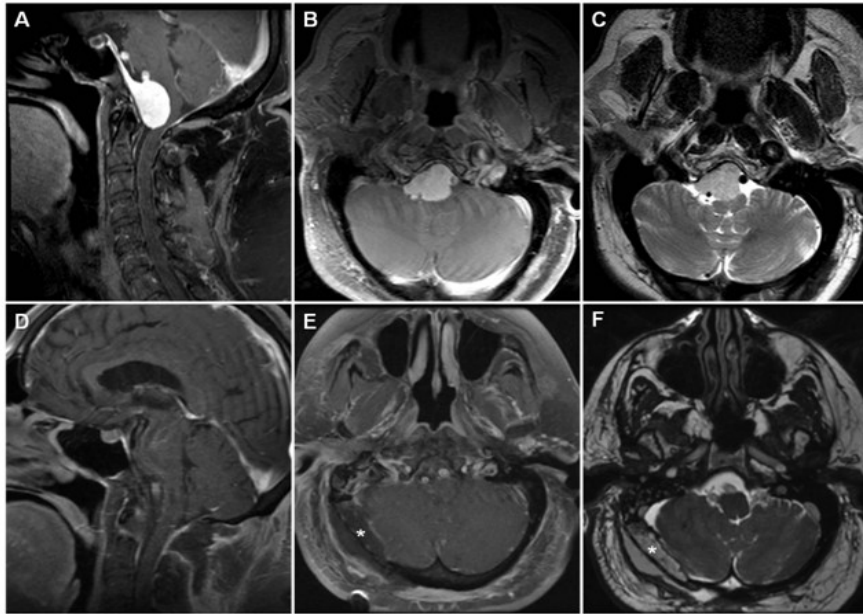


Figure 2. A-C: Preoperative MRI (A: T1 post-gadolinium sagittal, B: T1 post-gadolinium axial, C: T2 axial) demonstrating a ventral foramen magnum meningioma compressing the brainstem. D-F: Postoperative MRI (A: T1 post-gadolinium fat-suppressed sagittal, B: T1 post-gadolinium fat-suppressed axial, C: T2 FIESTA axial) showing complete tumor removal via a right far lateral transcondylar approach. The fat graft (asterisk) is seen filling the dead space of the craniectomy defect and upper cervical musculature.

Summary:

There were no instances of CSF leaks (incisional, rhinorrhea, and otorrhea), pseudomeningoceles, or meningitis in the immediate and delayed (30-day) postoperative period. There were no cases of postoperative headaches at the 3 month and most recent follow-up examination

CSF egress is eliminated through monolayered, watertight dural closure and meticulous waxing of mastoid air cells. The autologous fat graft provides an excellent natural sealant over the dural closure and obliterates any anatomic dead space, shrinking to size postoperatively. The Medpor Titan implant possesses high tensile strength and a modulus of elasticity comparable to the bony tissue it is intended to replace. Moreover, it is highly malleable, lacks sharp, penetrating edges, and is osteo and angioconductive. These properties allow the implant to both buttress the underlying fat graft and serve as a physical barrier between the dura and subcutaneous tissues to prevent postoperative headaches. The Medpor Titan is also radio-opaque and MRI-compatible with excellent cosmetic outcome. Additional tissue sealants and postoperative lumbar drainage may not be necessary with this technique. Our series demonstrates that skull base reconstruction using autologous fat graft-assisted Medpor Titan cranioplasty after the far lateral transcondylar approach is an excellent surgical technique for preventing postoperative CSF leaks and headaches.

Conclusion:

Postoperative CSF leaks and postoperative headaches were successfully prevented through our described repair technique using an autologous fat graft-assisted Medpor Titan reconstruction after the far lateral transcondylar approach.

Table 2: Summary of relevant studies on prophylactic techniques to prevent CSF leak after far lateral approaches

Authors & Year	Procedures with CSF leak (%)	Site of Leak	Prophylactic Technique
<u>Xiao et al., 2013</u>	0/11 (0.0)	N/A	fat graft* + vascularized muscle pedicle <u>with fascia</u>
Nanda et al., 2011	0/3 (0.0)	N/A	fat graft, muscle graft, or fascia as dural patch <u>graft</u> + bone wax + fascibrin glue
Wang et al., 2011	2/18 (11.1)	incisional	<u>unspecified</u> dural patch graft
Kumar et al., 2009	0/4 (0.0)	N/A	lumbar drainage
Menezes 2008	0/25 (0.0)	N/A	fat graft + bone wax
Cueva et al., 2005	1/10 (10.0)	rhinorrhea, incisional	fat graft* + bone wax + fascia + post-op mastoid pressure dressing
Day 2004	0/2 (0.0)	N/A	temporalis muscle <u>graft</u> pack + fibrin glue + <u>gelatin sponge to trap bone dust</u>
D' Ambrosio et al., 2004	3/20 (15.0)	Incisional	fat graft ^b + lumbar drainage
Nanda et al., 2002	0/10 (0.0)	N/A	Unspecified <u>none</u>
Banerji et al., 1999	3/7 (42.9)		fat graft + fascia + lumbar drainage + <u>bone graft</u>
Salas et al., 1999	7/69 (10.1)	Incisional	fat graft* + bone wax + fascia + fibrin glue + lumbar drainage
Babu et al., 1994	4/22 (18.2) ^a	incisional	fat graft + fascia + fibrin glue + lumbar drainage
Kratimenos et al., 1993	0/15 (0.0)	N/A	
current study	0/13 (0.0)	N/A	fat graft* + bone wax + Medpor Titan + post-op mastoid pressure <u>dressing</u>

*Fat graft used to fill defect/cavity; ^aincludes both CSF leak and pseudomeningocele; ^bused in four patient

Table 1: [Characteristics of patients who underwent autologous fat-assisted Medpor Titan cranioplasty after far lateral transcondylar resection of craniovertebral lesions*](#)

Variable	Value (%)
no. of cases	13
no. of patients	12
mean age (yrs)	34.6 ± 17.4
sex (M/F)	3/9
tumor location	
CPA	4 (30.8)
FM	5 (38.5)
Cerebellum	1 (7.7)
Neurenteric	2 (15.4)
PICA	1 (7.7)
far lateral approach	
hemilaminectomy	11 (84.6)
condylar resection	10 (76.9)
fibrin glue	5 (38.5)
mean follow-up (months)	13.0 ± 9.0
complications	
incisional CSF leak	0 (0.0)
CSF rhinorrhea	0 (0.0)
CSF otorrhea	0 (0.0)
pseudomeningocele	0 (0.0)
meningitis	0 (0.0)
headache	
preoperative headache	7 (53.8)
postoperative headache	0 (0.0)
*Values indicate number of cases unless specified. Means are presented with SD. Abbreviations: CPA = cerebellopontine angle; FM = foramen magnum; PICA = posterior inferior cerebellar artery	

RYAN MEYER (NJMS 2016)

PROJECT TITLE: EFFECT OF LOCAL VANADIUM TREATMENT ON FRACTURE HEALING IN THE ELDERLY RAT

MENTOR: SHELDON LIN, MD, ASSOCIATE PROFESSOR

DEPARTMENT: ORTHOPAEDICS

Participation Description:

When I started working in the lab in March of this year, my first role was to generate a sufficient quantity of diabetic-prone and diabetic-resistant BB Wistar rats for a variety of projects we have in the works by breeding existing rats belonging to our lab's BB Wistar breeding colony. Gestation is approximately 30 days. I weaned the pups at 24 days of age. Around 60-70 days of age, I began monitoring the blood glucose levels of the young diabetic-prone rats twice weekly, as approximately one-third of BB Wistar diabetic-prone rats spontaneously become diabetic (blood glucose > 150 mg/dL) around 75 days of age. I separated out any rats that became diabetic and maintained them in a loosely controlled diabetic state, as required for the project, by continuing to monitor blood glucose twice weekly and treating any rats with a blood glucose level above 450 mg/dL with a subcutaneous implant consisting of 86% palmitic acid and 14% bovine insulin. The implant slowly releases insulin at a rate of ~2 U/24 hour for >40 days. The animals required for this particular project needed to be diabetic-resistant BB Wistar rats aged 190-195 days. The surgery involved a parapatellar approach for an injection of either saline or vanadyl acetylacetonate into the femoral canal. Part of my role this summer was to perform some of these surgeries. Because the project requires that the femurs be harvested four weeks post surgery, I have not yet been able to analyze and collect data on the rats on which I myself performed surgery. Therefore, the data presented in my abstract were generated prior to the beginning of my tenure in this lab. This is one of multiple ongoing projects in this lab that I am currently involved in and plan on seeing through to completion.

Objective:

Local intramedullary delivery of insulin has been shown by Paglia et al. (2012) to stimulate bone regeneration and shorten fracture healing time in the non-diabetic Wistar rat. However, insulin can cause hypoglycemia when it is not administered in a slow-release form. Furthermore, as a protein, insulin is not compatible with many slow-release drug formulations and it cannot be stored at room temperature. As an alternative treatment option, vanadyl acetylacetonate (VAC), an organic vanadium salt, has been identified as an insulin-mimetic mineral that is compatible with slow-release formulations.

Facchini et al. (2006) showed that oral vanadium administration increases bone formation rate, osteoid volume, and osteoid surface area in both diabetic and non-diabetic female Wistar rats aged 9-12 months. Cortizo et al. (1995) showed in an in vitro model using osteoblast-like cells that vanadium exerted biphasic effects: a low concentration of vanadium stimulated osteoblast proliferation and differentiation, but a high concentration inhibited these effects. The purpose of the present study was to examine the effects of a 1.5 mg/kg dose of local vanadium on bone healing in an elderly rat femoral fracture model.

Methods:

7 male diabetic-resistant BB Wistar rats aged 190-195 days were randomly assigned to evaluate outcome parameters for VAC-treated compared to saline control rats. To prepare the VAC, glass vials were first placed in an autoclave and sterilized for two hours in a dry cycle. The 1.5 mg/kg VAC solution was prepared with sterile water. 1 cc sterile syringes were loaded with either the VAC solution or saline.

General anesthesia was administered by intraperitoneal injection of ketamine (60 mg/kg) and xylazine (8 mg/kg), the right leg of each rat was shaved, and the incision site was cleansed with Betadine. A 1 cm medial, parapatellar skin incision was made over the patella. The patella was dislocated laterally and the intercondylar notch of the distal femur was exposed. An entry hole was made with an 18 gauge needle and the femur was reamed with the same needle. After irrigation, 0.1 ml of either saline or 1.5 mg/kg VAC solution was injected into the intramedullary canal of the right femur using a 1 cc sterile syringe. The wound was closed with 4-0 vicryl resorbable suture and topical antibiotic was applied to the incision site. A closed, midshaft fracture was then created using a three-point bending fracture instrument (BBC Specialty Automotive, Linden NJ) and confirmed with X-rays immediately post-fracture.

Four weeks following surgery, the rats were euthanized and their femora were resected. The femora were prepared and mechanically tested to failure at a rate of 2°/s of torsion. The maximum torque to failure, maximum torsional rigidity, shear modulus, and maximum shear stress were determined using standard equations.

Summary:

The average maximum torque to failure (Nmm) for 1.5 mg/kg VAC treated femora at four weeks post fracture was significantly greater than that of the saline control femora ($p < 0.05$), signifying greater bone strength (Table 1).

Conclusion:

These preliminary data from this ongoing project support the concept introduced by Cortizo et al. (1995) that low dose VAC is effective stimulating bone growth. The fact that a significant increase in a bone strength parameter, average maximum torque to failure, with VAC treatment was seen even with small experimental groups suggests that local VAC treatment could help to improve fracture healing in the elderly population.

Figures:

	Maximum Torque to Failure (Nmm)	Maximum Torsional Rigidity (Nmm ² /rad)	Effective Shear Modulus (MPa)	Effective Shear Stress (MPa)	Mean Angle at Failure (degrees)
Saline Control (n=3)	220 ± 76	4.2x10 ⁴ ± 1.7x10 ⁴	2.2x10 ³ ± 1.5x10 ³	36 ± 5	6 ± 3
1.5 mg/kg VAC (n=4)	324 ± 83	3.0x10 ⁴ ± 1.8x10 ⁴	1.3x10 ³ ± 1.3x10 ³	43 ± 17	12 ± 4
	Percent Maximum Torque to Failure	Percent maximum Torsional Rigidity	Percent Effective Shear Modulus	Percent Effective Shear Stress	-----
Saline Control (n=3)	25 ± 7	62 ± 19	24 ± 10	15 ± 7	NA
1.5 mg/kg VAC (n=4)	44 ± 10*	56 ± 37	16 ± 18	16 ± 4	NA

Table 1. Mechanical testing data for elderly rat femora treated with 1.5 mg/kg VAC or saline at four weeks post fracture. The data represent average values ± standard deviation. * Represents values statistically higher than saline control, p < 0.05. Student t-test between two groups.

References:

Cortizo AM and Etcheverry SB. 1995. Vanadium derivatives act as growth factor—mimetic compounds upon differentiation and proliferation of osteoblast-like UMR106 cells. *Mol Cell Biochem* 145(2):97-102.

Facchini, DM, Yuen VG, Battell ML, McNeill JH, Grynpas MD. 2006. The effects of vanadium treatment on bone in diabetic and non-diabetic rats. *Bone* 38:368-77.

Paglia DN, Wey A, Breitbart EA, Faiwizewski J, Mehta SK, Al-Zube L, Vaidya S, Cottrell JA, Graves D, Benevenia J, O'Connor JP, Lin SS. 2012. Effects of local insulin delivery on subperiosteal angiogenesis and mineralized tissue formation during fracture healing. *J Orthop Res* 31:783-91.

SMIRNOV EXILUS (RUTGERS UNIVERSITY, 2016)

PROJECT TITLE: EFFECT OF A DEFICIENCY IN *USPA* (ENCODING A UNIVERSAL STRESS PROTEIN) ON ANTIMICROBIAL SUSCEPTIBILITY

MENTOR: XILIN ZHAO, PH.D, ASSOCIATE PROFESSOR

DEPARTMENT: NJMS– PUBLIC HEALTH RESEARCH INSTITUTE



Objective

Universal stress proteins comprehensively include an overwhelming variety of proteins synthesized by bacteria, archaea, fungi, flies, and certain plants. Universal stress proteins (Usp) are generally induced in response to exogenous stressors, such as starvation for carbon, nitrogen phosphate, or amino acids, exposure to extreme temperatures or antibiotics, and entering stationary growth phase. *Escherichia coli* has six different *usp* genes: *uspA*, *uspC*, *uspD*, *uspE*, *uspF*, and *uspG*. Each family of the *usp* genes is believed to be unique in its role to regulate some biochemical process within the cell though the exact function of the proteins has not been determined. The induction of *uspA* in *E. coli* occurs immediately after nutrient depletion that causes growth inhibition. In other words, *uspA* is induced as a result of starvation as the cells enter stationary phase. The transition from exponential growth to stationary phase significantly increases viability of cells when exposed to stressful conditions, such as oxidant, heat, and antibiotics. It is observed that a strain devoid of the *uspA* gene die prematurely in stasis. Thus we suspect that a *uspA* mutant might exhibit sensitivity to antibiotics when compared to its isogenic wild-type parental strain. Our objective is then to assay the relative viability of a *uspA* mutant to the wild-type strain when exposed to antibiotics.

Methods

The experiment is performed during stasis. To ensure that the cells are indeed in stationary phase, they are cultivated in Luria-Bertani (LB) broth and let grown overnight in 37 degree Celsius shaker with 250 rpm shaking. Two flasks containing 10 ml of LBbroth is inoculated with a single colony of *uspA* mutant and its wild-type control strain, respectively. The cultures are then incubated overnight. During the 24-hour period, the cells grow to maturity and divide until the medium is depleted of nutrients and enriched with wastes, thereby causing the cells to enter the phase of stasis. One ml of culture is then transferred to six different test tubes into which drugs are added. At the time of drug addition, a control is established by diluting 50 microliters of culture from each strain tenfold to 10 million-fold and plating them on LB agar. This control, referred to as time zero, will serve as a baseline against which viability percentages will be determined. Note that no drug is added to the control.

The drug concentration in the test tubes ranges from fifty times the minimum inhibitory concentration (MIC) to 1.5625 times MIC, with a differential drug concentration of two-fold between test tubes. The MIC is the minimum concentration of drug that inhibits growth of a diluted ($\sim 10^5$ bacteria/ml) culture after an overnight incubation. After the addition of the drug, the test tubes are placed in the 37 C shaker for two hours. After this time interval has elapsed, 50 microliters from each test tube is diluted and plated in the same manner as the control. The agar plates are then incubated overnight. The next day the bacterial colonies are counted and the survival percentage is obtained for each dilution and drug concentration using the time zero control.

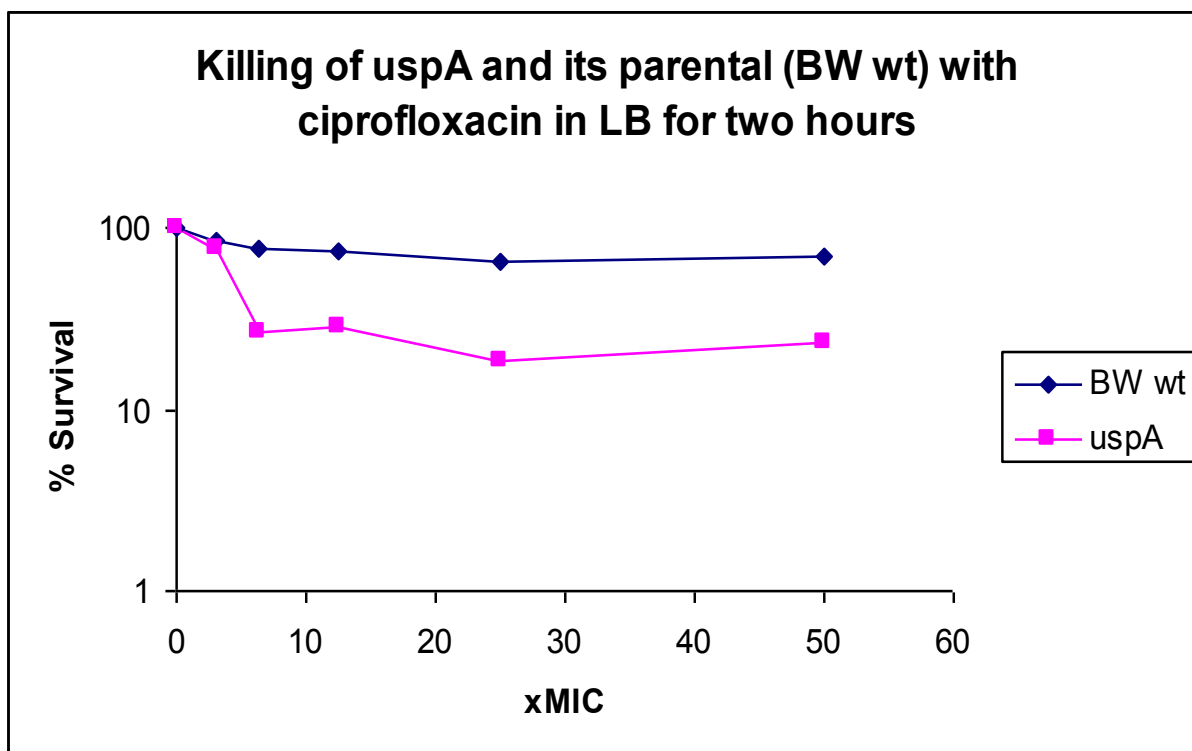
Summary

We assayed to determine the relative sensitivity of the *uspA* mutant using the above described methods on numerous occasions. Conventionally, an accepted difference in phenotypes between two strains should be no less than tenfold. Our results do not show such marked difference between the two strains. The largest separation between the two is threefold, which might be within the margin of experimental error. However, since the data obtained in numerous occasions show that the *uspA* mutant is at least twice as sensitive to antibiotics when compared to the isogenic wild-type, a small difference may indeed exist between the two strains.

Conclusion

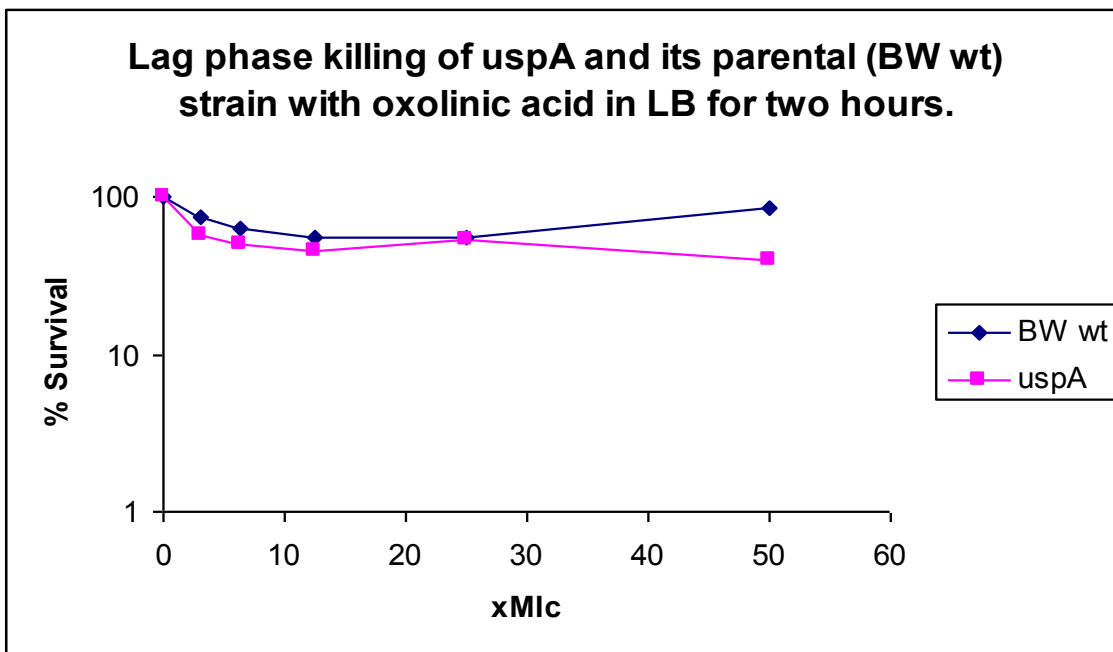
As demonstrated before, a *uspA* mutant survives poorly in stationary phase. This defect prompted us to suspect that the mutant might prove to be relatively sensitive to antibiotics during stasis. An experiment was design to explore our suspicion. The data reveals a very small difference between the wild-type strain and the *uspA* mutant using this particular approach. We cannot conclude, without reserve, that there is or there is not a solid difference between the two stains since the assay we used turn to have a two-fold error range. Consequently our findings are inconclusive. We look to reengineer our experiment and approach it from a different perspective.

Figure 1.



In figure one, the x-axis is calibrated with factors of the minimum inhibitory concentration and the y-axis represents the percent survival of the two strains. The killing is done with ciprofloxacin, a fluoroquinolone that interferes with DNA synthesis. During the stationary phase, the bacteria lack the nutrients to undergo division. Therefore there is little to no DNA synthesis during that phase. As a result, the graph shows that only marginal killing was observed even when the concentration of the drug is an impressive 50 times MIC. As the legend indicates, the diamonds represent the BW wild-type strain and the squares represent the *uspA* mutant. The largest difference between the two strains occurs at 25 x MIC where the survival of the wild type strain is roughly 66% and that of the mutant is 19%. This slight difference in viability is consistent in all the experiments performed.

Figure 2.

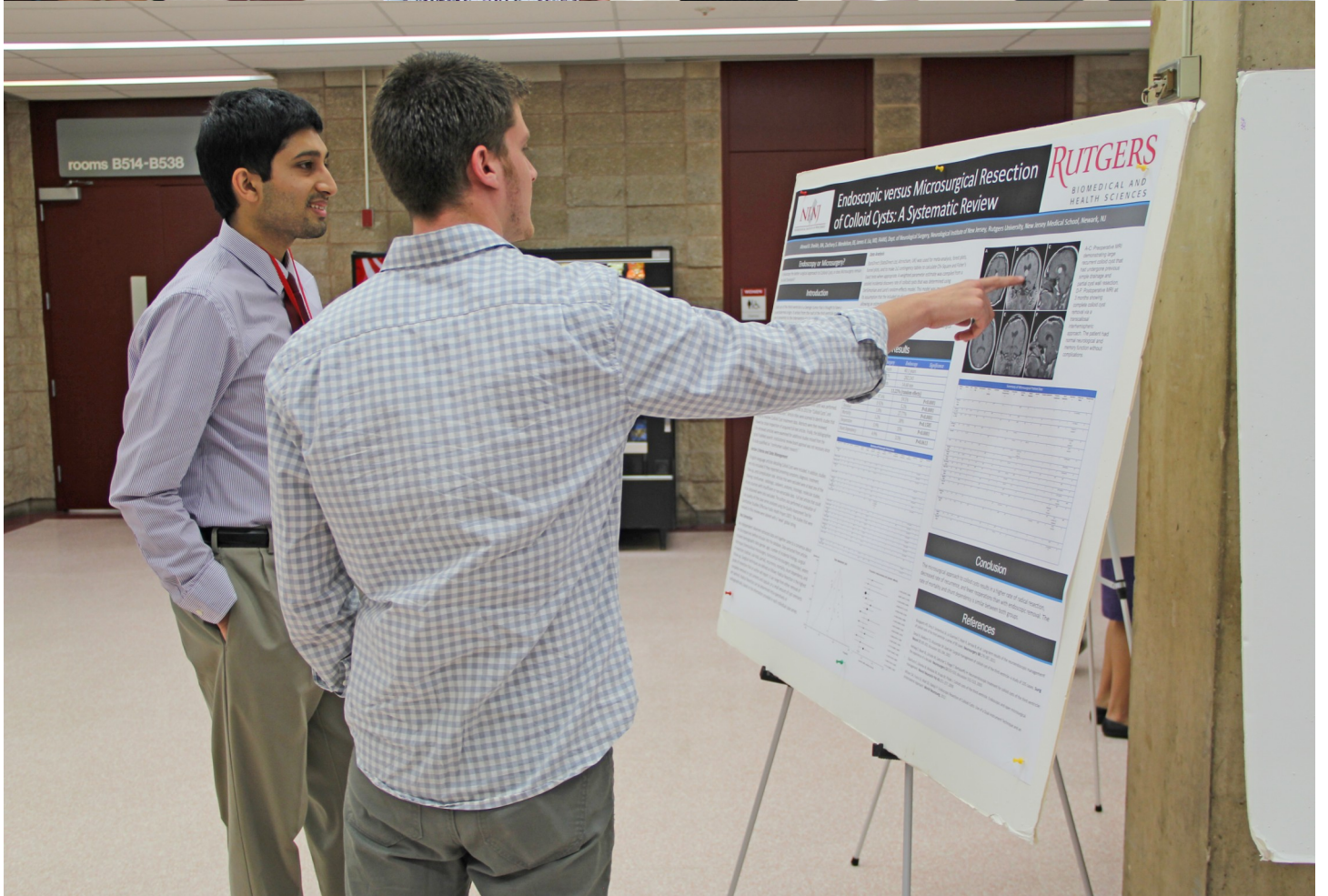
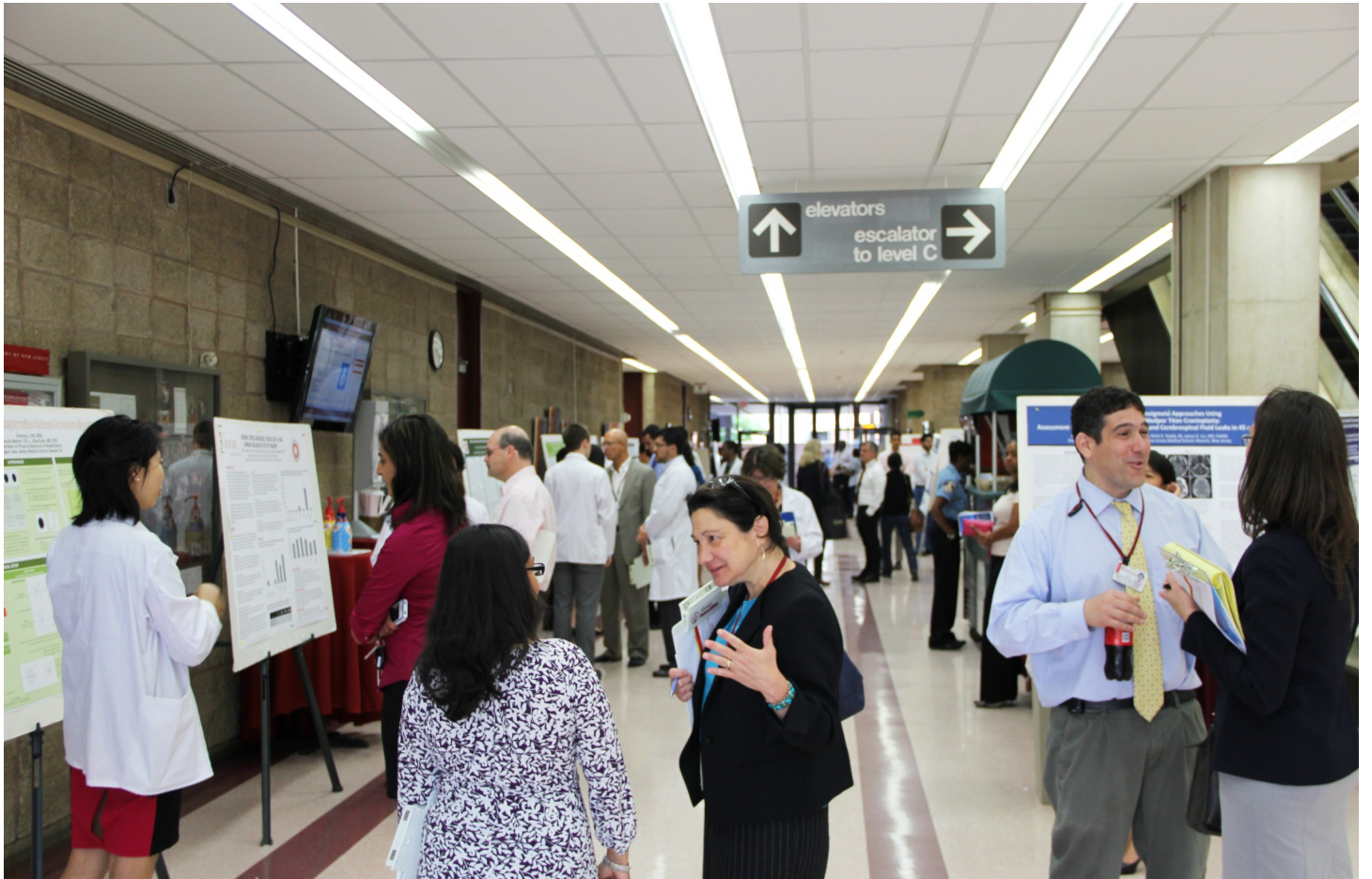


In figure 2, the axes are calibrated in the same manner as figure one. The graph represents an experiment performed during the lag phase of growth. During the lag phase the cells are maturing and adapting to environmental conditions and therefore are not yet ready to divide. Similar to stasis, there is little biochemical activity. The drug of choice for this experiment, oxolinic acid, is a broad spectrum quinolone and works best when the cells are actively replicating. As expected, there is minimal killing during that phase. We observe that the two strains show the same degree of viability under same conditions and that the threefold difference we saw earlier is no longer present. This might be due to the fact the cells are no longer in stasis and show similar characteristics. This leads us to believe that there is in fact something to explore during stasis and antibiotic sensitivity of *uspA* mutant.

HIGHLIGHTS FROM THE SSRP POSTER SYMPOSIUM THURSDAY, JULY 25, 2013

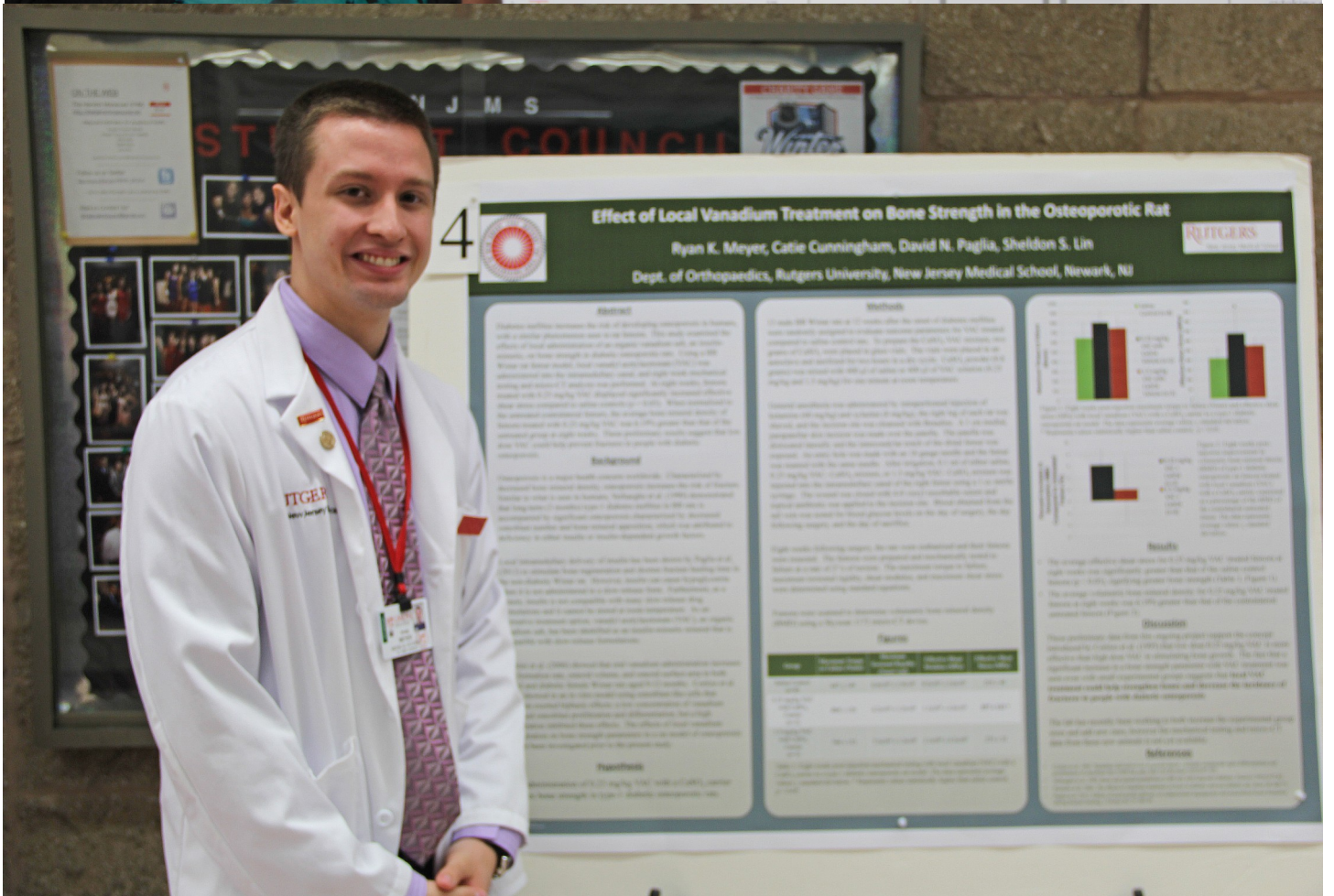
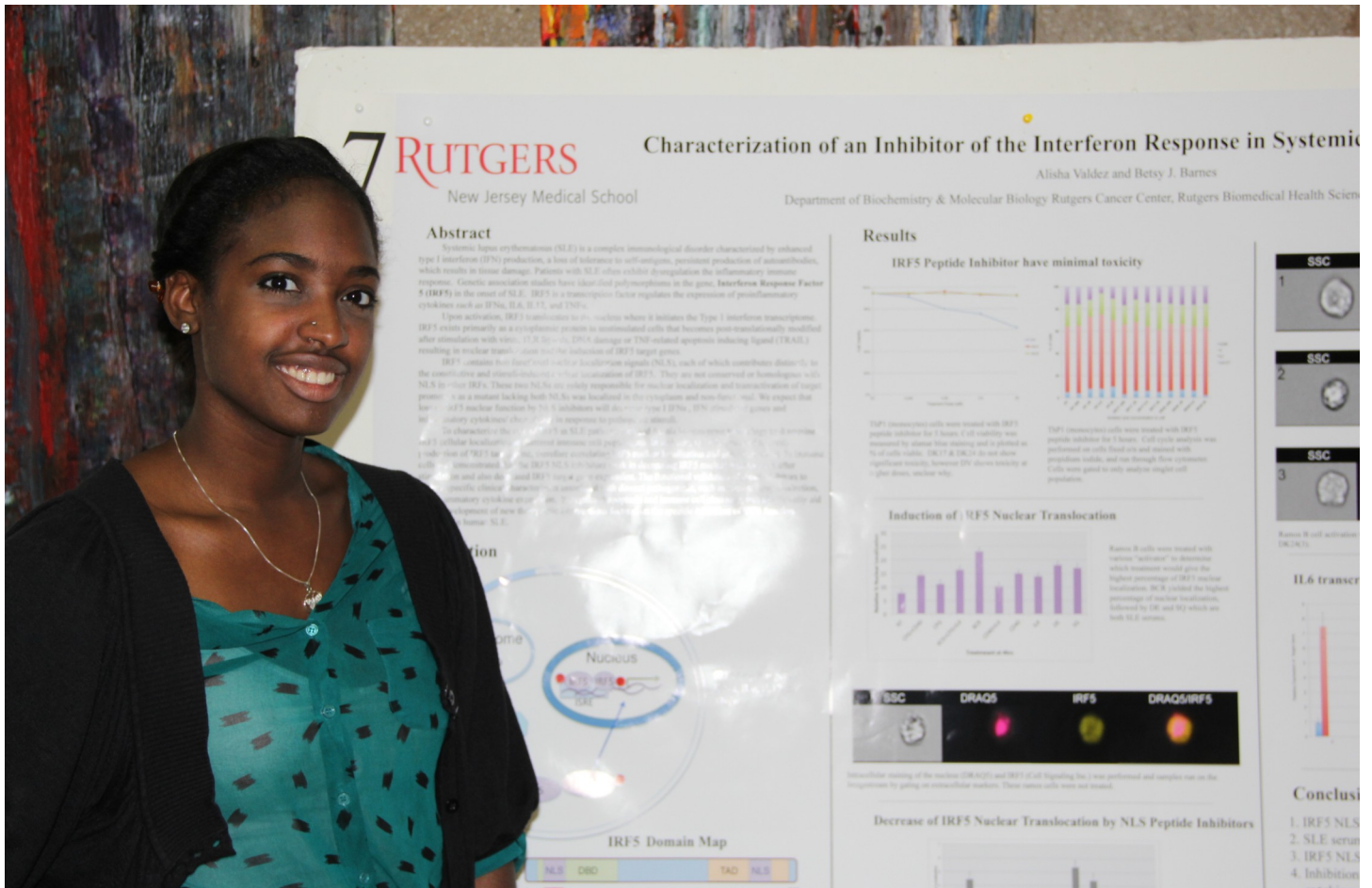














Vascular Techniques for Trauma Patients with Cerebrovascular Injuries

Ghislaine M. Cruz, Yazan Alderazi MD, Chirag D. Gandhi MD, E. Jesus Duffis MD
 Department of Neurological Surgery
 Rutgers, New Jersey Medical School, Newark, NJ

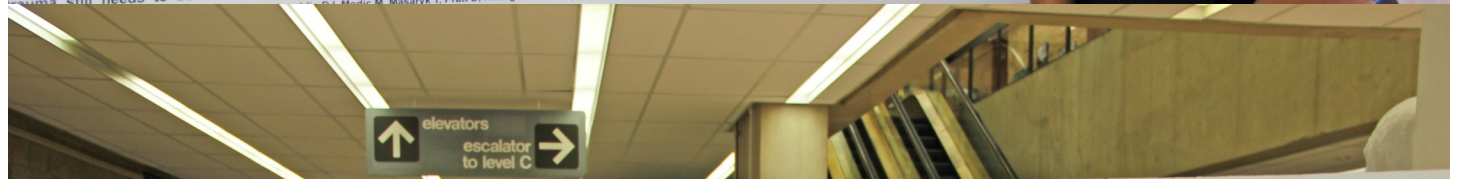


Type of Injury	Method of Diagnosis	Treatment
Carotid artery dissection	CT Angiography, Duplex Scan, Enhanced CT, Conventional Angiography	Anti-coagulants, Antiplatelets, Stent
Vertebral artery dissection	CT Angiography, CT Scan, DS Angiography, MRI	Anti-coagulants, Antiplatelets, Stent
Carotid-cavernous fistula (CCF)	DS Angiography, MRI, Conventional Angiography	Stent, Detachable balloon, Coil embolization
AV fistula	CT Angiography, CT Scan, Conventional Angiography	Covered stent, Coil embolization
VA occlusion	CT Angiography, Four vessel Angiography	Coil embolization
Transection	Conventional Angiography	Coil embolization
Pseudoaneurysm	CT Angiography, CT Scan, Duplex Scan, MDCT Angiography, Ultrasonography, Conventional Angiography	Coil embolization, Stent-graft, Gelfoam embolization
Intracranial Dissecting Aneurysms/Pseudoaneurysms	CT Angiography, Conventional Angiography	Coil embolization, Stent

Figure 1. Research Index for 150 patients that sustained blunt or penetrating injuries to the neck developed lesions to the carotid or vertebral artery; dissections with or without pseudoaneurysms (73.9%), carotid-cavernous fistula (CCF) (24.8%), Arteriovenous (AV) fistula (0.7%) or transection (0.7%). Based on the patients' clinical presentation and extent of injuries, patients were diagnosed and treated accordingly.

References

- Witz M, Gepstein R, Paron H, Shnaker A, Lehmann J, Gryton I, et al. Endovascular treatment of an open cervical fracture with carotid artery tear. *European Spine Journal*. 2006;15(5):650-2.
- Seth R, Obuchowski A, Zoarski G. Endovascular repair of traumatic cervical internal carotid artery injuries: a safe and effective treatment option. *American Journal of Neuroradiology*. 2013;34(6):1219-26.
- Faure E, Canaud L, Marry-Ane C, Ainc P. Endovascular Repair of a Left Common Carotid Pseudoaneurysm Associated With a Jugular-Carotid Fistula After Gunshot Wound to the Neck. *Annals of Vascular Surgery*. 2012.



The Utility of Pre-procedural Anti-platelet Assays For Neurovascular Stenting Procedures

C. Ayala NJMS'16, P. Jin NJMS'14, C. Gandhi MD, C. Prestigiacomo, T. Kass-Hout MD, J. Duffis MD
 Department of Neurosurgery, New Jersey Medical School, Newark NJ

Background and Purpose:

Previous studies have shown that patients with anti-platelet therapy resistance have a higher rate of thromboembolic complications such as stroke and hemorrhage. Others attempted to increase therapeutic dosages without success. Since 2007, UH has tested the platelet function of patients undergoing neurovascular stents (NS). Our data shows for the first time a change of treatment regimen away from traditional anti-platelets for those resistant. The purpose of this study is to compare the impact of this in outcomes and management compared to reported literature.

Methods:

NS patient data was peri-procedurally reviewed for stroke and hemorrhage. Platelet reactivity tested with VerifyNow to salicylic acid and clopidogrel pre-procedural therapy was recorded. Change in management was recorded. The PubMed database was searched for articles specifying complication rates of NS up to 30 days. Data was then compared.

Acknowledgments:

I would like to thank Dr. Duffis, Dr. Kass-Hout, Dr. Gandhi and Dr. Prestigiacomo for their kind advice and encouragement.

Results:

	UH	Reported
Cervical ICA	13	5218
IC stents	17	2105
IC Hemorrhage Studied	17	386
Non-Responder Salicylic Acid	2	N/A
Non-Responder Clopidogrel	9	N/A
Changed therapy regimen	8	N/A
30d Incidence Cervical Stroke	1	185
30d Incidence Intracranial Stroke	2	133
30d Incidence IC Hemorrhage	1	25
Percentage Stroke Cervical Stents	7.69%	3.52%
Percent Stroke IC Stents	11.76%	6.31%
Percentage Hemorrhage	5.88%	6.48%
Average Complication rate	8.44%	5.43%

Conclusions:

Our patient population showed a similar rate of complications to literature reported without pre-procedural testing. Our data reports for the first time a null impact to change in therapeutic agent for NS. A larger experimental population will be needed to verify the utility of pre-procedural anti-platelet assays for NS patients.

RUTGERS New Jersey Medical School

Reconstruction After Retrosigmoid Approaches Using Autologous Fat-Assisted Medpor Titan Cranioplasty: Assessment of Postoperative Headaches and Cerebrospinal Fluid Leaks in 45 cases

Phoebe Y. Ling, BS, Zachary S. Mendelson, BS, Rohit K. Reddy, BS, James K. Liu, MD, FAANS
Department of Neurological Surgery, Rutgers New Jersey Medical School, Newark, New Jersey

Introduction

The retrosigmoid approach used in skull base surgery offers an excellent corridor to access various tumors and vascular lesions in the posterior fossa and cerebellopontine angle. Postoperative CSF leaks and headaches, however, still remain frequent complications.^{1,2,4} Incidences for CSF leak (incisional, rhinorrhea, and otorrhea) after retrosigmoid approach have ranged from 2 to 30%^{3,4} and incidences for postoperative headaches have ranged from 4 to 73%.^{5,6} Meticulous dural and bony cranial repair is paramount for prevention of CSF leaks and headaches, and several different prophylactic surgical techniques have been proposed by others in the past.⁷

Purpose

We present a novel reconstruction technique with fat-assisted Medpor Titan cranioplasty after retrosigmoid approaches to minimize postoperative headaches and CSF leaks. We evaluate outcomes in all patients who have undergone the technique at our institution, and compare our findings with other prophylactic surgical techniques found in literature.

Methods

A retrospective chart review was conducted on all cases (n=45) with the reconstruction technique after a retrosigmoid approach performed by the senior author (J.K.L.) between September 2009 and May 2013. Factors analyzed were postoperative CSF leak (incisional, rhinorrhea, otorrhea), postoperative headache, length of hospital stay, and length of follow-up.

Results

The study population included 26 females and 19 males with a mean age of 47.5 years (range 27-80 years). Indications for surgery were meningiomas 12/45 (26.7%), acoustic neuromas 9/45 (20.0%), epidermoid tumors 6/45 (13.3%).

There were no postoperative CSF leaks (incisional, otorrhea) (0%), pseudomeningocele (0%), or meningeal cysts. There were no new onset of postoperative headaches at the 3-month and most recent follow-up.

Mean duration of postoperative hospital stay was 4.1 months. Mean of last follow-up with surgeon was 41.1 months.

Conclusion

Our preliminary assessment suggests that our novel technique for retrosigmoid approaches using an autologous fat-assisted Medpor Titan implant cranioplasty prevents postoperative headaches and CSF leaks. Meticulous dural closure, waxing off mastoid air cells to occlude the ear, obliterating the craniectomy dead space over with an autologous fat graft, and closing the craniectomy defect by performing a cranioplasty with a Medpor Titan implant is a material that is malleable yet retains shape, without sharp edges, conducive to rapid bony growths, ideal for rapid wound reentry, radiotherapy, and an excellent option for cranioplasty.

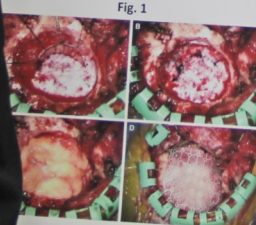


Fig. 1

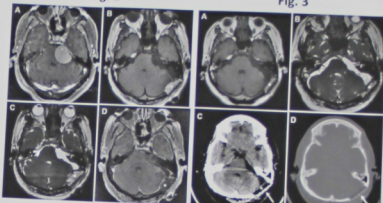


Fig. 2

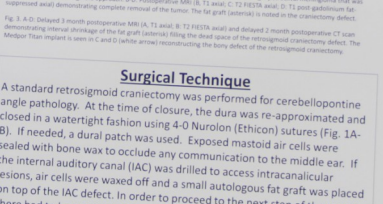


Fig. 3

Surgical Technique

A standard retrosigmoid craniectomy was performed for cerebellopontine angle pathology. At the time of closure, the dura was re-approximated and closed in a watertight fashion using 4-0 Nurodon (Ethicon) sutures (Fig. 1A-B). If needed, a dural patch was used. Exposed mastoid air cells were sealed with bone wax to occlude any communication to the middle ear. If the internal auditory canal (IAC) was drilled to access intracanalicular lesions, air cells were waxed off and a small autologous fat graft was placed on top of the IAC defect. In order to proceed to the next step of the repair, autologous fat graft was drilled to the dural suture line. Then, an autologous fat graft was harvested from the abdomen and placed over the craniectomy defect to just beyond the level of the outer table of the cranium (C). Finally, the fat graft was secured and bolstered up against the dural closure by performing a cranioplasty with a Medpor Titan implant (MTM, Porex Surgical), a titanium mesh plate embedded in two layers of porous polyethylene (D). The implant is readily shaped and contoured with surgical scissors to provide adequate coverage of the bony defect. The Medpor Titan is secured to the bone edges with titanium screws. Standard multilayer soft tissue wound closure is performed and a mastoid pressure dressing was applied postoperatively for 48 hours. Postoperative lumbar drainage was not used.

References

1. Anand SP, Terry C, Cohen-Gadol AA. Surgery for vestibular schwannoma: a systematic review. *Neurosurg Focus* 2012; 33:E14.
2. O'Brien MC, Niranjan TN, Mehta A. Retrosigmoid approach: indications, techniques, and outcomes. *Neurosurg Focus* 2012; 33:E14.
3. Kulkarni AV, Mehta TN, Gadhia JG, Cohen N, Mehta A. Prevention and management of cerebrospinal fluid leaks after retrosigmoid craniotomy. *J Neurosurg* 2004; 101:401-405.
4. Niranjan MC, Cohen N, Gadhia JG, Cohen N, Mehta A. Retrosigmoid approach for cerebellopontine angle meningiomas. *The Neurosurgeon* 2012; 122:2019-2023.
5. Niranjan MC, Cohen N, Gadhia JG, Cohen N, Mehta A. Retrosigmoid approach for cerebellopontine angle meningiomas. *The Neurosurgeon* 2012; 122:2019-2023.
6. Niranjan MC, Cohen N, Gadhia JG, Cohen N, Mehta A. Retrosigmoid approach for cerebellopontine angle meningiomas. *The Neurosurgeon* 2012; 122:2019-2023.
7. Niranjan MC, Cohen N, Gadhia JG, Cohen N, Mehta A. Retrosigmoid approach for cerebellopontine angle meningiomas. *The Neurosurgeon* 2012; 122:2019-2023.

Contact Information:
James K. Liu, MD
james.liu.md@rutgers.edu

Effect of Local Vanadium Treatment on Bone Strength in the Osteoporotic Rat

Ryan K. Meyer, Katie Cunningham, David N. Pagan, Dheeran S. Un
Dept. of Orthopaedics, Rutgers University, New Jersey Medical School, Newark, NJ

Abstract

Vanadium is a trace element that has been shown to have a beneficial effect on bone strength in the osteoporotic rat. The purpose of this study was to evaluate the effect of local vanadium treatment on bone strength in the osteoporotic rat. The study was conducted in a laboratory setting and involved the use of rats with osteoporosis. The rats were divided into two groups: a control group and a vanadium-treated group. The vanadium-treated group received a local injection of vanadium into the bone. The rats were then subjected to a mechanical test to measure bone strength. The results of the study showed that the vanadium-treated group had significantly higher bone strength compared to the control group. This suggests that local vanadium treatment may be a promising approach for improving bone strength in the osteoporotic rat.

Background

Osteoporosis is a common condition that affects millions of people worldwide. It is characterized by a loss of bone density, which makes the bones more fragile and prone to fractures. One of the main causes of osteoporosis is a deficiency of calcium and vitamin D. However, there are also other factors that can contribute to the development of osteoporosis, such as aging and certain medications. Finding effective treatments for osteoporosis is a major goal of medical research.

Methods

In this study, we used a rat model of osteoporosis. The rats were divided into two groups: a control group and a vanadium-treated group. The vanadium-treated group received a local injection of vanadium into the bone. The rats were then subjected to a mechanical test to measure bone strength. The results of the study showed that the vanadium-treated group had significantly higher bone strength compared to the control group.

Results

The results of the study showed that the vanadium-treated group had significantly higher bone strength compared to the control group. This suggests that local vanadium treatment may be a promising approach for improving bone strength in the osteoporotic rat.

Conclusion

Local vanadium treatment significantly improved bone strength in the osteoporotic rat. This suggests that vanadium may be a potential therapeutic agent for osteoporosis.



The Use of Deep Brain Stimulation in Tourette's Syndrome

Janine Rotsides, BS and Antonios Mammis, MD

Introduction

Tourette's syndrome (TS) is a childhood, psychiatric disorder characterized by the presence of multiple, involuntary motor and vocal tics, commonly associated with other behavioral disorders including attention deficit hyperactivity disorder, obsessive-compulsive disorder, self-injurious behaviors, anxiety, and depression. Symptoms typically begin during the first decade of life and wax and wane throughout its course. The developing neurophysiology of TS suggests that a dysfunction in the basal ganglia and cortical-striatal-thalamic-cortical circuitry underlies the generation of tics. TS can be effectively managed with psychobehavioral and pharmacological treatments and most patients experience a spontaneous improvement in tics in adulthood. However, symptoms may persist and cause functional impairment in a small subset of patients, necessitating available therapies.

In such patients, surgical intervention may be considered. In 1999, deep brain stimulation (DBS) was proposed as a possible treatment option for severe Tourette's syndrome. Since then, multiple target sites have been used, including the medial globus pallidus, anterior limb of the internal capsule/nucleus accumbens (ALIC-NA), and subthalamic nucleus. While stimulation at each of these target sites has been shown to reduce tic severity, the optimal target is yet to be determined.

Materials and Methods

Results

Table 1. Thalamic Targets of DBS for TS

Author & Year	n	Target	Follow-up	Outcomes
Vandewalle et al., 2003	3	CM-Vo-Sp	Patient 1: 5 years Patient 2: 1 year Patient 3: 8 months	90.1% reduction in tic score 72.2% reduction in tic score 82.6% reduction in tic score
Bayna et al., 2007	1	CM-Vo-Sp	2 years	66% reduction in tic score
Maciunas et al., 2007	5	CM-PT	3 months	Mean 44% tic reduction
Servello et al., 2008	18	CM-PT-Vo	3-18 months	Mean 28.6% reduction in tics
Shields et al., 2008	1	CM-PT-Vo	3 months	41% reduction in tic score 80% reduction in overall impairment
Porta et al., 2009	15	CM-PT-Vo	2 years	YGSS score: 76.5 → 36.6 YBOCS score: 20.9 → 14.4 BDI score: 30.7 → 22.7 STAI score: 44.2 → 29.5
Servello et al., 2010	19	CM-PT-Vo	2 years	YGSS score: 75.5 → 40 YBOCS score: 19.6 → 16.3 BDI score: 26.2 → 17.7 STAI score: 45.8 → 31.3
Ackermans et al., 2010	2	CM-Vo-Sp	Patient 1: 10 years Patient 2: 6 years	92.6% reduction in tic score 78% reduction in tic score
Ackermans et al., 2011	6	CM-Vo-Sp	1 year	Mean 49% improvement in tic severity
Kaibuchi et al., 2011	3	CM-PT-Vo	1 year	55.70% decrease in YGSS score
Pullen et al., 2011	1	CM-PT	18 months	YGSS score: 75 → 40
Lee et al., 2011	1	CM-PT	6 months	62% decrease in tic severity 70% reduction in tics
Savica et al., 2012	3	CM-PT	1 year	78% improvement in overall impairment

YGSS = Yale Global Tic Severity Scale, YBOCS = Yale-Brown Obsessive Compulsive Scale, BDI = Beck Depression Inventory, STAI = State-Trait Anxiety Inventory

Table 2. Pallidal Targets of DBS for TS

Author	n	Target	Follow-up	Outcome
Van der Linden et al., 2002	1	Posteroventral GPi	6 months	93% tic reduction
Diederich et al., 2005	1	Posteroventral GPi	14 months	78% decrease in tic frequency BDI score: 8 → 2 STAI score: 66 → 40
Houeto et al., 2005	1	Anteromedial GPi, thalamus (CM-PT)	2 months for each condition, 2 years	CM-PT: 65% tic reduction Gpi: 65% decrease in tics Both: 70% tic reduction Final: remained improved
Shahid et al., 2007	1	Posteroventral GPi	6 months	84% tic reduction 69% improvement in OCD symptoms
Weller et al., 2008	3	Anteromedial GPi, thalamus (CM-PT)	Patient 1: 60 months Patient 2: 27 months Patient 3: 20 months	82% reduction in tics with combined stimulation stable reduction in tics with pallidal stimulation 74% reduction in tics with combined stimulation
Wang et al., 2008	1	Posteroventral GPi	1 year	YGSS score: 93 → 40

Table 3. Other DBS Targets for TS

Author	n	Target	Follow-up	Outcomes
Flaherty et al., 2003	1	ALIC-NA	18 months	40% decrease in global tic severity
Kahn et al., 2007	1	ALIC-NA	2.5 years	40-50% tic reduction
Zaback et al., 2008	1	Unilateral right NA	28 months	Total # tics: 236 → 38
Shiels et al., 2008	1	ALIC-NA (later revised to thalamus)	18 months	21% reduction in tics 25% improvement in overall impairment
Neuner et al., 2009	1	ALIC-NA	36 months	44% tic reduction
Martinez-Torres et al., 2009	1	Subthalamic nucleus	1 year	97% decrease in tic frequency
Schwab et al., 2012	1	NA	7 months	YGSS score: 63 → 13 YBOCS score: 39 → 6

Discussion

Evidence supporting the effectiveness of deep brain stimulation for Tourette's syndrome has been growing in recent years and it may be an appropriate and beneficial treatment option in some cases. DBS targeting the medial thalamus, globus pallidus, anterior limb of the internal capsule/nucleus accumbens, and subthalamic nucleus have all shown to improve tic severity. Improvement in other behavioral symptoms varies among target sites. The medial thalamus is most widely used target, but increasing evidence supports the use of the globus pallidus well.

The lack of randomized, controlled trials makes definitive conclusions about the relative efficacy of target over another impossible. Further research comparing one target over another may have produced contradictory results. Future studies should aim to include larger sample sizes, standardized methods of evaluation, and standardized outcome measures, and follow-up periods.

Select Reference



Endoscopic versus Microsurgical Resection of Colloid Cysts: A Systematic Review

Ahmed B. Sheikh, BA, Zachary S. Mendelson, BS, James K. Liu, MD, FAANS, Dept. of Neurological Surgery, Neurological Institute of New Jersey, Rutgers University, New Jersey Medical School,

Endoscopy or Microsurgery?

Is Endoscopy the better surgical approach to Colloid Cysts, or does Microsurgery remain the Gold Standard?

Introduction

Colloid cyst of the third ventricle is a benign tumor that is thought to have a neuroectodermal origin. It arises from the roof of the third ventricle and extends into the lumen in proximity to the interventricular foramen of Monro. Symptoms develop when the foramen of Monro is obstructed, leading to a build-up of cerebrospinal fluid (CSF) resulting in acute hydrocephalus or in extreme cases sudden death. Of intracranial tumors, the incidence of colloid cyst ranges from 0.5-2.0%. Surgical resection is often chosen for large symptomatic colloid cysts, while small asymptomatic lesions require close observation with serial MR imaging. Currently, surgical interventions include CSF shunting, aspiration, microsurgical resection and recently endoscopic removal. There has been increased popularity in endoscopic approaches for colloid cyst resection because some feel that it is a less invasive technique than traditional transcortical or transcallosal microsurgical approaches.

Materials and Methods

Literature Search Strategy

A systematic review of published literature on cases of Colloid Cysts was performed. The PubMed database was searched from 1990 to 2013 for "Colloid Cysts", and "Colloid AND cyst AND resection." Article titles were scanned to identify studies that seemed to involve Colloid Cyst treatment data. Abstracts were then reviewed, followed by close inspection of acquired full-text articles. Finally, the bibliographies of the retrieved articles were examined for additional studies missed from the original PubMed search. Institutional review board approval was not necessary since this study qualified as "nonhuman subject research."

Selection Criteria and Data Management

All English-language articles detailing Colloid Cysts were included. In addition, studies were only included if they reported presenting symptoms, diagnosis, treatment, follow-up, and complication rate. Articles that were excluded were at least one of the following: nonhuman, radiologic, cadaveric, anatomic, histologic, molecular studies, and any sources with insufficient or non-extractable data. Full text articles that could not be obtained were also excluded. The authors also performed an evaluation of study quality of the case series analyzed using the Quality Assessment Tool for Quantitative Studies (Effective Public Health Project 2007). The studies that were assessed in this review were labeled with a "weak" global rating.

Data Extraction

Two independent observers extracted data and together came to a consensus about any discrepancies before inclusion into the database. Data extracted from articles included demographic data (gender, age), number of incidental findings, surgical technique (transcallosal microsurgery, transcortical microsurgery, endoscopy), extent of resection (radical, sub-total, partial), recurrence, mortality, shunt dependency, and follow-up. Surgical techniques are defined as follows: Radical Resection is the highest grade of resection that an author will report. It can range from either removal of complete removal or cyst contents and capsule, or a small amount of cyst remnants left behind. Radical Resection can be determined intra-operatively or radiographically, based on the information provided in each individual case series.

Results

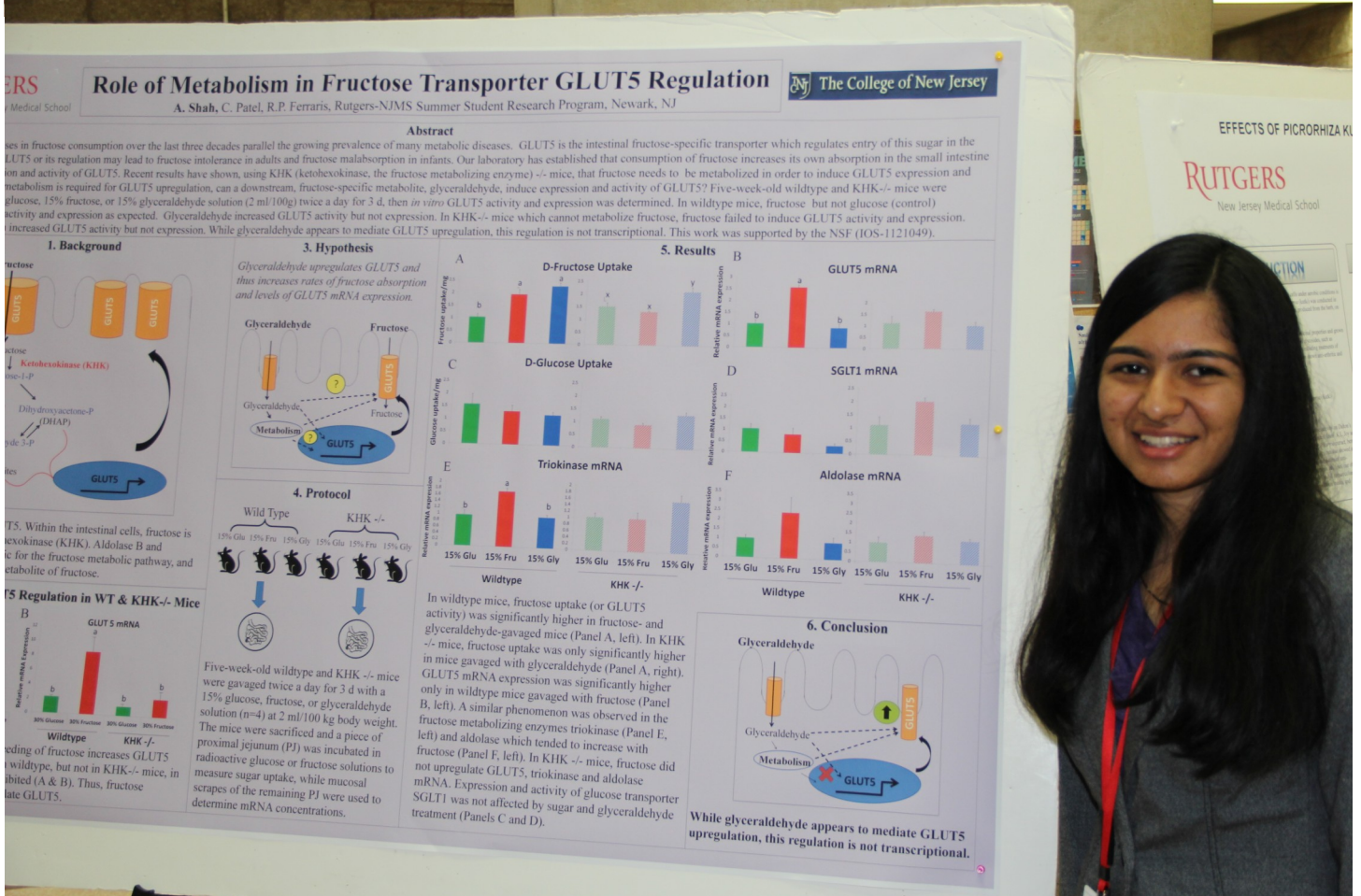
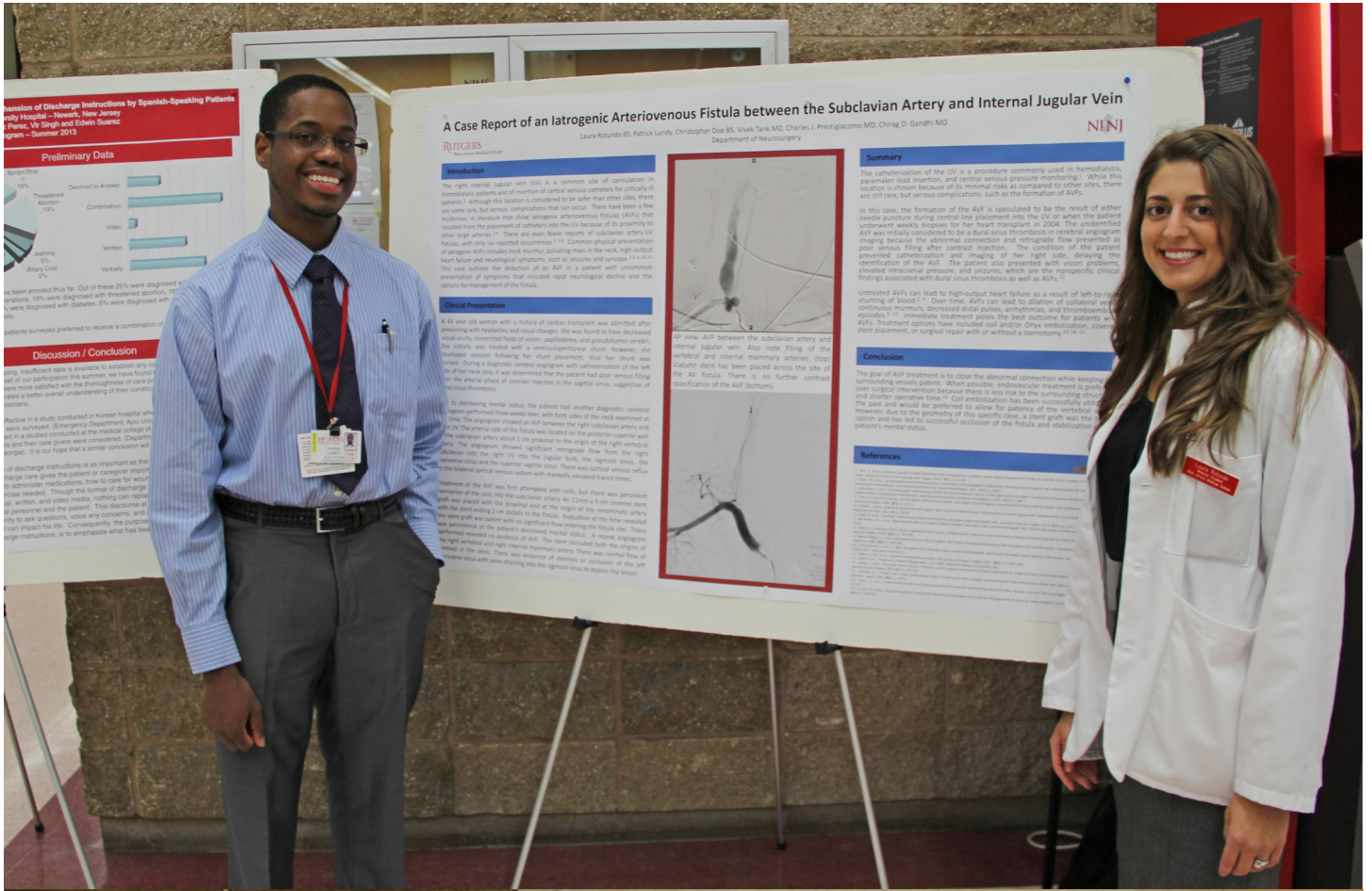
Measure	Microsurgery	Endoscopy	Significance
Age Mean	40.1 years	40.1 years	
Male/Female	335/279	282/243	
Cyst Size	12.4 mm	14.68 mm	
Incidental Findings			
Radical Resection	97.4%	59.5%	P<0.0001
Recurrence	0.92%	5.2%	P<0.0001
Residual	1.8%	27.77%	P<0.0001
Mortality	1.2%	38%	P<0.0001
Reoperation	3.9%	35%	P<0.0001
Shunt Dependency	4.9%	3.5%	P=0.0613

Conclusion

The microsurgical approach to colloid cysts results in a decreased rate of recurrence, and fewer reoperations rate of mortality and shunt dependency is similar bet

References

- Boggs HT, Ding R, Greenhaus JA, Le Guernec C, Nasser R, Estrada B, et al. Colloid cyst of the third ventricle: a series of 50 cases. *Neurosurgery*. 2002;51(2):295-302; discussion 302-294, 2002.
- Hollings G, Baur RL, Schmitz M, Galloway S, Riggl T, Mentelberg H. The experience of a decade. *Neurosurgery* 42:525-533; discussion 532-533.
- Shahmoradian L, Alkhatib M, Akshay M, Krupa M, Palka J. Colloid cysts of the management. *Neural Neurosurg* 64:205-213, 2009.
- Wilson DA, Fazio DS, West SD, Nakaji P. Endoscopic Resection of Colloid Cysts: Anatomic Approach. *World Neurosurg*. 2012.





EFFECTS OF PICORRHIZA KURROA (KUTKI) EXTRACT ON PROLIFERATION OF HUMAN COLON CANCER CELL LINES

Trinava Roy^{1,2}, Bishambar Dayal¹, and Michael A. Lea¹

¹Rutgers New Jersey Medical School, Newark, NJ,
²College of Natural Sciences-University of Massachusetts, Amherst, MA.



INTRODUCTION

The concept of chemoprevention is to prevent cells from becoming cancerous by blocking the carcinogenic process. Picrorhiza kurroa (P. kurroa) is a natural product from the bark of the Indian medicinal plant Picrorhiza kurroa (Rubiaceae). P. kurroa has been shown to have anticancer and chemopreventive activities in various cancer cell lines.

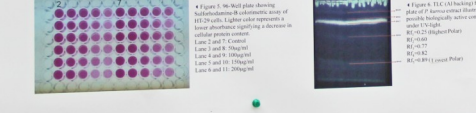
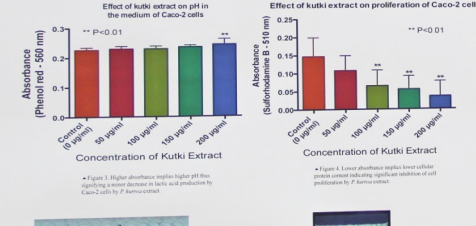
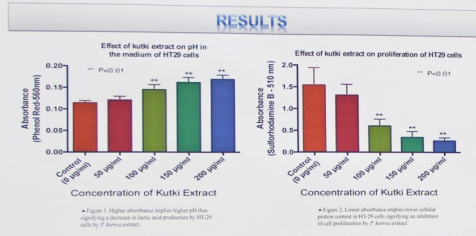
MATERIALS & METHODS

Picrorhiza Kurroa Extract

The extract was prepared using an approved protocol. The extract was then tested on HT29 and Caco-2 cells. The concentration of the extract was 0, 50, 100, 200, and 400 µg/ml. The absorbance was measured at 550 nm.

Cell Culture

HT29 and Caco-2 Human Colon Cancer Cell Lines (5000 cells) were plated in 96-well plates. The medium was changed to fresh medium containing the P. kurroa extract. The absorbance was measured at 550 nm.



SUMMARY

The results from our experiments show that Picrorhiza kurroa extract significantly inhibited the proliferation of HT29 and Caco-2 human colon cancer cell lines. The extract also caused a decrease in pH and a decrease in the proliferation of these cells. The extract also caused a decrease in the expression of p-Rpd3 and an increase in the expression of Rpd3.

CONCLUSIONS

The extract of Picrorhiza kurroa has a significant inhibitory effect on the proliferation of HT29 and Caco-2 human colon cancer cell lines. The extract also causes a decrease in pH and a decrease in the proliferation of these cells. The extract also causes a decrease in the expression of p-Rpd3 and an increase in the expression of Rpd3.

LITERATURE CITED

1. Gupta, R. K., et al. (2011). Picrorhiza kurroa extract inhibits proliferation of human colon cancer cell lines. *Journal of Cellular Biochemistry*, 101(1), 1-10.
2. Gupta, R. K., et al. (2012). Picrorhiza kurroa extract inhibits proliferation of human colon cancer cell lines. *Journal of Cellular Biochemistry*, 106(1), 1-10.
3. Gupta, R. K., et al. (2013). Picrorhiza kurroa extract inhibits proliferation of human colon cancer cell lines. *Journal of Cellular Biochemistry*, 109(1), 1-10.

ACKNOWLEDGEMENTS

We thank the National Institute of Health for their support of this project.



Regulating lifespan in *Drosophila melanogaster* by altering phosphorylation of Rpd3 protein in Loco signaling pathway

RADHIKA RAGAM*, ZACHARY KOPP, HARDIK PARIKH, and YONGKYU PARK
Department of Cell Biology and Molecular Medicine, Rutgers-New Jersey Medical School, Newark, New Jersey, USA

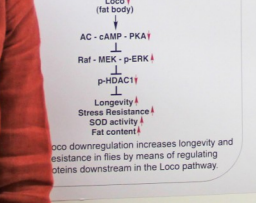


Abstract

Our research in the Loco longevity signaling pathway shows that decreased expression of Loco, a *Drosophila* RGS protein, leads to flies with increased lifespan and stronger stress resistance, and vice versa with reduced expression of Loco. Furthermore, downstream of Loco in this signaling pathway, we see that decreased Loco expression also leads to decreased levels of phosphorylated Rpd3/HDAC1 protein. We propose that Rpd3 protein regulates longevity and stress resistance downstream of Loco. Specifically, we propose that hyper-phosphorylation of Rpd3 protein will result in flies with decreased life span and stress resistance, and vice versa with no phosphorylation of Rpd3.

Introduction

G-proteins are molecular switches that are regulated by GTPase-activating proteins and guanine exchange factors. An RGS protein is a GTPase-activating protein, in that it inactivates G-protein by hydrolyzing its GTP and rejoining the beta and gamma subunits to the heterotrimeric G-protein. Loco therefore, is a G-protein inactivating protein. Overexpression of Loco has downstream effects in Figure 1. We want to focus specifically on the interaction between Loco and Rpd3/HDAC1.



Hypothesis

We hypothesize that regulating phosphorylation of Rpd3/HDAC1 protein directly affects stress resistance and longevity in *Drosophila melanogaster*; specifically that hyper-phosphorylation will result in a decreased life span and stress resistance in *Drosophila melanogaster* and vice versa with no phosphorylation.

Methods

Polymerase Chain Reaction

Amplified our three different Rpd3 gene inserts (WT, ADA, DDD) by PCR to be inserted into our vector. Also used colony PCR to confirm inserted was successfully ligated into our vector.

Molecular Subcloning

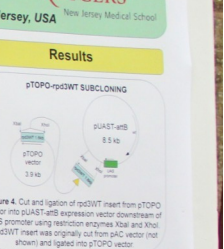
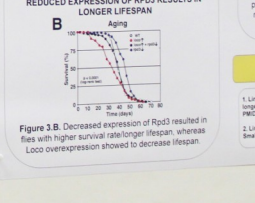
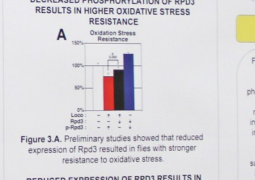
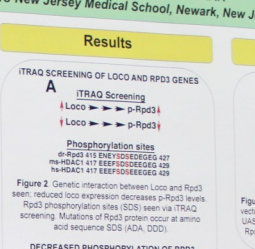
Three types of subcloning using performed pTOPO-pRW3, pUAST-p3A, and pTOPO-p3DD. We created three different subcloning constructs for wild-type phosphorylation (WT), hyper-phosphorylation (DDD), and no phosphorylation (ADA) of Rpd3 protein.

Miniprep

After successful subcloning experiments, we performed miniprep to extract and purify the plasmid DNA.

Experiment

We are testing if change of the phospho-Rpd3/HDAC1 resistance and lifespan through the target genes of Rpd3. We are testing this by creating mutated versions of Rpd3 protein specifically at the SDS phosphorylation site (mutations: ADA, DDD). We are focusing on the genetic interaction between Loco and Rpd3 genes and how regulation of p-Rpd3 levels affects lifespan and stress resistance in *Drosophila melanogaster*.



Conclusion

From the data collected thus far, we conclude that both Loco and Rpd3 genes affect longevity and stress resistance. Decreasing levels of phosphorylated Rpd3 with Loco downregulation were shown in flies with longer lifespan and stronger resistance to oxidative stress, and vice versa with increasing levels of p-Rpd3. We observed a genetic interaction between Loco and Rpd3, as well as the Rpd3 phosphorylation sites through ITRAQ screening, which we mutated for our different subcloning experiments. We expect that mutation of SDS phosphorylation site, DDD, results in hyper-phosphorylation and decreases lifespan and stress resistance, whereas no phosphorylation mutation, ADA, increases lifespan and stress resistance.

References

1. Liu, Y., Kim, K., Tang, Y., Jaisa, A., Sudojima, J., Park, Y. Regulation of longevity by phosphorylation of Drosophila Loco. *Agging Cell* 2011; 13:441-451.
2. Liu, Y., Park, H., and Park, Y. Loco signaling pathway in longevity. *Small GTPases* 2011; 2:3, 108-110. DOI: 10.1081/S1600





A Meta-Analysis of Drug Eluting Stents vs Bare Metal Stents for Treatment of Extracranial Vertebral Arteriovenous Malformations

Vikas Gupta, MD, Nakul Sheeth, BA, Ritam Ghosh, BA, Shariyah Gordon, Wenzhuan He, MD, Stephen F Modica, M.S., Charles J. Prestigiacomo, MD and CF

Department of Neurological Surgery, University of Medicine and Dentistry of New Jersey, Newark New Jersey, USA.

Introduction

Angioplasty and stenting offers an attractive treatment option for medically refractory patients with symptomatic vertebral artery stenosis (VAS). However, a major problem with bare metal stents (BMS) for VAS is the high in-stent restenosis (ISR) rate, which has ranged from 10% to 37%.

Methods

A meta-analysis was performed using the terms "drug eluting stents", "vertebral artery", and "vertebrobasilar insufficiency". The search and clinical success, postoperative morbidity, and overall survival outcomes measures were calculated using the Mantel-Haenszel method with fixed effect heterogeneity. Sensitivity analyses were performed with the studies included in the meta-analysis.

Compiled Data from Eligible Studies

Outcome parameter	Drug Eluting Stents	Bare Metal Stents
Technical Success	96.5% (102/106)	100% (10/10)
Clinical Success	90.7% (106/118)	80.0% (14/17)
Postoperative morbidity rate (days)	1.8%	2.8%
Postoperative mortality (30 days)	0%	0%
Postoperative morbidity (30 days)	0%	0%
Postoperative mortality (30 days)	0%	0%
Postoperative morbidity (30 days)	0%	0%
Postoperative mortality (30 days)	0%	0%
Postoperative morbidity (30 days)	0%	0%
Postoperative mortality (30 days)	0%	0%
Postoperative morbidity (30 days)	0%	0%
Postoperative mortality (30 days)	0%	0%

Anatomical Implications for In-Stent Restenosis (ISR)

In addition to neointimal hyperplasia, the unique anatomical properties of the vertebral artery column contribute to ISR rates.

- Elastic recoil after PTA due to a thick tunica media with its elastic and smooth muscle may promote ISR even after stent deployment. DES with higher metal loss may be a solution.
- Tortuous radius and continuous mobility of the vertebral artery may promote the subacute VA junction may promote mechanical strain.
- Longer lesion lengths are associated with higher ISR rates.

Illustrative Case: In-Stent Restenosis on Follow-Up

Fig 2. Treatment with BMS (A) Left subclavian angiography shows severe stenosis at the C4-C5 vertebral artery junction. (B) Post-stenting angiography shows sufficient dilation of the lesion. (C) Follow-up angiography at 4 months shows in-stent restenosis. (D) Follow-up angiography at 4 months after stent placement shows in-stent restenosis. (E) Deflation of the stent is seen on a simple radiograph during follow-up at 4 months (arrow).

Illustrative Case: Normal Follow-Up

Fig 3. Short balloon-expandable DES treatment in a 62-year-old male. (A) Preoperative angiography shows significant stenosis at the C4-C5 vertebral artery junction. (B) Postoperative angiography shows sufficient dilation of the lesion. (C) Follow-up at 5 months shows no in-stent restenosis. Source: Yokoi et al.

Meta-Analysis Results

Outcomes	Q	P	OR	P	95% CI	Model Used
Technical Success Rate	0	<0.001	0	1.528	0.622	Random Effect Model
Clinical Success Rate	0.096	0.992	N/A	1.917	0.263, 8.238	Random Effect Model
Non-complicate	0	<0.001	0	0.597	0.290	Fixed Effect Model
Mortality	0	<0.001	0	0.741	0.614	Random Effect Model
Postoperative Morbidity	0	<0.001	0	0.741	0.614	Random Effect Model
Postoperative Symptoms	5.391	0.068	N/A	0.965	0.231, 2.375	Random Effect Model
Restenosis	2.52	0.284	0	3.219	0.011	Fixed Effect Model

Endoscopic Transphenoidal Surgery of Rathke's Cleft Cyst: Endocrinologic Results With Less Aggressive Resection

Dhanraj S. Meenadath, BS, *Qasim Hussain, MD, *Vivek V. Kamdar, BS, *Peter F. Sulder, MD, FACS, *James K. Liu, MD, FACS

Departments of Neurological Surgery, *Otolaryngology - Head & Neck Surgery, *Center for Skull Base and Pituitary Surgery, Neurological Institute of New Jersey, Rutgers University, New Jersey Medical School, Newark, New Jersey

ABSTRACT

Rathke's cleft cysts (RCC) are benign lesions that originate from remnants of the Rathke pouch. They can compress adjacent structures causing neurological symptoms and may require surgical treatment. In the last decade, endoscopic endonasal transphenoidal surgery has gained popularity in the surgical management of pituitary and parasellar tumors. Nevertheless, postoperative cyst recurrence and endocrine dysfunction remain major concerns despite transphenoidal surgery. The purpose of this study was to review the outcomes for endoscopic transphenoidal resection of RCC and weigh the risk of postoperative morbidity of an aggressive resection with the potential for recurrence.

A non-aggressive strategy via endoscopic transphenoidal surgery is a safe and effective approach for surgical treatment of RCC with a low rate of postoperative endocrinopathy.

BACKGROUND

Rathke's cleft cysts (RCC) are benign saccular and/or suprasellar lesions that originate from congenital remnants of the Rathke pouch. The cysts can be filled with a mucinous, gelatinous, or caseous cystic fluid, which can affect imaging characteristics. They are relatively common, frequently found on autopsy, but are usually asymptomatic. However, some lesions can exhibit symptomatic growth or present as pituitary apoplexy, affecting critical surrounding structures resulting in headaches, cranial nerve palsies, visual and/or endocrine disturbances.

Although most RCC can be managed conservatively with observation, surgery is warranted in symptomatic cases. Typically, cyst decompression through a microsurgical transphenoidal approach with either partial or gross total resection (GTR) of the cyst wall is performed.¹⁻³ A purely endoscopic endonasal transphenoidal approach (ETTA) has gained popularity in the last decade with favorable results.⁴⁻⁶

A major concern with RCC is the risk of recurrence postoperatively. There is an incomplete understanding of the etiology of recurrence although some have suggested certain histologic features may predict recurrence.⁷ Partial resection with complete drainage as well as radical resection of the cyst wall have been reported to have similar efficacy, although the various approaches to achieving this resection have been less well studied.⁸

OBJECTIVES

- Differentiate between Gross Total Resection (GTR) and Subtotal Resection (STR).
- Weigh the morbidity of a GTR vs STR via ETTA.
- Attempt to elucidate when the high risk of morbidity of a single GTR is appropriate.
- Determine if multiple STRs may be a better intervention option than a single GTR with respect to recurrence rate and risk of endocrinologic dysfunction.

METHODS

Retrospective Chart Review

The database of endoscopic skull base cases of the senior authors were searched for diagnosis of Rathke's Cleft Cyst.

Specific data were extracted regarding patient demographics, presenting symptoms, cyst characteristics, surgical treatment, and postoperative outcomes.

TABLE 1: Patient Characteristics

Case	Sex	Age	Presenting Symptom	Visual	Endocrine	Resection	Follow-up (months)
1	M	52	Headache	Yes	None	GTR	8
2	F	35	Headache	Yes	None	GTR	2
3	M	35	Headache	Yes	None	GTR	2
4	M	57	Headache	Yes	None	GTR	34
5	M	38	Headache	Yes	None	GTR	1
6	F	33	Headache	Yes	None	GTR	1
7	F	46	Headache	Yes	None	GTR	1
8	F	34	Headache	Yes	None	GTR	1
9	F	48	Headache	Yes	None	GTR	1
10	M	41	Headache	Yes	None	GTR	1
11	M	50	Headache	Yes	None	GTR	1

ETTA: Endoscopic Endonasal Transphenoidal Approach

Figures 1 A and D: Preoperative MRI of a patient with a RCC. B and E: Intraoperative endoscopic views showing drainage of the RCC and partial resection of cyst wall. C and F: Delayed 2-year postoperative MRI showing observation imaging with no evidence of recurrence.

ILLUSTRATIVE CASE

This 49-year-old male patient presented with complaints of a persistent headache, visual loss, nausea, and endocrine dysfunction. Imaging found a 13mm x 13mm x 12mm (APxACxSI) saccular mass with suprasellar extension. The mass appeared as hyperintense on T1 MRI and hypointense on T2. Gross total resection was achieved. ETTA with a STR was determined to be the appropriate intervention. A small flow flow cyst was observed which was sealed with a nonabsorbable flap. Postoperative course was unremarkable. Pathology did not report any presence of squamous metaplasia. When the patient was re-evaluated for all presenting symptoms had improved and by the time of discharge were entirely alleviated. At a 17-month follow-up there was no radiographic evidence of recurrence and the patient reported that all pre-op symptoms had disappeared.





Skull Base Reconstruction after Far Lateral Transcondylar Approach using Autologous Fat-assisted Medpor Titan Cranioplasty: Surgical Technique and Nuances

Rohit K. Reddy, BS, Zachary S. Mendelson, BS, Phoebe Y. Ling, BS, James K. Liu, MD, FAANS
Department of Neurological Surgery, Rutgers University - New Jersey Medical School, Newark, NJ
Center for Skull Base and Pituitary Surgery, Neurological Institute of New Jersey, Rutgers University - New Jersey Medical School, Newark, NJ

Introduction

Various surgical approaches exist to access lesions located at the ventral foramen magnum and craniovertebral junction, one of which is the far lateral transcondylar or "far lateral" approach. Postoperative cerebrospinal fluid (CSF) leak after the far lateral transcondylar approach is considered an infrequent complication but remains a major factor to consider.¹⁻³ Currently, there is no consensus on which approach is best to prevent CSF leak.⁴⁻⁶ CSF leak following this surgical approach has ranged from 0% to 42.86%, with an average of 8.25%.⁷⁻¹¹ It is widely understood that meticulous repair of the dura and the cranial defect is vital for the prevention of postoperative CSF leaks; several prophylactic surgical techniques have been described by others in the past.¹²

Objective

We describe a novel multi-layer repair technique using an autologous fat graft-assisted Medpor Titan cranioplasty after a far lateral transcondylar approach as a way to prevent post-operative CSF leaks. We describe our surgical nuances and report our incidence of postoperative CSF leak and postoperative headaches.

Methods

Between September 2009 and June 2013, 13 patients underwent an autologous fat graft-assisted Medpor Titan cranioplasty after a far lateral skull base approach. There were a total of 13 procedures performed during this period (one patient had bilateral procedures). Lesions resected included 6 foramen magnum (FM) meningiomas, 2 cerebellopontine angle (CPA) epidermoid cysts, 1 bilateral neurenteric cyst (2 separate operations), and 1 CPA schwannoma. Factors examined included postoperative CSF leak length to follow-up (Table 1).

Variable	Value
no. of cases	13
no. of patients	12
mean age (yr)	34.6 (10-71)
sex (M/F)	3/9
far lateral approach	3/9
hemilaminectomy	11
condylar resection	10
fibre flap	5
mean follow-up (mos)	12 (1-39)

Surgical Technique

A standard far lateral approach was used for tumor resection in all patients. Lesions were accessed through a suboccipital craniotomy to the foramen magnum and the craniovertebral junction, which was performed with hemilaminectomy (11 cases) and condylar resection (10 cases). At the time of closure, any exposed mastoid air cells were sealed with bone wax. Primary watertight closure of the dura was performed using 4-0 Nuroleth (Ethicon) sutures, with a dural allograft as needed. A Valsalva maneuver was performed after dural closure to assess for any CSF egress through the suture line. An autologous fat graft was then harvested from the abdomen and placed over the dead space of the far lateral craniotomy defect. The fat graft was strategically positioned over the dural suture line and up against the waxed off mastoid air cells and the suture line, with the fat graft placed into the mastoid craniectomy defect and in the dead space of the cervical musculature. A Medpor Titan cranioplasty (76 reconstruct the suboccipital bony defect. Care was taken not to overpack the fat graft in order to avoid and meticulous multi-layer soft tissue wound closure was performed. Postoperatively, a mastoid pressure dressing was applied for 48 hours and no lumbar drainage was used.

Figure 1: A. Dural incision of a right-sided far lateral craniotomy. B. Primary watertight dural closure performed with an allograft. C. Mastoid air cells waxed off. D. An autologous fat graft placed into the craniotomy defect over the suture line and against the dead space of the cervical musculature. E. Medpor Titan cranioplasty is used to reconstruct the far lateral craniotomy defect.

Figure 2: A-C. Postoperative MRI (A: T1 post-gadolinium sagittal, B: T2 axial demonstrating a medial foramen magnum meningioma compressing the brainstem, D: post-operative MRI (A: T1 post-gadolinium for supratentorial sagittal, B: T2 axial demonstrating complete tumor removal and a well-defined fat graft), E: T2 axial demonstrating the fat graft (hypointense) is seen filling the dead space of the craniotomy defect and upper cervical spine.

Figure 3: A-C. Postoperative T1 axial MRI (A and B) and axial CT (C) craniotomy defect (B) and the upper cervical musculature (B) and postoperative axial CT shows the Medpor Titan cranioplasty reconstructing the far lateral craniotomy defect.

The patient cohort (Table 1) had an average age of 34.6 years, up to 12 months (1-39 months). Hemilaminectomy was performed, condylar resection was performed (fibre flap) was used. There were no instances of CSF otorrhea, pseudomeningocele, and delayed (30-day) postoperative headaches at follow-up examination.

Postoperative CSF leaks and postoperatively prevented through autologous fat graft-assisted far lateral approach. The autologous fat graft placed over the dead space of the craniotomy defect and against the dead space of the cervical musculature. The Medpor Titan cranioplasty is used to reconstruct the far lateral craniotomy defect. The Medpor Titan cranioplasty is used to reconstruct the far lateral craniotomy defect. The Medpor Titan cranioplasty is used to reconstruct the far lateral craniotomy defect.

Emergency Department Administration and Prescription Patterns of Opioid Analgesics

Daniel Funch Jr. MS-2, Vir Singh MS-1, Seth Lichtenstein MS-2, John Cafaro MS-2, Larrisha Love MS-2, Colleen Rivers MD, Steven Keller PhD, Roxanne Nagarika BA, Sangraeta Lamba MD, Sandra Scott, MD
DEPARTMENT OF EMERGENCY MEDICINE
NEW JERSEY MEDICAL SCHOOL
RUTGERS, THE STATE UNIVERSITY OF NEW JERSEY, NEWARK, NEW JERSEY

INTRODUCTION

- Usage of prescription opioid analgesics is a growing concern amongst healthcare providers in the US.
- Up to 61% of Emergency Department (ED) visits in the US are related to painful conditions and 29% of all pain-related ED visits result in opioid prescriptions.¹
- Many patients with addictions to illicit opiate drugs and/or prescription opioid analgesics seek medication from EDs.
- Patients may develop habits for prescription opioid analgesics after exposure from an ED visit.

OBJECTIVE

- Characterize the administration and prescription patterns of opioid analgesics including specific opioid, dosage, and quantity dispensed.
- Describe the chief complaints and diagnoses of patients receiving opioid analgesics.
- Evaluate substance abuse histories and number of ED visits of patients receiving opioid analgesics.

METHODS

- Retrospective chart review of opiate analgesic prescription and administration during 60 randomly selected days in 2012 for patients presenting to University Hospital ED. This sample represented approximately 11% of the total days in 2012.
- Data entry and analysis was performed after removing pediatric patients, restricted access patients (patients whose charts were unavailable due to administrative reasons), and patients who left the ED before triage.

RESULTS

Initial data for presentation: 2/3/2012, 7/26/2012, 8/5/2012, 9/1/2012

- 988 total visits to University Hospital ED
- 674 patients qualified for chart review
- 146 (21.7%) patients received opioid analgesic drugs
- 74 (50.7%) males and 72 (49.3%) females
- Medications administered include: Dilaudid® (hydromorphone), Morphine Sulfate, Oxycodone® (oxycodone), Percocet® (oxycodone/acetaminophen), Sublimaze® (buprenorphine), and Ultram® (tramadol)
- Medications prescribed include: Dilaudid®, Percocet®, Tylenol® (acetaminophen/codeine), Ultram® (tramadol/acetaminophen), Ultram® and Vicodin® (hydrocodone/acetaminophen)
- 34 (23.3%) patients had repeat visits involving opioid analgesics within 1 year
- Of patients with a substance abuse history, 13 (11.6%) were administered opioid analgesics, 5 (6.3%) received a prescription

RESULTS CONTINUED

EM Opioid Distribution: Pain Intensity

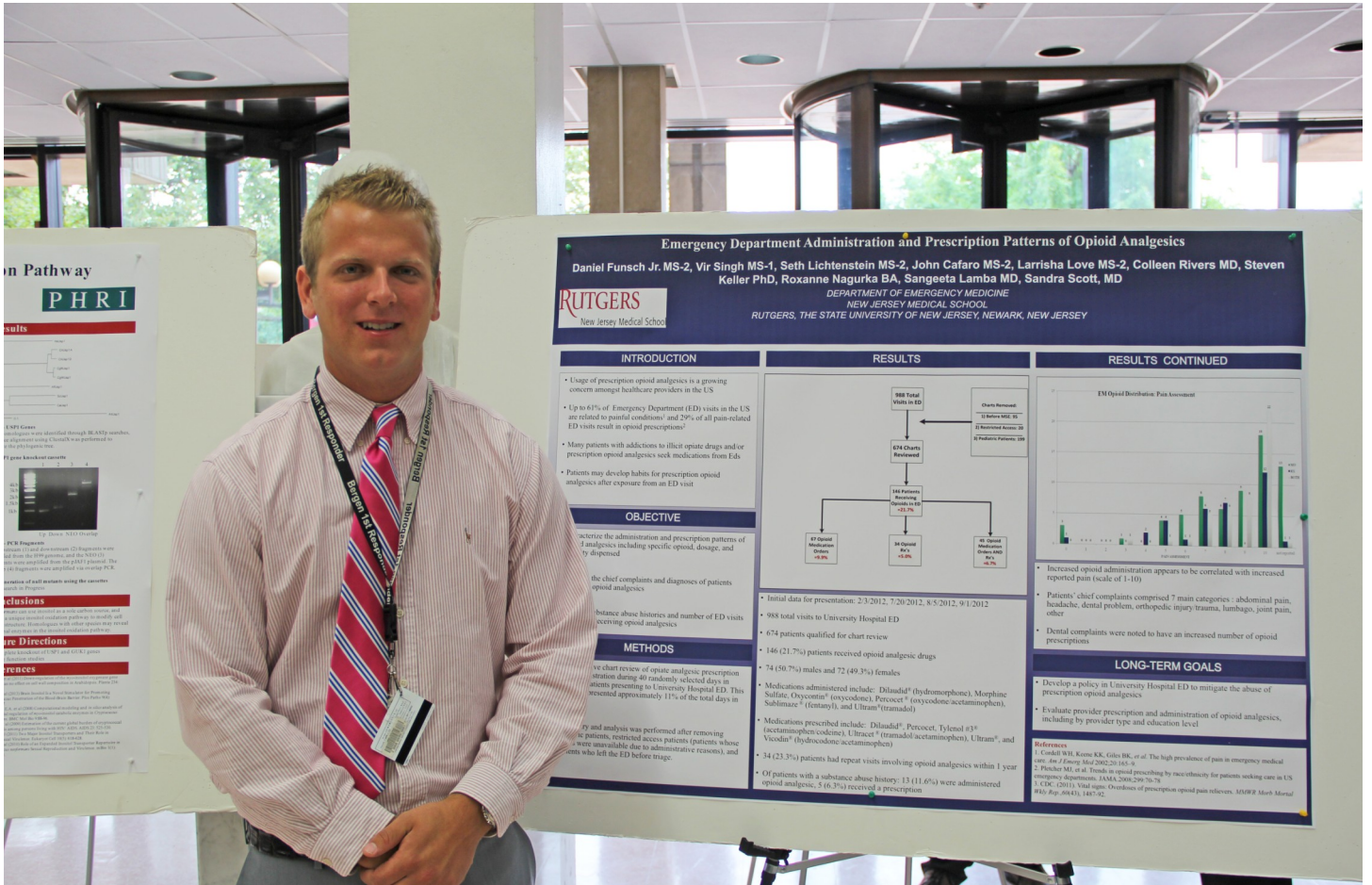
Increased opioid administration appropriate reported pain (scale of 1-10)

Patients' chief complaints comprise headache, dental problem, orthopedic, other

Dental complaints were noted to have prescription

LONG-TERM

- Develop a policy in University Hospital prescription opioid analgesics
- Evaluate provider prescription and administration including by provider type and education

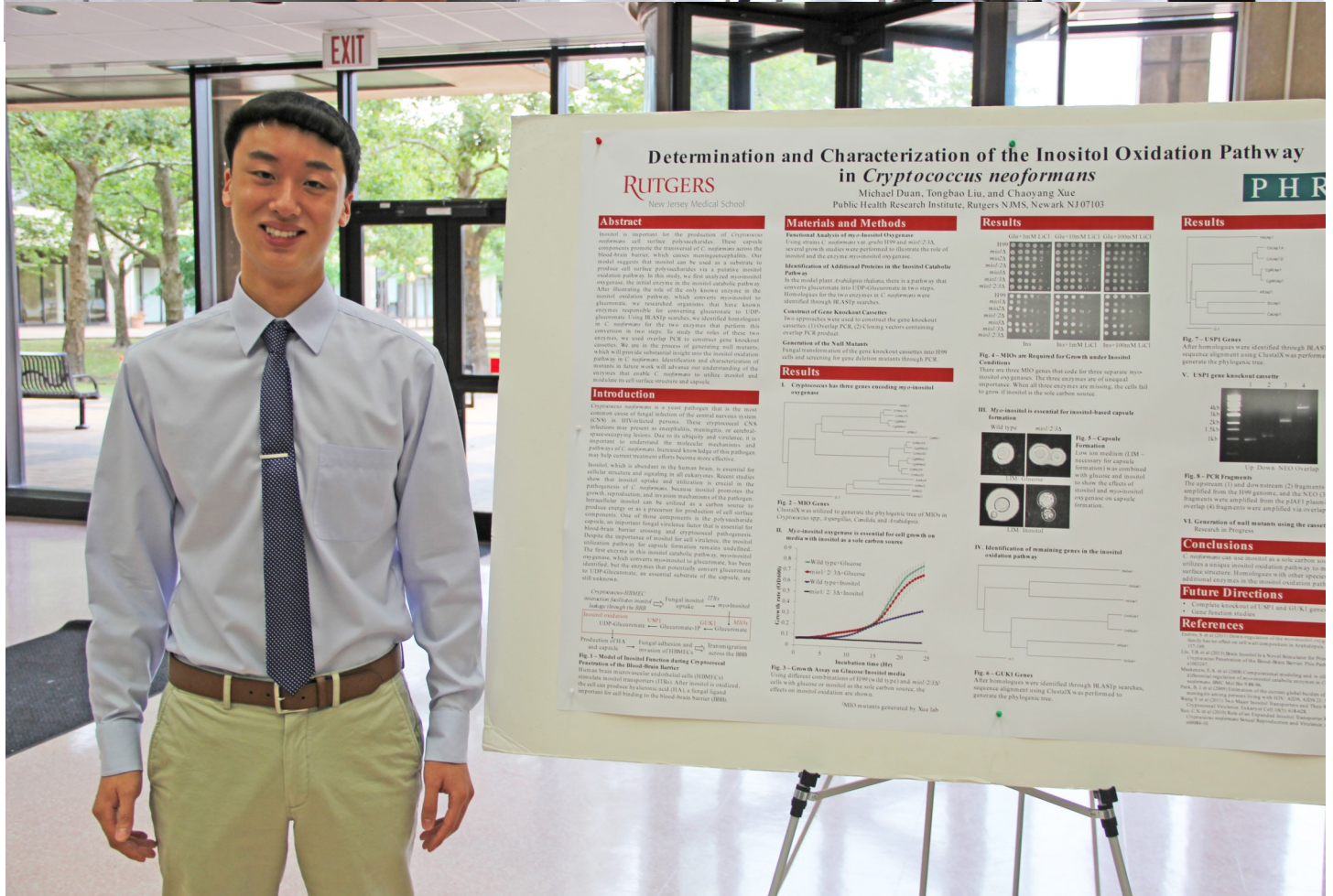


Emergency Department Administration and Prescription Patterns of Opioid Analgesics

Daniel Funsch Jr. MS-2, Vir Singh MS-1, Seth Lichtenstein MS-2, John Cafaro MS-2, Larrisha Love MS-2, Colleen Rivers MD, Steven Keller PhD, Roxanne Nagurka BA, Sangeeta Lamba MD, Sandra Scott, MD

RUTGERS
New Jersey Medical School
DEPARTMENT OF EMERGENCY MEDICINE
NEW JERSEY MEDICAL SCHOOL
RUTGERS, THE STATE UNIVERSITY OF NEW JERSEY, NEWARK, NEW JERSEY

INTRODUCTION	RESULTS	RESULTS CONTINUED
<ul style="list-style-type: none"> Usage of prescription opioid analgesics is a growing concern amongst healthcare providers in the US Up to 63% of Emergency Department (ED) visits in the US are related to painful conditions and 29% of all pain-related ED visits result in opioid prescriptions¹ Many patients with addictions to illicit opiate drugs and/or prescription opioid analgesics seek medications from EDs Patients may develop habits for prescription opioid analgesics after exposure from an ED visit 	<p>888 Total Opioid Prescriptions</p> <p>674 Charts Reviewed</p> <p>44 Patients Requiring Opioid Prescriptions</p> <p>47 Opioid Analgesic Opioids</p> <p>44 Opioid Analgesic Opioids</p> <p>44 Opioid Analgesic Opioids</p>	<p>ED Opioid Distribution: Pain Assessment</p> <p>Increased opioid administration appears to be correlated with increased reported pain (scale of 1-10)</p> <p>Patients' chief complaints comprised 7 main categories: abdominal pain, headache, dental problem, orthopedic injury/trauma, lumbago, joint pain, other.</p> <p>Dental patients were noted to have an increased number of opioid prescriptions</p>
<p>OBJECTIVE</p> <p>Describe the administration and prescription patterns of analgesics including specific opioid, dosage, and type dispensed.</p> <p>Identify the chief complaints and diagnoses of patients receiving opioid analgesics.</p> <p>Identify substance abuse histories and number of ED visits receiving opioid analgesics.</p>	<p>RESULTS</p> <ul style="list-style-type: none"> Initial data for presentation: 2/3/2012, 7/20/2012, 8/5/2012, 9/1/2012 988 total visits to University Hospital ED 674 patients qualified for chart review 146 (21.7%) patients received opioid analgesic drugs 74 (50.7%) males and 72 (49.3%) females Medications administered include: Dilaudid® (hydromorphone), Morphine Sulfate, Oxycodone® (oxycodone), Percocet® (oxycodone/acetaminophen), Sublimaze® (fentanyl), and Ultram® (tramadol) Medications prescribed include: Dilaudid®, Percocet, Tylenol 3® (acetaminophen/codone), Ultracet® (tramadol/acetaminophen), Ultram®, and Vicodin® (hydrocodone/acetaminophen) 34 (23.3%) patients had repeat visits involving opioid analgesics within 1 year Of patients with a substance abuse history: 13 (11.6%) were administered opioid analgesic, 5 (6.7%) received a prescription 	<p>LONG-TERM GOALS</p> <ul style="list-style-type: none"> Develop a policy in University Hospital ED to mitigate the abuse of prescription opioid analgesics Evaluate provider prescription and administration of opioid analgesics, including by provider type and education level



Determination and Characterization of the Inositol Oxidation Pathway in *Cryptococcus neoformans*

Michael Duan, Tongbao Liu, and Chaoyang Xue
Public Health Research Institute, Rutgers NJMS, Newark NJ 07103

PHRI

Abstract

Inositol is important for the production of *Cryptococcus neoformans* cell surface polysaccharides. Opioid analgesics promote the conversion of C-6 inositol to produce cell surface polysaccharides via a putative inositol oxidation pathway. In this study, we first analyzed inositol oxidation, the initial step in the inositol oxidation pathway. After illustrating the role of the only known enzyme in the inositol oxidation pathway, which converts inositol to glucose, we searched organisms that have known enzymes responsible for converting glucose to UDP-glucose. Using RAMP searches, we identified homologous genes in *C. neoformans* for two enzymes that perform this conversion in yeast. To study the roles of these two enzymes, we used overlap PCR to generate gene knockout strains. We then in the process of generating null mutants, which will provide substantial insight into the inositol oxidation pathway in *C. neoformans*. Identification and characterization of mutants in future work will advance our understanding of the enzymes that enable *C. neoformans* to utilize inositol and modify its cell surface structure and capsule.

Introduction

Cryptococcus neoformans is a yeast pathogen that is the most common cause of fungal infection of the central nervous system (CNS) in HIV-infected patients. These cryptococcal CNS infections may present as meningitis, myelitis, or abscesses, and are often fatal. Due to its ubiquity and virulence, it is particularly of interest. Increased knowledge of this pathogen pathogenesis is important. Increased knowledge of this pathogen pathogenesis is important. Increased knowledge of this pathogen pathogenesis is important.

Materials and Methods

Functional Analysis of an Inositol Oxidase

Using yeast 2-hybrid screens and growth on inositol and maltose, several growth studies were performed to illustrate the role of inositol and the enzyme inositol oxidase.

Identification of Additional Proteins in the Inositol Oxidation Pathway

In the model plant *Arabidopsis thaliana*, there is a pathway to synthesize inositol from D-glucose. In *C. neoformans*, we hypothesized that the inositol oxidase is a membrane-associated protein. Homologues for the two enzymes in a membrane-associated complex were identified through RAMP searches.

Construction of Gene Knockout Strains

Two approaches were used to construct the gene knockout strains: (1) homologous recombination and (2) CRISPR-Cas9 using vectors containing overlapping PCR products.

Generation of the Yeast Mutants

Fungal transformation of the gene knockout cassette into H99 cells and screening for gene deletion mutants through PCR.

Results

I. *Cryptococcus* has three genes encoding myo-inositol oxidase

Genetic analysis of the three genes revealed that the *INO1* gene is essential for growth on inositol as a sole carbon source.

II. *Myo*-inositol is essential for inositol-based capsule formation

Low iron medium (LIM) is necessary for capsule formation. In our study, we combined LIM with glucose and inositol to show the effects of inositol and myo-inositol on capsule formation.

III. *Myo*-inositol is essential for inositol-based capsule formation

Low iron medium (LIM) is necessary for capsule formation. In our study, we combined LIM with glucose and inositol to show the effects of inositol and myo-inositol on capsule formation.

IV. Identification of remaining genes in the inositol oxidation pathway

Using different combinations of H99 cell types and maltose/inositol as carbon sources, the effects on inositol oxidation are shown.

Fig. 3 - Growth Assay on Glucose-based media

Using different combinations of H99 cell types and maltose/inositol as carbon sources, the effects on inositol oxidation are shown.

Fig. 4 - MDOs are Required for Growth on Inositol

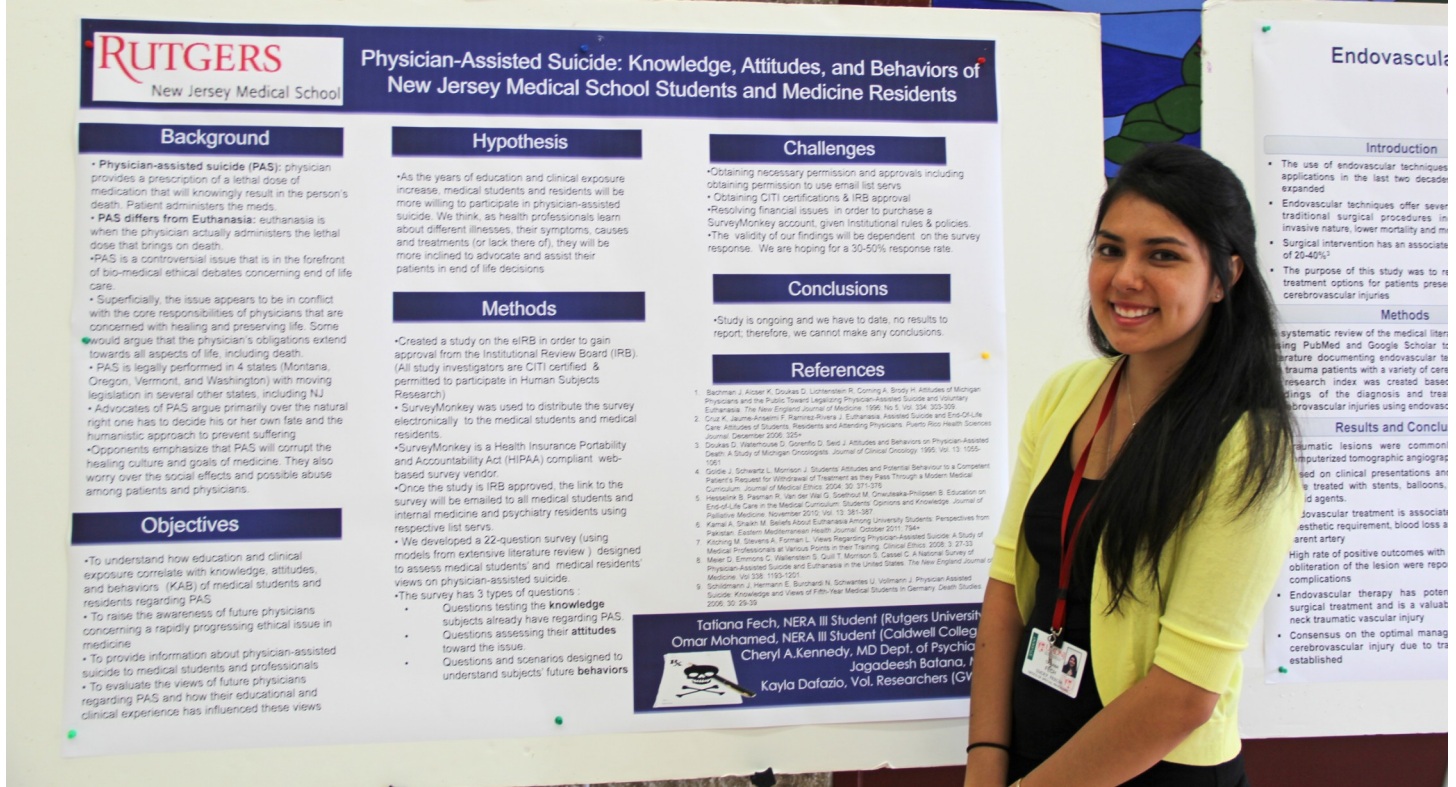
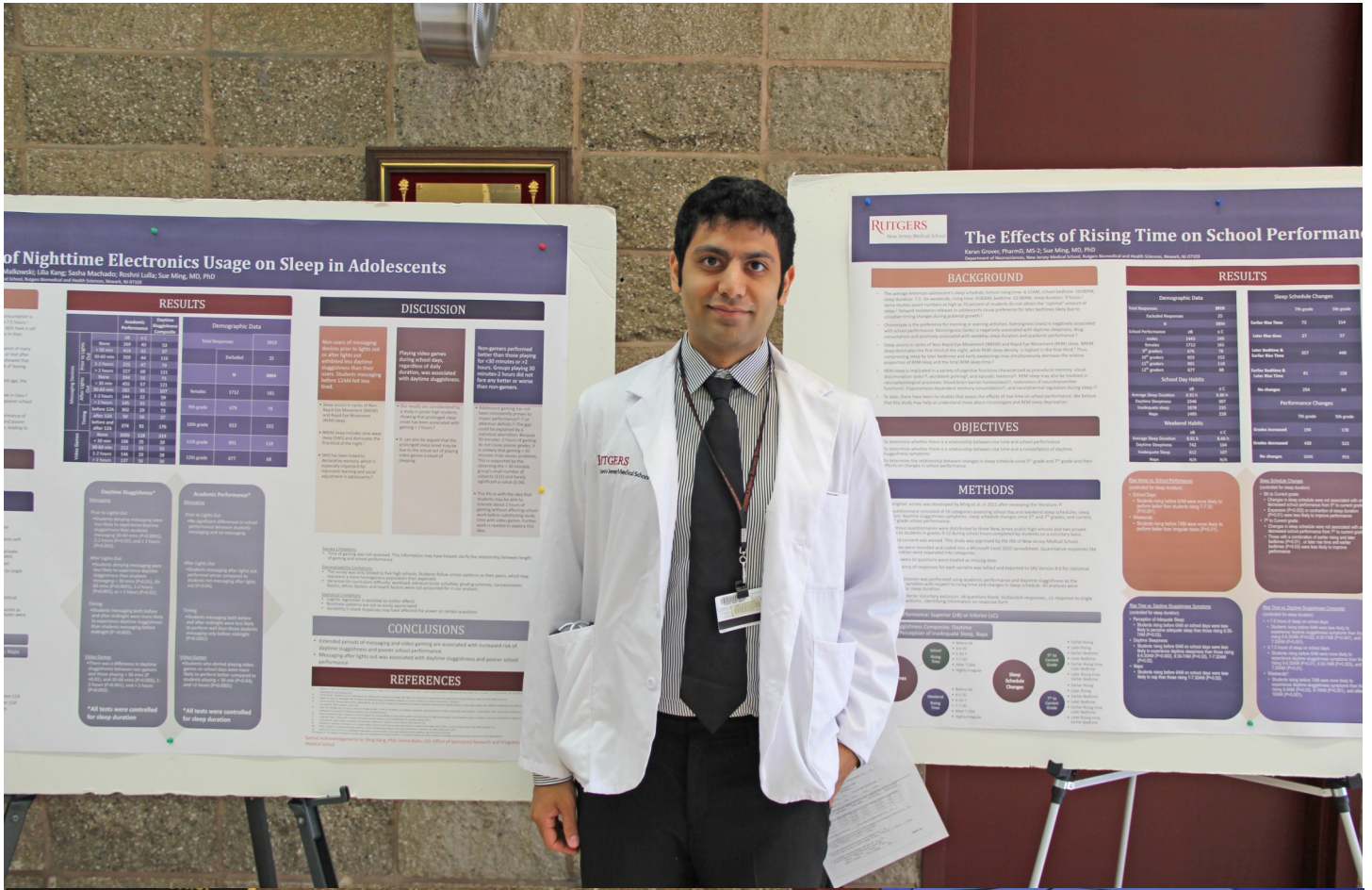
Three or three MDO genes that code for three separate myo-inositol oxidases. The three genes are of unequal importance. When all three genes are missing, the cells fail to grow if inositol is the sole carbon source.

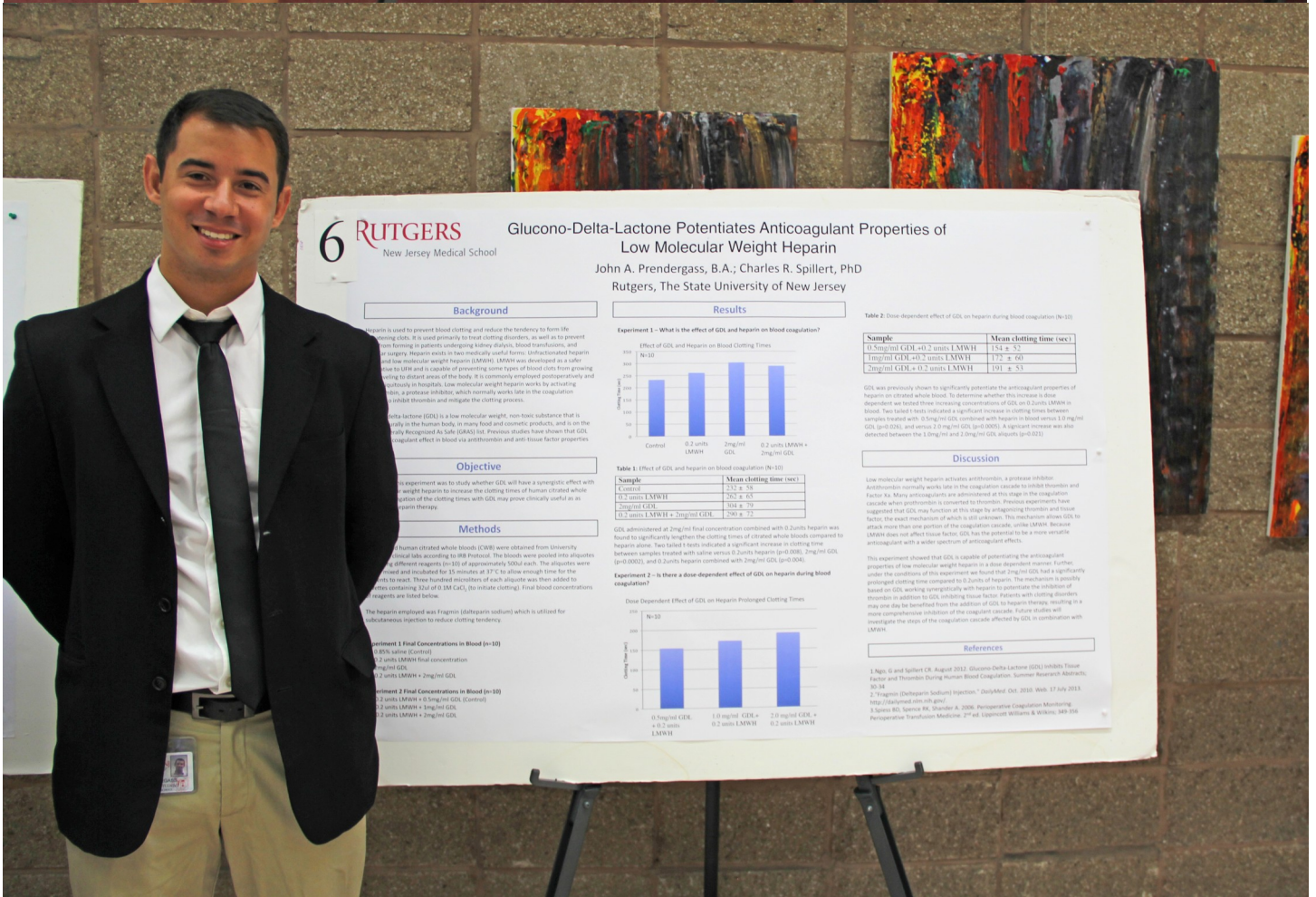
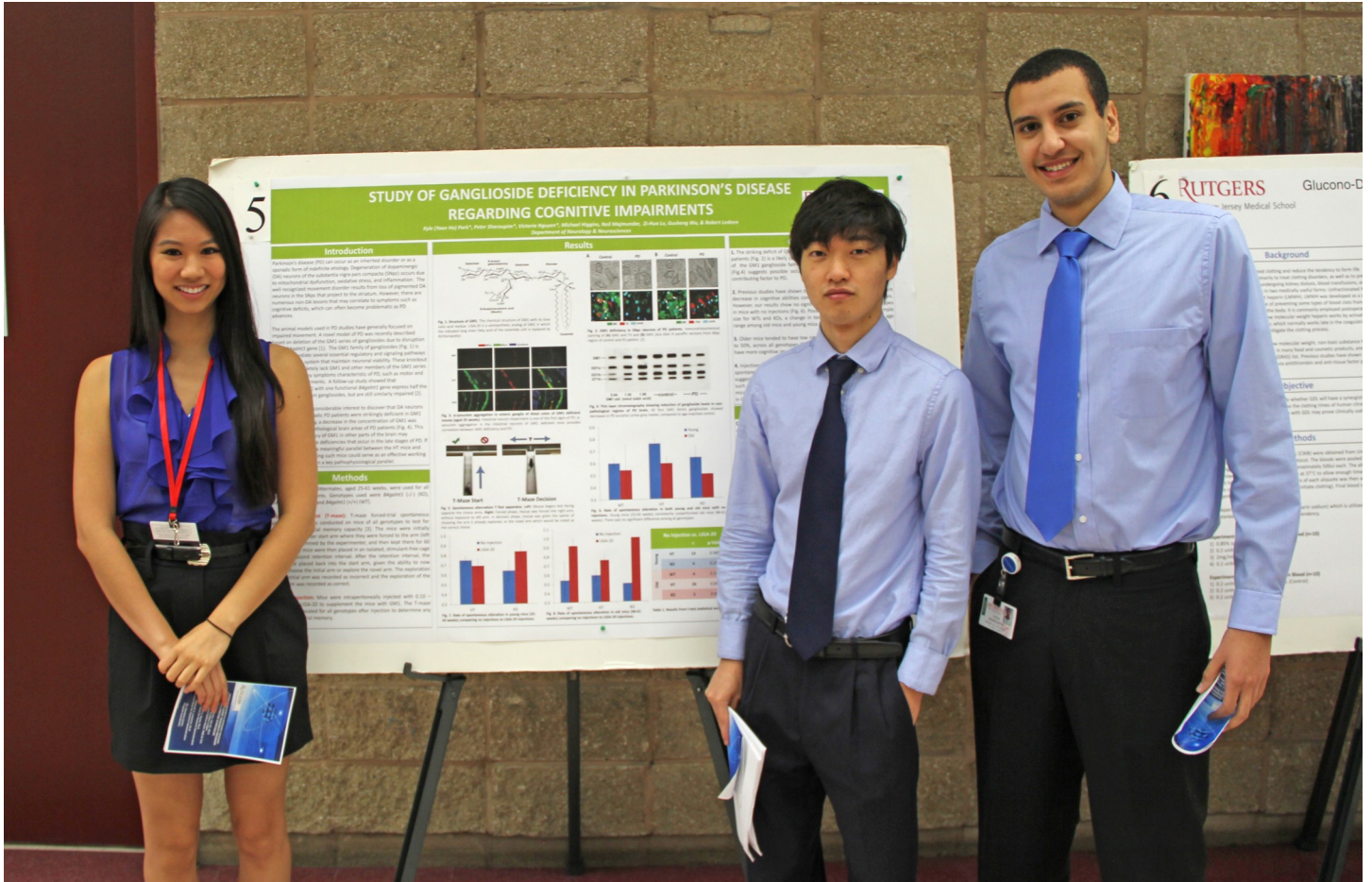
Fig. 5 - Capsule Formation

Low iron medium (LIM) is necessary for capsule formation. In our study, we combined LIM with glucose and inositol to show the effects of inositol and myo-inositol on capsule formation.

Fig. 6 - CRISPR Genes

After homologues were identified through BLAST searches, sequence alignment using ClustalW was performed to generate the phylogenetic tree.

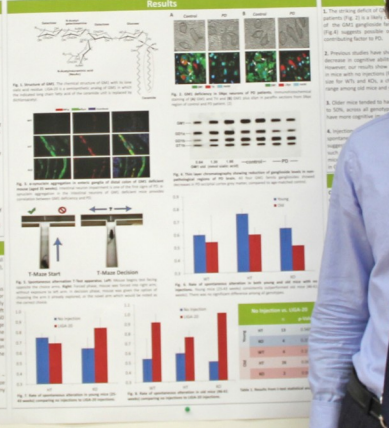




STUDY OF GANGLIOSIDE DEFICIENCY IN PARKINSON'S DISEASE REGARDING COGNITIVE IMPAIRMENTS

Introduction
Parkinson's disease (PD) can occur as an isolated condition or as part of a neurodegenerative syndrome. Dysregulation of ganglioside synthesis leads to cognitive impairment, including attention, and information processing. Ganglioside deficiency results from loss of ganglioside transferase in the brain that impairs the brain. However, there are numerous gene mutations that may contribute to ganglioside synthesis defects, which can often become problematic as PD advances.

Methods
The animal model used in PD studies has generally focused on the loss of a single gene. We have recently identified a mutation in the GDI1 gene that encodes for the enzyme responsible for the synthesis of GM1. The GDI1 gene is expressed in the brain and is essential for the synthesis of GM1. We have identified a mutation in the GDI1 gene that encodes for the enzyme responsible for the synthesis of GM1. We have identified a mutation in the GDI1 gene that encodes for the enzyme responsible for the synthesis of GM1.



Results
The study of the effect of the GDI1 gene mutation on the synthesis of GM1 and its effect on cognitive impairment in Parkinson's disease. The study found that the mutation in the GDI1 gene significantly reduced the synthesis of GM1 and led to cognitive impairment. The study also found that the mutation in the GDI1 gene was associated with a decrease in the levels of GM1 in the brain.

Background
Ganglioside synthesis is a complex process involving several enzymes. The GDI1 gene is essential for the synthesis of GM1. The study found that the mutation in the GDI1 gene significantly reduced the synthesis of GM1 and led to cognitive impairment.

Glucono-Delta-Lactone Potentiates Anticoagulant Properties of Low Molecular Weight Heparin

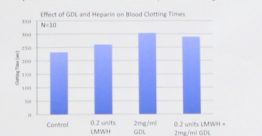
John A. Prendergast, B.A.; Charles R. Spillert, PhD
Rutgers, The State University of New Jersey

Background
Heparin is used to prevent blood clotting and reduce the tendency to form life-threatening clots. It is used primarily to treat clotting disorders, as well as to prevent from forming in patients undergoing kidney dialysis, blood transfusions, and surgery. Heparin exists in two medically useful forms: unfractionated heparin and low molecular weight heparin (LMWH). LMWH is developed as a safer drug to use in patients with kidney disease. LMWH is commonly employed postoperatively and in hospitals. Low molecular weight heparin works by activating antithrombin, a natural inhibitor which normally works late in the coagulation cascade to inhibit thrombin and mitigate the clotting process.

Objective
This experiment was to study whether GDL will have a synergistic effect with LMWH to increase the clotting times of human citrated whole blood.

Methods
Human citrated whole blood (CWB) were obtained from University of New Jersey labs according to IRB Protocol. The bloods were pooled into aliquots of approximately 500uL each. The aliquots were mixed and incubated for 15 minutes at 37°C to allow enough time for the blood to reach 200 hundred micrometers of each aliquot was then added to test tubes containing 20uL of 0.3M CaCl₂ (to initiate clotting). Final blood concentrations of reagents are listed below.

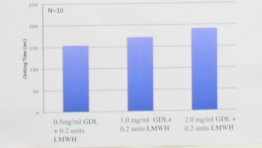
Experiment 1 - What is the effect of GDL and heparin on blood coagulation?



Sample	Mean clotting time (sec)
Control	212 ± 52
0.2 units LMWH	262 ± 65
2mg/ml GDL	358 ± 72
0.2 units LMWH + 2mg/ml GDL	590 ± 72

GDL administered at 2mg/ml final concentration combined with 0.2units heparin was found to significantly lengthen the clotting times of citrated whole bloods compared to heparin alone. Two tailed t tests indicated a significant increase in clotting time (p<0.0001), and 0.2units heparin combined with 2mg/ml GDL (p<0.004).

Experiment 2 - Is there a dose dependent effect of GDL on heparin during blood coagulation?



Dose Dependent Effect of GDL on Heparin Prolonged Clotting Times
The results of this experiment show that GDL has a dose-dependent effect on the anticoagulant properties of LMWH. As the concentration of GDL increases, the clotting time of the blood also increases.

Table 2: Dose-dependent effect of GDL on heparin during blood coagulation (N=10)

Sample	Mean clotting time (sec)
0.2mg/ml GDL + 0.2 units LMWH	174 ± 52
1mg/ml GDL + 0.2 units LMWH	172 ± 60
2mg/ml GDL + 0.2 units LMWH	191 ± 53

GDL was previously shown to significantly potentiate the anticoagulant properties of heparin on citrated whole blood. To determine whether this increase is dose dependent we tested three increasing concentrations of GDL on 0.2units LMWH in blood. Two tailed t tests indicated a significant increase in clotting times between samples treated with 0.2mg/ml GDL combined with heparin to blood versus 1.0 mg/ml GDL (p<0.0001), and versus 2.0 mg/ml GDL (p<0.0001). A significant increase was also observed between the 1.0mg/ml and 2.0mg/ml GDL aliquots (p<0.002).

Discussion

Low molecular weight heparin activates antithrombin, a protease inhibitor. Antithrombin normally works late in the coagulation cascade to inhibit thrombin and Factor Xa. Many anticoagulants are administered at this stage in the coagulation cascade when prothrombin is converted to thrombin. Previous experiments have suggested that GDL may function at this stage by inhibiting thrombin and Factor Xa, the exact mechanism of which is still unknown. The mechanism allows GDL to attack more than one portion of the coagulation cascade, unlike LMWH. Because LMWH does not affect Factor Xa, GDL has the potential to be a more versatile anticoagulant with a wider spectrum of anticoagulant effects.

This experiment showed that GDL is capable of potentiating the anticoagulant properties of low molecular weight heparin in a dose dependent manner. Further, under the conditions of this experiment we found that 2mg/ml GDL had a significantly prolonged clotting time compared to 0.2units of heparin. The mechanism is possibly LMWH working synergistically with heparin to potentiate the inhibition of thrombin in addition to GDL inhibiting Factor Xa. Patients with clotting disorders may also benefit from the addition of GDL to heparin therapy, resulting in a more comprehensive inhibition of the coagulation cascade. Future studies will investigate the usage of the coagulation cascade affected by GDL in combination with LMWH.

References

1. Ngai, G. and Spillert, C.R. August 2012. Glucono-Delta-Lactone (GDL) Inhibits Tissue Factor and Prothrombin During Purkiné Blood Coagulation. Summer Research Abstracts, 2012.
2. "Trisodium (heparin sodium) injection." *Drugs@FDA*. Oct. 2008. Web. 17 July 2013. <http://drugs.fda.gov/>
3. Spring, M.S., Sprague, M., Shuster, A. 2006. Perioperative Coagulation Monitoring. *Perioperative Transfusion Medicine*. 2nd ed. Lippincott Williams & Wilkins, 349-358.



3 RUTGERS New Jersey Medical School

CHRONIC STRESS INCREASES TISSUE SDF-1 AND IMPAIRS HEALING AT SITE OF INJURY

Andrew A. Marano, BA, Letitia E. Bible, MD, Walter Alzate, MS, Kannan B. Kolenkote, PhD
David H. Livingston, MD, Ziad C. Sifri, MD, Alicia M. Mohr, MD
Department of Surgery, Rutgers, The State University of New Jersey, Newark, New Jersey

INTRODUCTION

Patients who have experienced severe injury and hemorrhagic shock suffer prolonged anemia due to bone marrow (BM) mobilization. Hematopoietic progenitor cell (HPC) growth is suppressed in BM and mobilization of progenitors to peripheral blood and site of injury is increased. This anemia persists in trauma patients, but studies in animals that have undergone traumatic injury and hemorrhagic shock. The difference in the duration of the anemia may be due to the persistent hypercoagulable state that trauma patients experience from the stresses of hospitalization. In order to mimic these conditions, animals were subjected to chronic stress and evaluated for factors affecting HPC growth and mobilization.

A major player in the HPC mobilization process is the cytokine stromal cell-derived factor-1 (SDF-1). It is a chemotactic factor that serves as a homing mechanism for HPCs. The direction of net movement of HPCs is determined by an SDF-1 gradient between the BM and the tissues. The purpose of this study is to evaluate the effect of chronic stress on the SDF-1 and determine its effect on HPC mobility seven days after injury.

METHODS

Animals: Sprague-Dawley rats weighing between 250-300g (Charles River, Wilmington, MA) were housed in a barrier-contained facility at 25 C with 12-hour light/dark cycle. They had free access to water and chow (Teklad 220 Rodent Diet W-8640, Harlan Teklad, Madison, WI). All rats were maintained in accordance with the recommendations of the Guide for the Care and Use of Laboratory Animals.

Lung Contusion (LC)

A unilateral lung contusion was introduced by using the blast wave of a percussive nail gun (Cathren 96054 Skoper, Sears Roebuck, Chicago, IL) applied to a 12-mm small metal plate placed on the right axilla of the rat. This model has been shown to produce a clinically relevant LC, as demonstrated by radiography and histology.

Hemorrhagic Shock (HS)

Animals underwent blood withdrawal until the mean arterial pressure was reduced to 30 mmHg. Body temperature was maintained using an electric heating pad. After 45 minutes, the shed blood was reinfused at a rate of 1ml/min.

Chronic Stress (CS)

Animals underwent a daily two-hour period of restraint stress. During these periods, rats were probed by repositioning and alarm every thirty minutes. Animals were sacrificed on day 7, after 6-day restraint periods.

Sample Collection and Preparation

Animals were sacrificed by cardiac puncture and serum was collected. Samples were then centrifuged and the plasma supernatants were stored at -80 C for detection of SDF-1 by ELISA.

Animals were sacrificed by cardiac puncture and serum was collected. Samples were then centrifuged and the plasma supernatants were stored at -80 C for detection of SDF-1 by ELISA.

Lungs were harvested from the animals immediately after sacrifice. They were flash frozen in dry ice and stored at -80 C. Sections of approximately 4mg were taken from each lung tissue sample and placed in 1ml cold PBS (pH 7.4) (GIBCO). Samples were homogenized (BioGen Pro 200 Homogenizer) and then centrifuged at 10,000 RPM for 10 minutes at 4 C. The supernatants were transferred to clean tubes and stored at -80 C.

SDF-1 ELISA

All samples were tested using a Quantikine mouse CXCL12/SDF-1 ELISA kit (R&D Systems, R&D Systems) in accordance with the manufacturer's protocol. Each sample was tested in duplicate and the average of the two results was recorded. 1 µl of each sample was used for determination of protein concentration by spectrophotometry using Protein Assay Reagent (BioRad, Richmond, CA, USA). Results were calculated as pg/ml protein.

Lung Injury Score

Lungs were harvested and fixed in 10% buffered formalin. They were then dehydrated, embedded in paraffin, cut into 4µm slices, and stained with hematoxylin and eosin. A blinded reader examined the slices under a light microscope for pulmonary edema, interstitial edema, alveolar integrity, and inflammatory cells and rates it on a scale of 0-11.

Statistical Analysis

All groups comprised 4 to 7 animals. Analysis of variation was performed using a one-way ANOVA with Tukey's Multiple Comparison post-test in GraphPad Prism 5 (GraphPad Software, Inc.). Data is presented as the mean ± standard error.

RESULTS

Figure 1: Addition of CS to LC and LCHS leads to increased Lung Injury Score at day 7 following injury (n=4/group)

Group	Lung Injury Score
LC	~1.5
CS	~1.5
LC+CS	~4.5
LCHS	~3.5
LCHS+CS	~5.5

Figure 2: Addition of CS to LC and LCHS does not cause significant variation in plasma SDF-1 at day 7 following injury (n=4/group)

Group	Lung Injury Score	Inflammatory Cells
LC	0.0	0.8
CS	1.8	0.4
LC+CS	0.4	1.75
LCHS	0.4	1.75

Figure 3: Addition of CS to LCHS leads to increased SDF-1 concentration in injured lung tissue at day 7 following injury (n=2/group)

Group	SDF-1 (pg/ml protein)
LC	~1000
CS	~1000
LC+CS	~5000
LCHS	~1000
LCHS+CS	~6000

Figure 4: Addition of CS to LC and LCHS does not increase plasma SDF-1 at day 7 following injury (n=4/group)

Group	SDF-1 (pg/ml protein)
LC	~1000
CS	~1000
LC+CS	~1000
LCHS	~1000
LCHS+CS	~1000

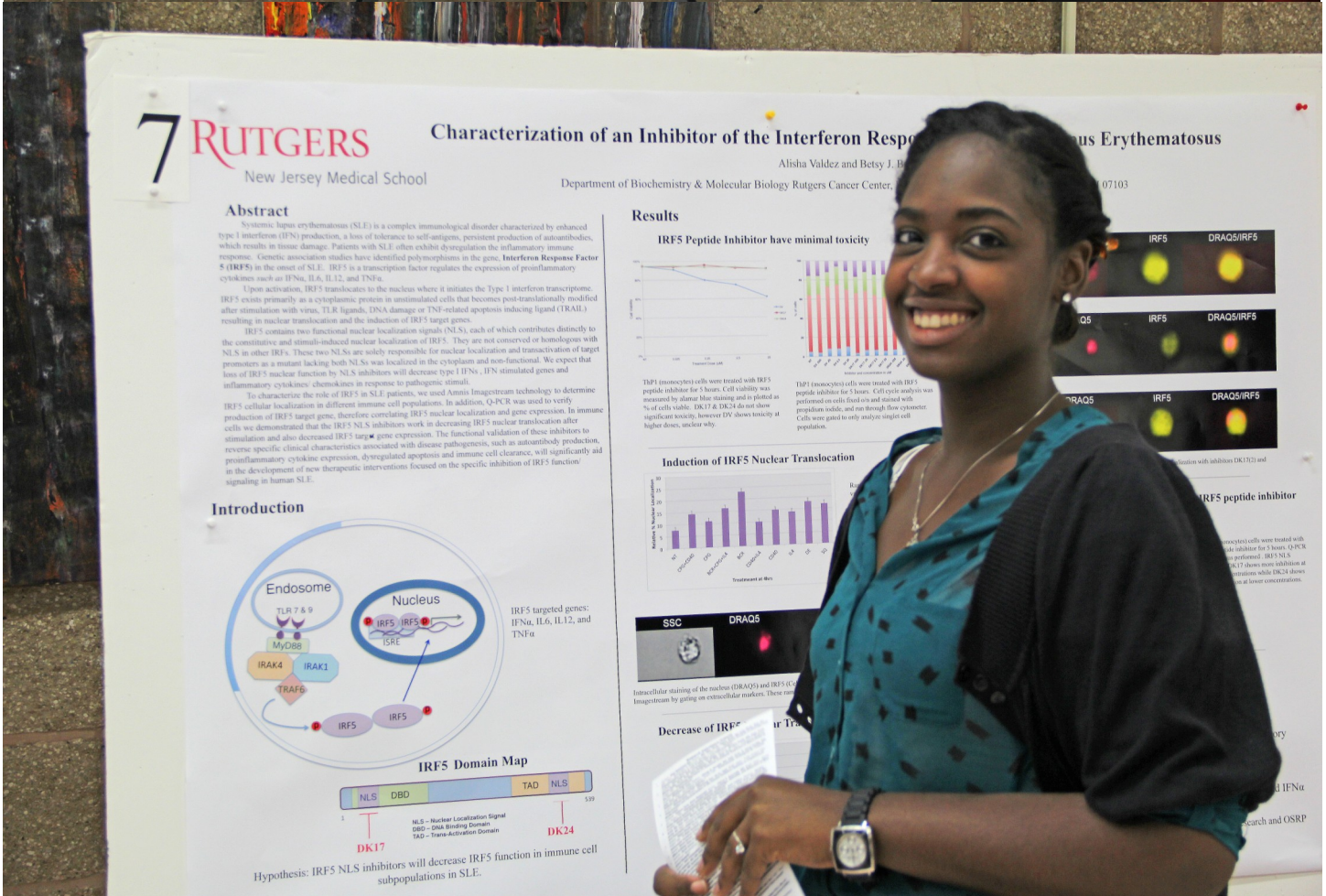
CONCLUSIONS

- Chronic stress impairs healing following LC and LCHS.
- Chronic stress following LCHS significantly increases SDF-1 levels in the injured lung but has no impact on SDF-1 plasma concentration.
- The mechanism responsible for chronic stress-induced impaired healing following injury requires further investigation and may be related to increased SDF-1 levels at the site of injury.

FUTURE STUDIES

We are currently investigating the effect chronic stress has on SDF-1 levels in the bone marrow to determine the BM-to-tissue gradient responsible for the mobilization and homing of HPCs. This data, in conjunction with measurements of BM and lung tissue cellularly, may give us insight into the mechanism by which injury and stress lead to anemia.

REFERENCES



7 RUTGERS New Jersey Medical School

Characterization of an Inhibitor of the Interferon Response in Systemic Lupus Erythematosus

Alisha Valdez and Betsy J. ...
Department of Biochemistry & Molecular Biology Rutgers Cancer Center, ...

Abstract

Systemic lupus erythematosus (SLE) is a complex immunological disorder characterized by enhanced type I interferon (IFN) production, a loss of tolerance to self-antigens, persistent production of autoantibodies, which results in tissue damage. Patients with SLE often exhibit dysregulation of the inflammatory immune response. Genetic association studies have identified polymorphisms in the **Interferon Response Factor 5 (IRF5)** in the onset of SLE. IRF5 is a transcription factor regulates the expression of proinflammatory cytokines such as IFN α , IL-6, IL-12, and TNF α .

Upon activation, IRF5 translocates to the nucleus where it initiates the Type I interferon transcription. IRF5 exists primarily as a cytoplasmic protein in unstimulated cells that becomes post-translationally modified after stimulation with virus, TLR ligands, DNA damage or TNF-related apoptosis inducing ligand (TRAIL), resulting in nuclear translocation and the induction of IRF5 target genes.

IRF5 contains two functional nuclear localization signals (NLS), each of which contributes distinctly to the constitutive and stimuli-induced nuclear localization of IRF5. They are not conserved or homologous with NLS in other IRF5s. These two NLSs are solely responsible for nuclear localization and transactivation of target promoters as a mutant lacking both NLSs was localized in the cytoplasm and non-functional. We expect that loss of IRF5 nuclear function by NLS inhibitors will decrease type I IFN, IFN stimulated genes and inflammatory cytokines/chemokines in response to pathogenic stimuli.

To characterize the role of IRF5 in SLE patients, we used Amnis ImageStream technology to determine IRF5 cellular localization in different immune cell populations. In addition, qPCR was used to verify production of IRF5 target genes. Therefore, correlating IRF5 nuclear localization and gene expression. In immune cells we demonstrated that the IRF5 NLS inhibitors work in decreasing IRF5 nuclear translocation after stimulation and also decreased IRF5 target gene expression. The functional validation of these inhibitors to reverse specific clinical characteristics associated with disease pathogenesis, such as autoantibody production, proinflammatory cytokine expression, dysregulated apoptosis and immune cell clearance, will significantly aid in the development of new therapeutic interventions focused on the specific inhibition of IRF5 function/signaling in human SLE.

Introduction

TLR 7 & 9
MyD88
IRAK4
IRAK1
TRAF6
IRF5
IRF5

IRF5 Domain Map

NLS - Nuclear Localization Signal
DBD - DNA Binding Domain
TAD - Trans-Activation Domain

DK17
DK24

Hypothesis: IRF5 NLS inhibitors will decrease IRF5 function in immune cell subpopulations in SLE.

Results

IRF5 Peptide Inhibitor have minimal toxicity

THP1 monocytic cells were treated with IRF5 peptide inhibitor for 5 hours. Cell viability was measured by Annexin flow staining and is plotted as % of cells viable. DK17 & DK24 do not show significant toxicity, however DV shows toxicity at higher doses, unclear why.

Induction of IRF5 Nuclear Translocation

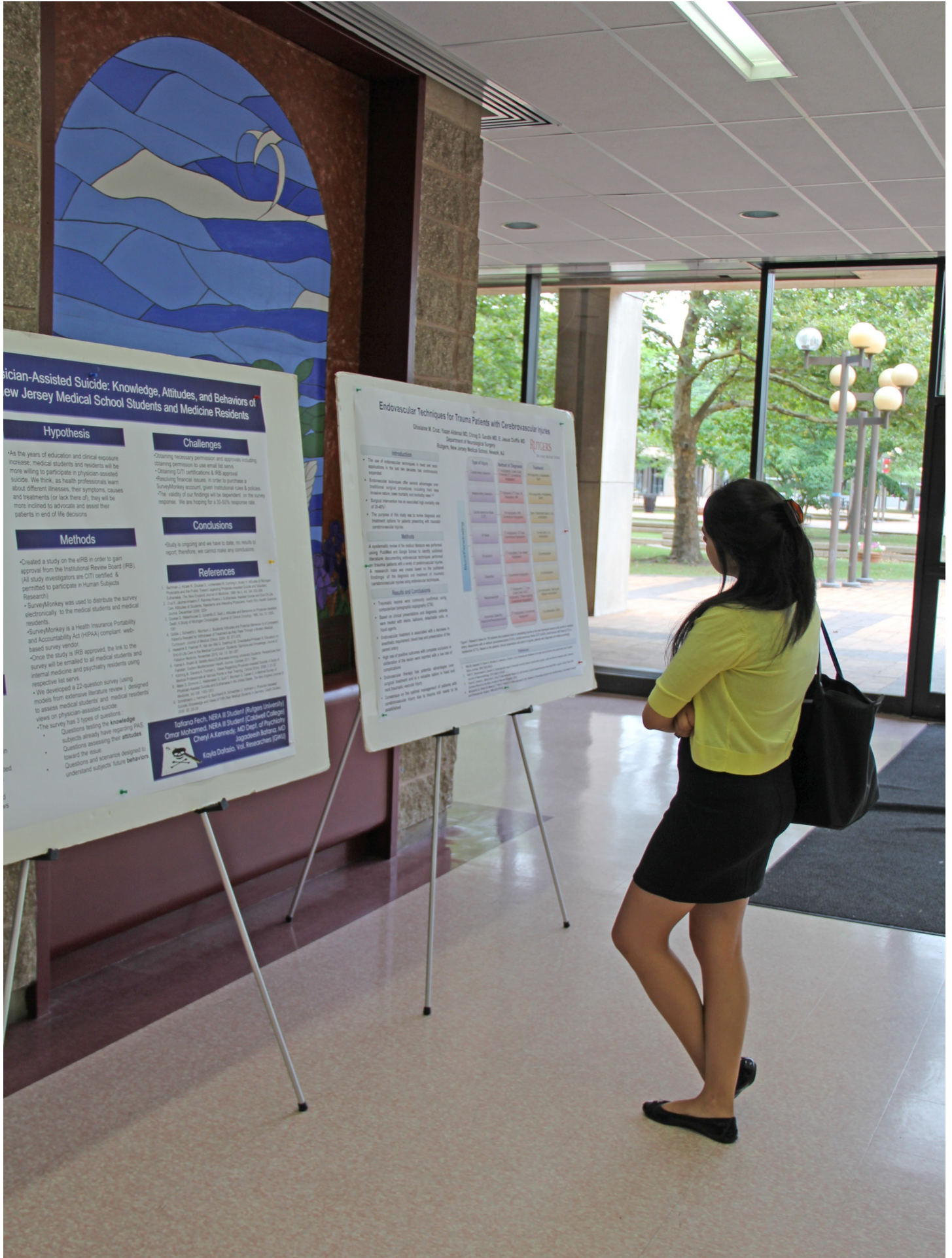
THP1 monocytic cells were treated with IRF5 peptide inhibitor for 5 hours. Cell cycle analysis was performed on cells that did not and treated with propidium iodide, and no flow through cytometer. Cells were gated to only analyze single cell population.

IRF5 peptide inhibitor

THP1 monocytic cells were treated with IRF5 peptide inhibitor for 5 hours. qPCR was performed. IRF5 NLS inhibitors DK17 shows some inhibition at 100nM while DK24 shows inhibition at lower concentrations.

Decrease of IRF5 Nuclear Translocation

Intracellular staining of the nucleus (DRAQ5) and IRF5 (Cy5) was performed by gating on extracellular markers. These are SSC and DRAQ5.



Physician-Assisted Suicide: Knowledge, Attitudes, and Behaviors of New Jersey Medical School Students and Medicine Residents

Hypothesis

- As the years of education and clinical exposure increase, medical students and residents will be more willing to participate in physician-assisted suicide. We think, as health professionals learn about different illnesses, their symptoms, causes and treatments (or lack thereof), they will be more inclined to advocate and assist their patients in end of life decisions.

Challenges

- Obtaining necessary permission and approvals including obtaining permission to use email list serves
- Obtaining CITI certifications & IRB approval
- Resolving financial issues in order to purchase a SurveyMonkey account, given institutional rules & policies
- The validity of our findings will be dependent on the survey response. We are hoping for a 50-55% response rate.

Conclusions

Study is ongoing and we have to date, no results to report, therefore, we cannot make any conclusions.

References

1. ...
2. ...
3. ...
4. ...
5. ...
6. ...
7. ...
8. ...
9. ...
10. ...

Tatiana Fecht, MBA B Student (Rutgers University)
Omar Mohamed, MBA B Student (Caldwell College)
Cheryl A Kennedy, MD Dept of Psychiatry
Jagadeesh Balaram MD
Kavita Datta, Vol. Researcher (CITC)

Endovascular Techniques for Trauma Patients with Cerebrovascular Injuries

Chaitan M. Cruz, Yogan Arinze MD, Ching D. Gandy MD, E. Jason Duffy MD
Department of Neurological Surgery
Rutgers, New Jersey Medical School, Newark, NJ

Introduction

- The use of endovascular techniques is well established in the field of stroke and cerebrovascular disease.
- Endovascular techniques offer several advantages over traditional surgical approaches including less invasive nature, lower mortality rates, and reduced hospitalization time in emergency settings (1-3).
- The purpose of this study was to assess diagnosis and treatment outcomes for patients presenting with traumatic cerebrovascular injuries.

Methods

A retrospective review of medical records was performed using PubMed and Google Scholar to identify published literature discussing endovascular techniques for trauma patients with cerebral cerebrovascular injuries. A research team was created based on the published findings of the literature and consisted of neurologists, neurosurgeons, and endovascular specialists.

Results and Conclusions

- Endovascular treatment is associated with a decrease in mortality compared to traditional open craniotomy in patients with acute intracerebral hemorrhage.
- High rates of patient outcomes will require further investigation.
- Endovascular techniques offer several advantages over traditional surgical approaches including less invasive nature and reduced hospitalization time.
- Consistent to the published literature, patients with endovascular treatment (ET) had a higher rate of survival.

Type of Injury	Method of Diagnosis	Treatment
Subarachnoid Hemorrhage (SAH)	CT Scan	Endovascular Treatment
Intracerebral Hemorrhage (ICH)	CT Scan	Endovascular Treatment
Subdural Hematoma (SDH)	CT Scan	Endovascular Treatment
Epidural Hematoma (EDH)	CT Scan	Endovascular Treatment
Extradural Hematoma (XDH)	CT Scan	Endovascular Treatment
Dissecting Aneurysm	CTA	Endovascular Treatment
Arteriovenous Malformation (AVM)	CTA	Endovascular Treatment
Cerebral Aneurysm	CTA	Endovascular Treatment
Carotid Artery Dissection	CTA	Endovascular Treatment
Vertebral Artery Dissection	CTA	Endovascular Treatment



RUTGERS

New Jersey Medical School

**RESEARCH OFFICE
SUMMER STUDENT RESEARCH PROGRAM**

**2013
ANNUAL REPORT OF ACCOMPLISHMENTS**